



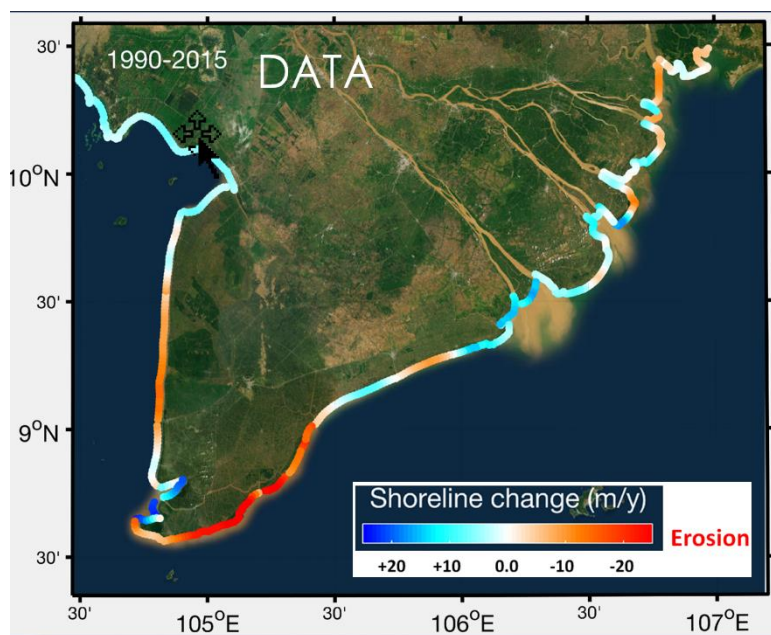
AGENCE FRANÇAISE DE DÉVELOPPEMENT (AFD) & EUROPEAN UNION (EU)  
SOUTHERN INSTITUTE OF WATER RESOURCES RESEARCH (SIWRR)

Contract No: AFD-SIWRR 2016

PROJECT

Erosion processes in the Lower Mekong Delta Coastal Zones and measures for  
protecting Go-Cong and Phu-Tan

## Final report



Ho Chi Minh City – December 2017

**Southern Institute of Water Resources Research (SIWRR)**  
658 Vo Van Kiet, Ward 1, District 5, Ho Chi Minh City, Vietnam  
Tel. 84.28.38380990, Fax: 84.28.39235028  
Website: <http://www.siwrr.org.vn>

**Contract No: AFD-SIWRR 2016**

**PROJECT**

**Erosion processes in the Lower Mekong Delta Coastal Zones and measures  
for protecting Go-Cong and Phu-Tan**

## **Final report**

**Team Leader**

**Dr. Patrick Marchesiello**

**Coordinator**

**Dr. Dinh Cong San**

**SIWRR DIRECTOR**

**Dr. Tran Ba Hoang**

# Executive Summary

## Context

The Lower Mekong Delta Coastal Zone (LMDCZ) is emblematic of the coastal erosion problem in tropical delta regions. It is strongly influenced by very large sedimentary fluxes reaching the ocean (about 50 million tons per year<sup>1</sup>), but also by waves and currents, which, in combination, redistribute the river intake to the southwest. This process has formed the Ca Mau peninsula for the last 3500 years. But now, in addition to natural forces, the LMDCZ is affected by local human activity, including possible reduction of river sediment fluxes due to damming and sand mining, as well as a reduction of protective coastal mangroves in favor of agriculture and aquaculture. Coastal erosion is observed in many places, with a rate of up to 50 m per year in some areas. Global warming has as yet a much lower impact than land subsidence<sup>2</sup>, associated with groundwater depletion, but the expected increase in sea level will undoubtedly contribute to an already large relative sea level rise.

The LMD has prograded for thousands of years during the Holocene, advancing southeastward along the river flow direction (16 m/y), then southwestward even faster due to redistribution by coastal currents (26 m/y). However since the middle of the 20<sup>th</sup> century, progradation has shown signs of weakening, while land use is accelerating. The general tendency of the system is not a settled matter. From satellite investigations of shoreline change rates (including our own), the general tendency of the whole LMDCZ is uncertain with large interannual to interdecadal variations. However, the system can be separated into subregions of common dynamics, which have a much clearer signature in their evolution. Within these subregions, local variations driven by local processes can also occur. Erosion can thus be seen in generally accretive zones, and that may be the case of our study sites (Phu-Tan and Go-Cong). Clearly, regional and local scales need to be distinguished as they hold different types of processes.

**In this project, we provide arguments to separate local from regional phenomena and natural redistribution by currents from actual effect of river sediment supply deficit. This investigation is first conducted at regional scale to assess system-wide sediment budgets using in-situ (WP1) and remote observations (WP3), combined with regional numerical modeling (WP2). We then assess the local sediment budgets in two selected sites: Go-Cong (Tien Giang Province) and Phu-Tan (West coast of Ca Mau Province). Based on regional and local sediment budget understanding (WP4 and WP5), we test soft and hard measures of protection using physical models (SIWRR flume facility) and local numerical models (WP6). Model assessments are also examined in the face of on-site observations and monitoring of existing protection measures along the LMDCZ (particularly at U-Minh**

<sup>1</sup> Estimates of the Mekong sediment discharge are uncertain. Depending on limited measurements and on the methods of computation, these estimates range from 50 to 160 Mt/y in the literature, but at different locations and not always including sedimentation in Vietnam's Mekong delta plain (Anthony et al., 2015). From our own calculations based on 2009-2016 high-frequency data collected in Can Tho and My Thuan, sediment discharge is currently at 42 Mt/y in average, but varied much between 18 and 86 Mt/y in the last 8 years.

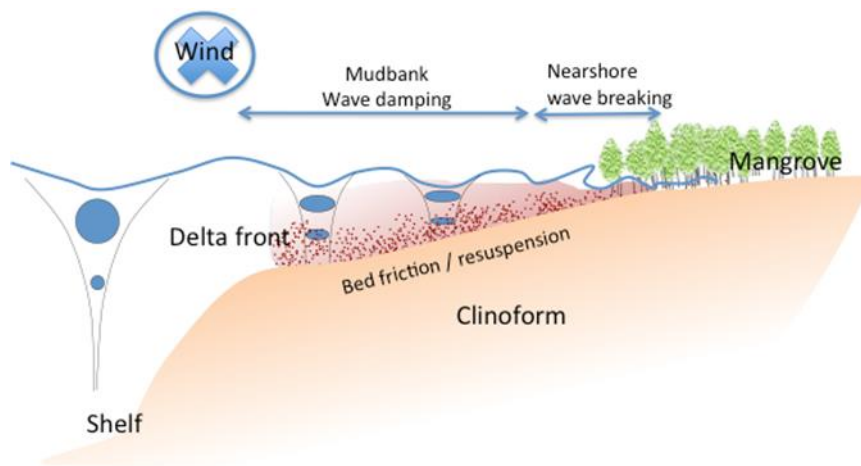
<sup>2</sup> Global sea level change and subsidence rates are respectively estimated in average at 4 and 16 mm/y, but local subsidence rates can range from 1-4 cm/y in the lower Mekong Delta with higher values in the Ca Mau peninsula and Ho Chi Minh City (Erban et al., 2014, Minderhound et al., 2017).



project also uses a large set of observational tools to complement our general knowledge and validate the models, from in-situ to satellite observations and coastal video cameras. Laboratory studies were also used for calibrating sediment model parameters (CARE lab) and to test protection measures (SIWRR flume). Capacity building was also part of the project's objectives, through formal training (video camera, ADCP measurements) and regular exchange with international experts.

## Erosion processes

Based on observations and model solutions, we revisited some of the important processes of erosion. In some cases, we contributed important results to previous studies, and in others, we reviewed the current state of knowledge.



Schematic view of coastal regions and main driving forces in the LMDCZ

### Natural redistribution

Deltas are coupled hydro-morphodynamic systems, which are generally unstable and vary following cycles of advance and retreat with time-scales from intra-seasonal to multi-decadal (Winterwerp, 2005). These natural processes certainly explain part of observed erosion in the LMDCZ. In Europe, almost all mudflats are in estuaries or tidal inlets, mainly because the exposure to waves on the open coast is too great to allow any significant amount of mud to accumulate (Roberts et al., 2000). In the tropical zone, there are situations where open coast mudflats exist. These are usually associated with areas having a very large fluvial source of muddy sediments, e.g., the Mekong delta system. In this case, mud and sand are transferred from the river to the coastal zone, but the displacement of mud is much faster than that of sand, so that mud keeps accumulating in southern shores, forming the Ca Mau peninsula. Western shores of the peninsula are less exposed from waves than eastern muddy shores and thus naturally experience less erosive attacks.

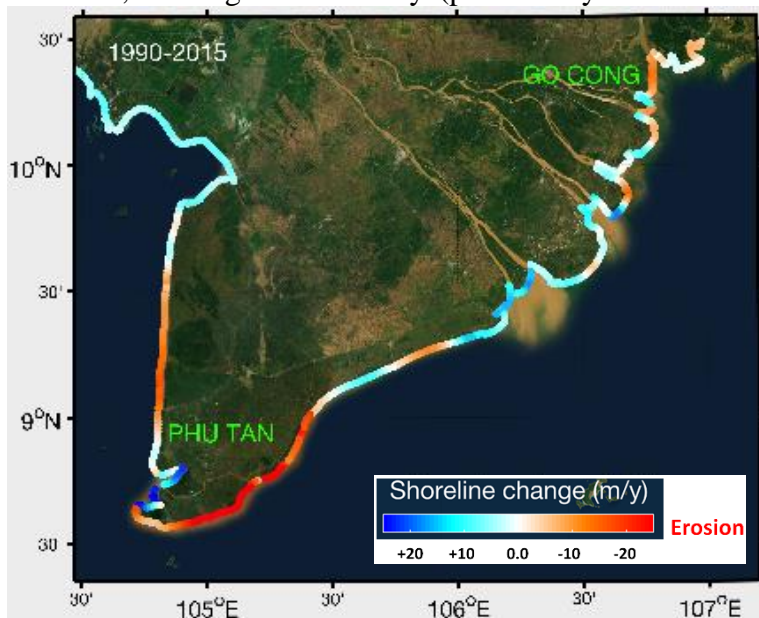
Owing to the project results, the regional picture of sediment transport and budget is now substantially improved. It is based on an ensemble of data from in-situ and satellite observation, laboratory analysis and modeling. These comparisons allows us to estimate the part of shoreline changes that results from a natural redistribution of sediments by waves and currents, and the part from other sources (river supply deficit, coastal squeeze, subsidence...). We find that our



models can reproduce essential regional patterns of erosion and deposition, featuring three dynamically consistent coastal zones: Estuary zone, East coast and West coast. These patterns thus appear to be largely a result of redistribution processes by waves and currents. The largest subregional erosion is in the southern shores of Ca Mau.

It is important to note that our numerical models suggest erosion to be primarily a result of wave-driven re-suspension and wind-driven transport occurring over a particularly shallow cliniform<sup>3</sup> along the LMDCZ (about 10-km wide across-shore), rather than strictly over the nearshore zone (less than 1 km). Therefore, simpler nearshore models, which only deal with wave-driven longshore drift, cannot explain the observed regional phenomenon. These so-called one-line models or associated paradigm of littoral dynamics (e.g., Albers et al, 2013) were sometimes applied to the LMDCZ; they are inherited from sandy littoral applications where they provide reliable answers, but shallow muddy environments have different dynamics. Our study provided a better-suited paradigm for LMDCZ processes.

However, looking more closely (particularly in our two study sites), we notice that some



Map of shoreline change rates in m/y estimated from satellite images. Red/blue colors are erosive/accretive shores.

likely candidate for that severe erosion is a deficit in river supply from the Saigon-Dong-Nai River, upstream from Go-Cong (see below).

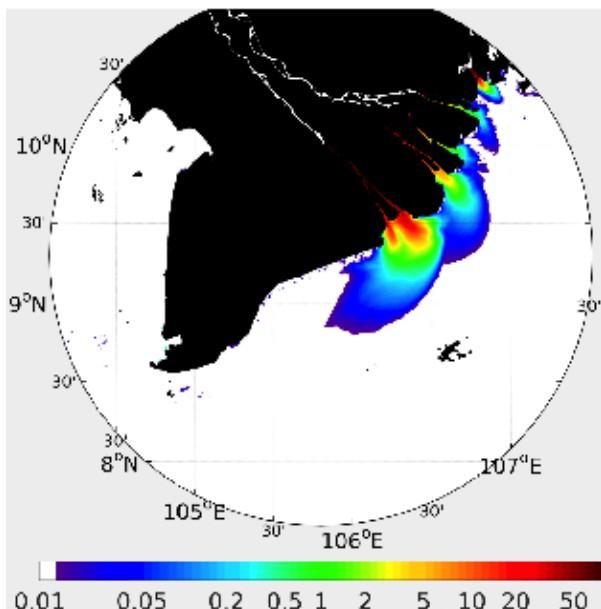
patterns cannot be explained by natural redistribution of subaqueous sediments. For example, the models do not predict the recently observed strong erosion at U-Minh and the fact that our bathymetry survey shows little erosion in waters deeper than 2 m suggests that other processes might be involved, including subsidence and/or coastal squeeze. On the contrary, the Go-Cong area shows the most consistent erosion of the whole Estuary zone (seen both in satellite-based shoreline analysis and comparison of bathymetric surveys at a 6-year interval). A

<sup>3</sup> Here, we may use indifferently the words mudbank or cliniform to describe the total wedge-shaped package of sediments contained in the subaqueous-delta deposits. Subaqueous cliniforms serve as the marine foundation for subaerial delta progradation. In the Mekong delta, the transition between the broad cliniform topset and steeper foreset is located at about 5 m depth (rollover depth), much shallower than in many large-river deltas (Eidam et al., 2017).

## Sediment river supply

Because sediment river supply is the source of delta progradation, a decrease of this supply would certainly affect the delta's morphology. One objective of the project was to try and estimate the tendency of sediment input into the coastal ocean. Our estimation of sediment flux in the lower Mekong River<sup>1</sup> is on the lower end of previous estimates. Whether this is the expression of a real change or a bias due to low-frequency data used in historical studies, it is hard to conclude. The scarcity of in-situ data still precludes us from accurately assessing this tendency. Yet, we can provide answers by indirect methods (through satellite observation and model testing). From our model results, a decrease of river supply about 100km upstream has a rapid decay downstream with significant impact only in the estuary and mouth area (where a fraction of the signal is left). This is consistent with recent observations of sedimentation rates, showing a majority of deposition near the river mouths (DeMaster et al., 2017). Therefore, if sediment is missing from the river, it should first be seen in the estuary zone.

In this sense, the observation by Loisel et al. (2014) of a decrease of suspended particulate



Model sensitivity of coastal surface sediment concentration to river supply. The difference of SSC in mg/l is between two simulations with upstream river SSC fixed at 200 mg/l and 50 mg/l.

such as the West coast of Ca Mau (see also Winterwerp, 2005, for similar conclusions for the gulf of Thailand).

**Yet, our results also suggest that extreme erosion in Go-Cong is likely a result of sediment supply deficit, but from the Saigon-Dong Nai river system rather than the Mekong River.** Here follows another novel proposition, which surprisingly was not put forward before. If Go-Cong has such a singular behavior in the Estuary zone (which is in general still accretive), it is likely because it is under direct influence of the Saigon Dong Nai river system. Massive dams and reservoirs were built in the 1980s and 1990s: for example Dau Tieng dam in the Saigon river operated in 1984 and Tri An dam in the Dong Nai river operated in 1991. These dams would modify sediment supply to the coastal zone much faster than those of the Mekong



system. Therefore, we need to study more closely the possibility that erosion in Go-Cong may result from these dams. **If it were confirmed, then the Go-Cong coastal area would be a predictor of the Mekong system. It is a relatively small-scale real-world laboratory that will help predict what will probably be the effect of Mekong dams on the LMDCZ.**

### Coastal mangrove squeeze

A well-known problem in coastal zones is the squeeze of coastal habitats before a dyke, a road or any structure parallel to coastline. Coastal mangrove squeeze is a particular case of coastal squeeze that has been identified as a serious issue for the LMDCZ (Winterwerp, 2013; Phan et al., 2015) because dykes were built all around very close to the shoreline (often less than 500m). Phan et al. (2015) estimated that a critical mangrove width of at least 500m is needed around the LMDCZ to sustain the coastal mangrove belt. Loss of these coastal mangroves is detrimental to shoreline protection because mangroves are a natural protection, i.e., buffer zones acting as barriers to wave energy and in the same time helping nearshore sediment trapping. But, there are still doubts about the correlation between mangrove belt width and its sustainability, which we investigated in this project.

Our study confirms previous findings but with a slightly more complex picture. **A minimum size of mangrove belt of 500-800 m appears as necessary but not sufficient condition for sustainability.** For example, the southern Ca Mau province is so naturally exposed to erosion that no amount of mangrove can stop erosion there. The same may probably be true for Go-Cong. On the other hand, the West coast of Ca Mau would more fully profit from mangrove restoration. In erosion-prone areas, the addition of bamboo/melaleuca fences appears as a very efficient complement to mangrove planting, as it promotes sedimentation by flocculation and settling in calmer water.

### Onshore flow blocking

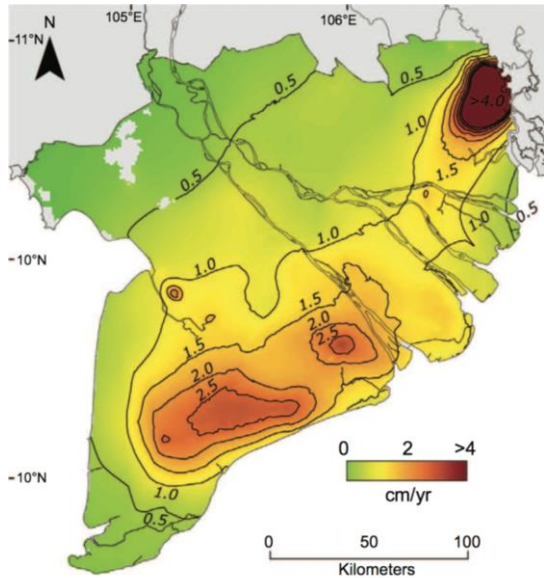
The cross-shore profiles of mudflats can be classified according to the relative contributions made by waves and tidal currents to the total sediment transport. Traditionally, we see at one end of the range erosional flats dominated by waves, which are characterized by a concave profile; at the other end are tidally dominated flats with a convex profile, which are believed to have a long-term tendency to accrete. Cross-shore tidal flow promotes onshore sediment transport and accretion while waves tend to produce erosion (Le Hir et al., 2000), although there are also wave processes (gravity and infragravity waves) associated with onshore transport (not yet well understood and handled by models, especially for muddy environments). Even though the amount of water flowing towards the coast during rising tides equals that flowing off the coast during falling tide, a net onshore sediment transport is explained by a number of asymmetries in the water movement (tidal asymmetry) and sediment behavior (settling and scour lag; van Straaten, and Kuenen, 1958). Onshore winds can also participate in coastal sediment accretion. The Ekman drift is a process that tends to carry water properties to the right of the wind (less so in shallow water). During winter, northeastern monsoon winds thus provide some ways of accumulating sediments to shore.

In any case, constructing dykes or breakwaters parallel to shore can block the onshore water flux (tidal prism; e.g., Winterwerp, 2013) and associated onshore sediment flux, not only near the wall but also over long distances seaward from it. Our model results seem to confirm the role of tides in onshore sedimentation. Therefore, wherever possible, a submerged or porous barrier would be preferred. The final answer is in the trade-off between reducing detrimental

high-energy waves and blocking beneficial currents. Where erosion is severe and waves are high, such as in Go-Cong, damping waves is a priority.

### Subsidence and sea level rise

Global warming might not be significant in the current situation because its impact remains low



Anthropogenic subsidence rates from Minderhoud et al. (2017) subsidence. It would be consistent with a stable offshore bathymetry, as suggested by our survey.

in the face of tectonic subsidence (1.6 cm/y in average for the LMD and up to 5 cm/y locally<sup>2</sup>), due to groundwater depletion, but the expected increase in sea level will undoubtedly contribute to its aggravation in the future. Subsidence is not part of the present study as it involves very different techniques of investigation and would represent an entire new project. However, in present literature, this process is considered a serious risk for flood and shoreline retreat, which should be better evaluated in the future. Right now, subsidence may account for about **10 m/yr** of shoreline retreat along the LMDCZ (based on a foreshore slope of 1/1000), although it has large regional variations and appears to be particularly strong on Vietnam’s west coast, i.e. away from the Mekong floodplains. Some of the erosion seen at U-Minh in recent years can possibly be explain by

U-Minh in recent years can possibly be explain by

### Synthesis for Go-Cong and Phu-Tan

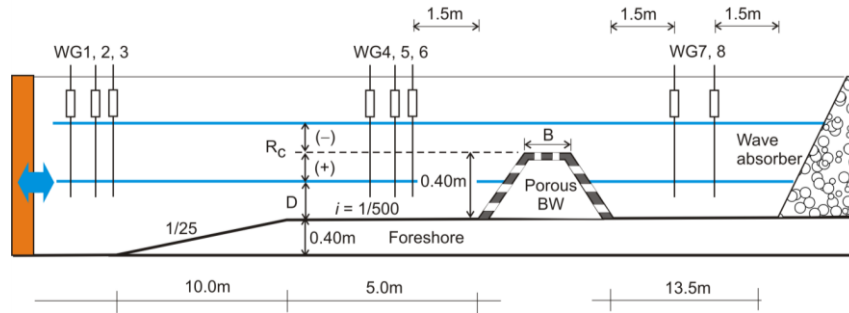
	Shoreline retreat	Subsidence contribution	River supply deficit	Dynamic redistribution	Mangrove squeeze
<b>GO-CONG</b>	15 m/y	< 5m/y	<b>Large sensitivity to Soai Rap river</b>	Erosive (export south)	NA
<b>PHU-TAN</b>	5 m/y	< 5m/y	Small	Neutral or accretive (from south)	<b>Probable</b>

## Protection measures

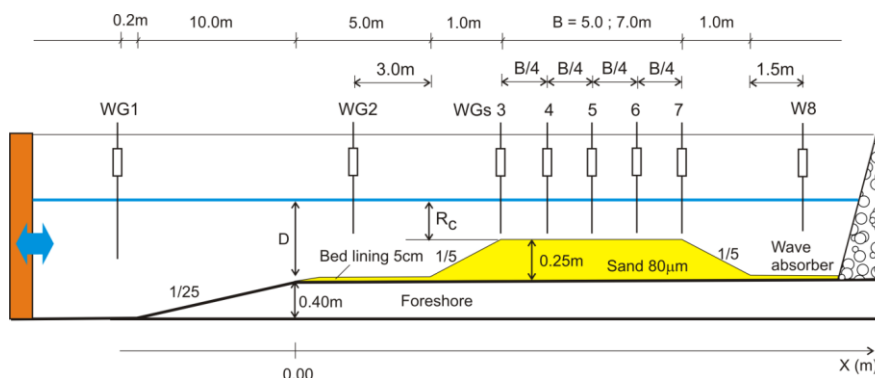
The proposed measures were based on surveys of the study sites (Go-Cong and Phu-Tan), physical and numerical modeling, and also importantly on the review of existing protection measures, their success and failure. Much can be learned from pilot experiments in the past.

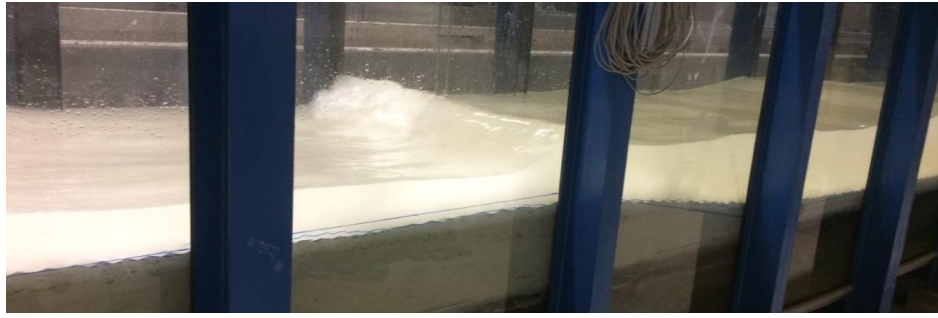
The first selection was provided by the SIWRR physical model (flume) with 1/10 length scale, and essentially consisted in two solutions: hard solutions (breakwater) and soft solutions (nourished sand bar, possibly completed with mangrove replanting and bamboo fencing).

**POROUS BREAKWATERS:** the selected porous breakwater is shown to work as a mean to reduce wave transmission, but it must be higher than the Maximum High Water line. However, the flume experiment shows serious reflection, which can produce some amount of scouring in the seaward side of a breakwater. Preliminary tests with kaolinite sediment showed that sediment is clearly transported through the breakwater. With tidal flow cycles, we expect an easy exchange of sediment through the structure. Our understanding is that any porous structure that allows the tide to enter will allow the fine sediment to pass the breakwater.



**NOURISHED SAND BARS:** the flume experiment also shows significant reduction of the wave spectrum due to the presence of a wide sand bar (50-70m). Narrower sand bars are less efficient. Deformation of the bar can be significant although it maintains integrity and positive damping effect remains over most tested wave conditions. Overall, the test of nourished sand bars is positive.





Then, these measures were tested in local models and assessed against in-situ and remote observations and sediment budget model results. Note that protection measures need to be implemented in a depth of a few meters. Sandbar elevation should be at mean sea level. In Go-Cong, this corresponds to a position only 300m from shore, but in Phu-Tan, it is further offshore, 500m, since the water is shallower there. In addition to breakwater and sandbars, the local numerical models allowed us to carry a preliminary test of the damping effect of mangroves as a complement to soft measures (it is qualitative and more would need to be done on this matter).

### Go-Cong

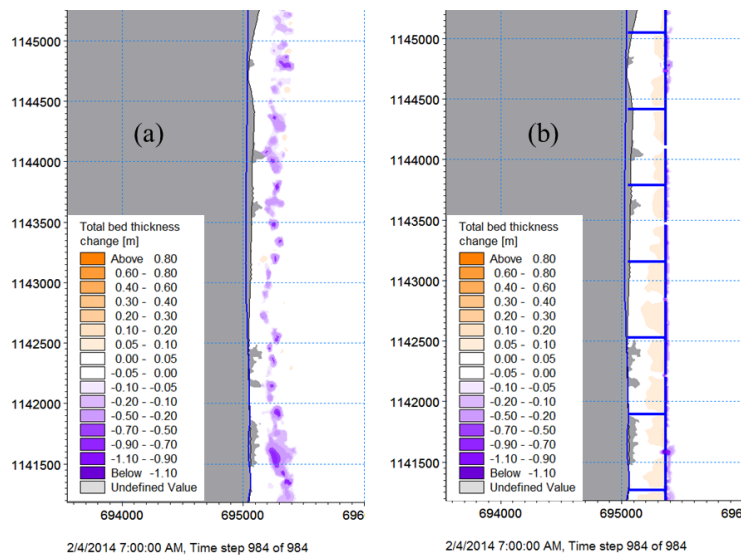
Shoreline change observation shows consistent erosion in Go-Cong from 1990 to 2015. This is unique within the Estuary zone. As said before, it is consistent with the fact that Go-Cong shores are under direct influence from the Saigon/Dong-Nai river system, rather than the Mekong River. Our bathymetric survey compared with a previous survey done 15 years ago, confirms severe erosion (on the order of 1 Mt/y), which is on the order of estimated Saigon Dong Nai river flux. The same comparison in the West coast of Ca Mau does not show such a large difference, which means that there is consistency between satellite analysis of shoreline changes and bathymetric surveys.

Erosion in Go-Cong is massive and has reached the level of dykes, drastically affecting the mangrove belt. Geotextile tubes (geo-tubes) implemented along part of the coast are unconvincing as yet. There is little evidence of small accretion (anecdotic), no effect of vegetation growth, and there are still large waves accessing the shore. A systematic monitoring of these geotubes would be needed for more reliable conclusions.

Below is a summary of model test results in terms of mean bed thickness evolution for various scenarios and combination of summer and winter months (Jan/Sep 2014), with comments that follow:

Go-Cong simulations	Baseline	Breakwater	Sandbar	Baseline -75% supply	Breakwater -75% supply	Sandbar -75% supply
Jan/Sep 2014 Sedimentation in 2-km coastal area (cm)	0.4	0.8	1.1	-1.2	-0.6	-0.3
<b>Jan/Sep 2014 Sedimentation inside structure (cm)</b>	<b>-2.8</b>	<b>4.0</b>	<b>2.7</b>	<b>-3.6</b>	<b>3.7</b>	<b>1.6</b>
Comments		Scouring	No scouring Small bar deformation		Scouring	No scouring Small bar deformation

**MODELED BREAKWATER:** The modeled breakwater is a T-groyne structure 300m from shore, and has a crest elevation above the highest water level (2.2m). It is composed of sections 600m wide with gaps of 30-50-70m (3 scenarios). The model testing of protection measures shows that the breakwater promotes reduced erosion and inshore accretion. There is a 50% decrease of net erosion in winter (lower erosion and higher accretion), reversing the erosive balance. Gaps between shore-parallel breakwaters were tested as well. It appears that the gap needs to be optimized to get the most effective accretion inside the structure and to reduce wave effect. It should be noted that the smaller gaps also produce sensibly larger **scouring between gaps and outer structure toe**. In addition, larger gaps are more efficient to mitigate river sediment flux deficit (see below).



Erosion and accretion in Jan. Left: model erosion without protection; Right: accretion with T-groyne structures (30m gap). It should be noted that the smaller gaps also produce sensibly larger **scouring between gaps and outer structure toe**. In addition, larger gaps are more efficient to mitigate river sediment flux deficit (see below).

**NOURISHED SAND BAR:** We also tested the effect of a nourished sand bar. The modeled nourished sandbar is a shore-parallel structure 500m from shore, 50 or 70 m wide, with gaps of 200 m and crest level at mean sea level +0.0 m (deeper crest level proved inefficient in this high-energy environment). The model was first tested for sandbar integrity under high-energy NE monsoon waves. The results confirmed that of the physical model in producing only mild morphological changes on the outer slope of the bar. The damping of waves by the bar was less efficient than with breakwaters. Even though accretion inside the protection structure is lower, scouring is much reduced for sandbars compared with breakwaters. **The overall accretion with sandbars (over a section of 2km from shore) is higher by 30%**. Interestingly, during the low-energy season (SW monsoon), sandbars are more effective for accretion inside the



protection structure, which adds to the overall efficiency. Finally, sandbar nourishment can also be useful as sediment storage in this sediment starved area. However, how helpful this might be for mangrove rehabilitation is an open question.



Photos of mud and sand during a field trip to Go-Cong in Dec 2017. The shore near the Soai Rap river mouth (the Saigon-Dong Nai river system) was sandy (left hand on left panel) and mud is only retained within mangrove roots (right hand). Further south near the Mekong river branch (Tieu river), large amounts of mud were deposited.

**SEDIMENT SUPPLY:** A test of sediment supply from the Soai Rap river (Saigon/Dong Nai river system) was also performed. When sediment input is reduced by **75%** (100 km upstream), net erosion increases along the coast of Go-Cong. There is about **60% deficit** of accretion in the nearshore area. The rest is deposited offshore or compensated by river erosion (“hungry water” process). **The deficit of accretion in the river supply model experiment results in a large increase of net erosion over the combined seasons (an order of magnitude).** This result confirms that of the regional model, indicating that erosion in Go-Cong is highly sensitive to sediment supply by the Saigon Dong Nai river system. This seems also confirmed by our video camera images of summer 2017 and by SIWRR surveys showing only thin layers of mud deposition during the low-energy season (summer), contrasting with thicker layers that are deposited further south in the mouths of Mekong branches (Tieu and Dai rivers), albeit with interannual variability. Importantly, protection measures can mitigate river deficit. Inside the protection zone, breakwaters work better than sandbars as they trap almost as much sediment as without river deficit. However, there is much larger scouring around breakwaters, so that looking at an extended area (2-km) breakwaters can only reduce erosion by half in case of river deficit, while sandbars lead to a closer mitigation.

### Phu-Tan

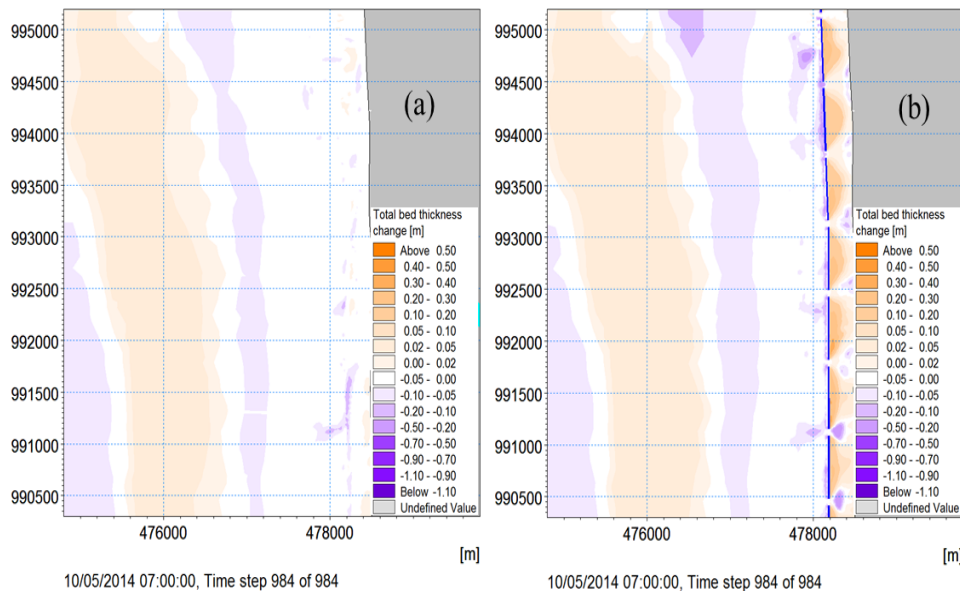
If U-Minh shows erosion, Phu-Tan, our study site on the West coast, is more of a neutral zone, receiving sediments from the eroding East Coast. Yet, local zones of erosions are an increasing concern. Note that the case of Phu-Tan may be different from U-Minh, and even more so from Go-Cong. Phu-Tan is a subregion of mild erosion compared with U-Minh, which has showed steady erosion in recent years. Our bathymetric survey compared with a survey performed a few years ago shows little evolution. If there is local erosion, then it may be due to local causes. As subsidence is lower than at U-Minh, mangrove squeeze may be a factor or variability of the coupled hydro-geomorphologic system (e.g., reduced sediment supply from Ca Mau cap).



Our local model results can shed some light. The erosive season in Phu-Tan is summer monsoon, with maximum wave height in August. Waves are the dominant cause of erosion, while winds and tides drive sediment transport: northward and shoreward to a lesser extent. This tendency would contribute to shoreline stability. Offshore wave intensity is generally correlated with wind magnitude. On reaching the shore, they rapidly decrease in intensity. Confirming the result of the regional model, we show that, contrarily to sandy environments with steep beach profiles, the effect of waves here is not confined to the surf zone, but extend over a shallow mud seafloor where bed shear stress is dominated by wave orbital velocities to a depth of about 10m.

Below is a summary of model test results in terms of mean bed thickness evolution for a combination of summer and winter months (Jan/Sep 2014), with comments that follow:

Phu-Tan simulations	Baseline	Breakwater	Sandbar
Jan/Sep 2014 Sedimentation (cm) in 2-km nearshore area	-1.8	-1.1	-0.4
<b>Jan/Sep 2014 Sedimentation (cm) in area inside structure</b>	<b>-0.8</b>	<b>8.0</b>	<b>9.4</b>
Comments		Scouring Wind contribution to trapping	Sandbar deformation Wind contribution to trapping

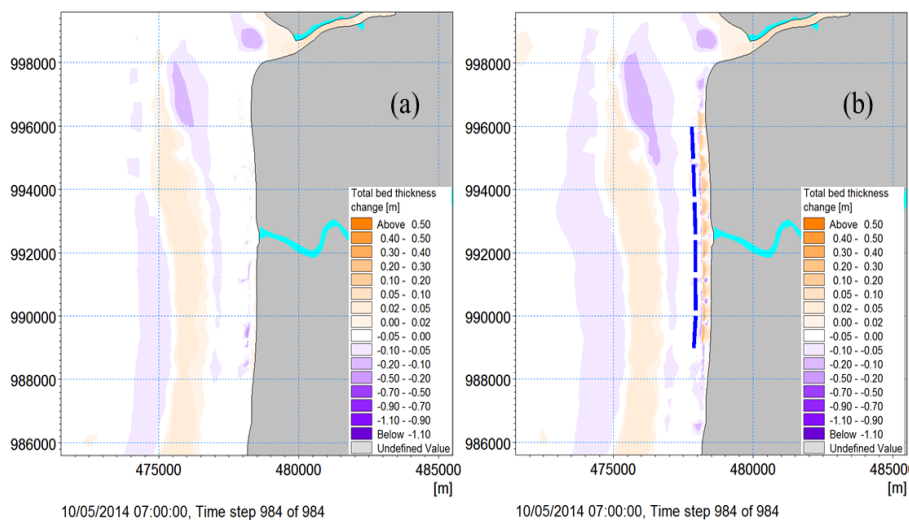


Monthly erosion and accretion off Phu-Tan district in Sep 2014 (SW monsoon). Left: without protection, erosion is apparent nearshore (on the right of the panel); Right: with breakwaters, strong accretion occurs but with scouring within gaps and outer toe of structures.

**MODELED BREAKWATER:** The modeled breakwater is a shore-parallel structure 300m from shore, with gaps of 70 m, and has a crest elevation above the highest water level. Our results show that it can efficiently remove inshore wave energy. Because erosion results from wave-enhanced bed friction, the breakwater efficiently controls it. **The sediment budget changes from moderate bed erosion of a few cm/y to strong accumulation of many tens of**

cm/y. This result tends to confirm the result of our survey on existing breakwater structures in U-Minh. At U-Minh, erosion stopped and sediments accumulated inside the breakwater. Interestingly, accretion is much stronger during the SW summer monsoon because SSC is higher due to stronger waves outside the protected zone, so that a larger sediment load can be brought inside and deposited. Without protection, the same waves would lead to offshore export of mud and erosion. Therefore, some amount of wave energy can be beneficial to accretion, provided that the nearshore area is protected. To confirm this, a model test with double wave height was conducted, which led to 50% increase of sediment deposition inside the protected area.

**NOURISHED SAND BAR:** We also tested the effect of a nourished sand bar. The modeled nourished sand bar is a shore-parallel structure ~500m from shore, 70 or 120 m wide, with gaps of 200m and height at mean sea level. The damping of waves by the bar was also an efficient process, provided that the bar width is in the order of a wavelength (120m is more efficient than 70m in our simulations but with bar height at mean sea level, the difference is not important). Sandbars are a bit less efficient for wave blocking than a shore-parallel breakwater and has lower peak accretion inside the structure, but it has the **advantage of avoiding scouring at the breakwater toe and within gaps, which gives better overall accretion**. Finally, the addition of simulated mangrove effect on wave and flow dissipation showed to be a good complement to nourished sandbar as it carries wave damping further inshore and allows a more positive nearshore sediment budget in the model. As this is a preliminary experiment, the results remain qualitative.

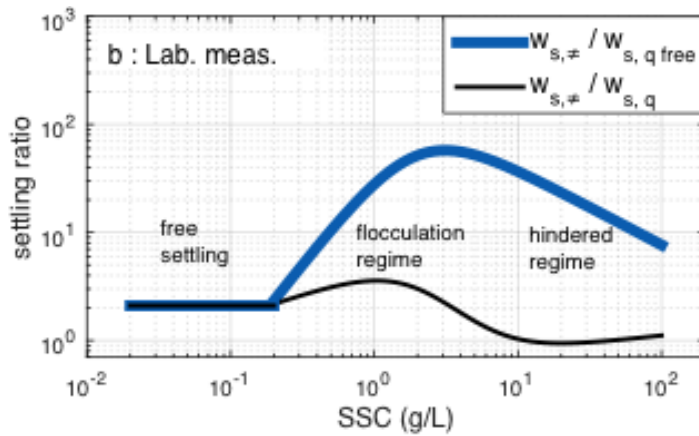


Same as previous figure but with sandbar for protection instead of concrete breakwaters. Accretion is also strong with sandbars. Although peak values are a bit less than with breakwaters The absence of scouring between gaps and outside the structure makes it more efficient overall.

### Flocculation in protected waters

In successful existing protection measures, the source of deposited sediment deposited is not always clear but is assumed to result from onshore fluxes through porous structures. Shore-parallel walls can maintain part of the alongshore transport, but it blocks the residual onshore sediment flux associated with winds and tides. Porosity can significantly increase the retention capability of protection measures, as also seen for porous bamboo/melaleuca fences (e.g.,

Cuong et al., 2015). Fortunately with fine sediments, porosity is easily achieved, which explains some of the successes observed on the west coast.



Regimes of settling velocities of LMD cohesive sediments from laboratory experiments (published in Gratiot et al., 2017)

We expect that porous structures such as bamboo/melaleuca fences should also greatly help accumulating sediments in the mangrove area. Above is a figure from laboratory experiments conducted during our project. It shows at least two regimes of settling sediment velocity depending on sediment concentration. In the fluvial and coastal environment, sediment concentration is generally lower than 200 mg/l and settling velocity is low, in the range  $1-8 \cdot 10^{-5}$  m/s; particles are flocculi in great majority (more than 80%) of size 8-20 microns. We use these parameters for our models. However, very near shore, the regime can change due to two possible processes:

- Sediment concentration increases due to very shallow water conditions, i.e., high bed friction from tides and waves. It may reach a few grams per liter, which is optimal for flocculation. Our surveys confirm the increase of SSC very near shore.
- Turbulence may also decrease due to protections from fences or mangroves. In this case, flocculation by differential settling can occur.

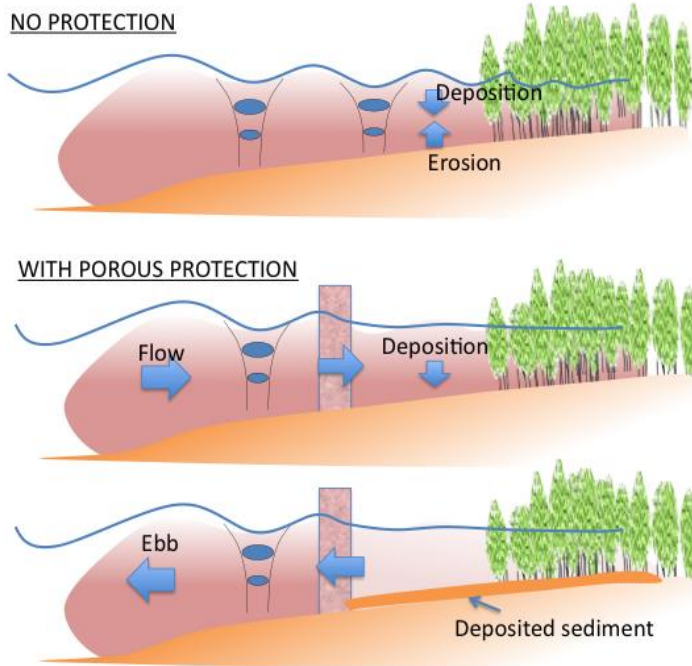
If the two processes are combined (optimal concentration; weak turbulence), then settling velocities, and thus sediment accumulation, may increase by two orders of magnitude.

### Upper limits of sedimentation

This very near shore processes are not well resolved in current models, but we can consider an upper limit of what to expect in terms of sedimentation rate, provided that erosion is controlled and protection measures are porous to tides (almost everywhere, regardless of the structure type, as long as the tidal range behind the structure is the same as in front of it). For cases where a sheltered region is created, let's assume that tides are the main driver for exchanging sediment. The total inflow in one tidal cycle is the product of tidal volume and nearshore concentration; the outflow depends on the efficiency in capturing the sediment. If we assume complete effectiveness as an upper limit the sedimentation rate per year is:

$$\text{MaxSed (m/y)} = \frac{\text{Tidal Range (m)} \cdot \text{SSC (kg/m}^3) \cdot 700 \text{ tides/y}}{\text{bed density (kg/m}^3)}$$

For Phu-Tan, tidal range is  $\sim 1.5$  m; concentration  $\sim 100$  mg/l; bed density  $\sim 1000$  kg/m<sup>3</sup>, which



leads to  $\sim 10$  cm/yr. For nearshore SSC above 300 mg/l as measured during our nearshore surveys, accumulation of **30 cm/y is possible**. For Go-Cong, higher tidal ranges will double that estimation and more if considering higher SSC. Since the sediment has about 6 hours to settle, the part of the water column that can settle depends on fall velocity. For 0.25 mm/s, the whole water column is involved, but material with smaller fall velocities would not have time to sediment. As seen previously, fall velocities of 0.25 mm/s can only occur for high nearshore SSC concentration. Therefore, if all conditions are met, i.e., well-sheltered conditions but with high

SSC in places with tidal exchange, then we can expect accumulation of order 10 cm/y or more.

At U-Minh observation of existing breakwaters show that accretion can easily reach this limit. It is true also in our model simulations, as long as flocculation is represented within a cohesive sediment approach. Our sensitivity experiments show that favorable **onshore winds can also increase this upper limit by 30%**. However, the exact numbers are dependent on an accurate knowledge of sediment concentrations in shallow areas, which still needs further evaluation for both the muddy environment of Phu-Tan or the mixed one of Go-Cong.

### Conclusion on structure efficiency

1. **PHU-TAN:** from existing experiments and model results, we can expect high accretion of order 5-40 cm/y inside any structure that is sufficiently porous for tides to get through. It is important to note that accretion here does not result primarily from longshore drift due to nearshore breaking of oblique waves (littoral drift paradigm) but from a combination of alongshore transport over the entire subaqueous delta front and onshore transport associated with tides and winds. This means that the protection structure may have **limited impact on the surrounding area**, as opposed to what is common in sandy beach environments. This is confirmed by our model results, where only limited erosion is observed on either side of the structures. The paradigms of sandy littoral protection, which has been the focus of most engineering work may not be applicable to mud coasts.
2. **GO-CONG:** the conclusions above must be moderated for Go-Cong. Our modeling experiments show that Go-Cong being directly under the influence of the Soai Rap river, **SSC and nearshore accretion efficiency also largely depends on river sediment supply**. Protection structures can turn annual net erosion to large net deposition if sediment supply is available (with 50% less net erosion in winter). With a 75% decrease of river flux, the efficiency of protection measures is greatly reduced in models and

cannot overcome erosion. The exact numbers will thus be dependent on an exact knowledge of river fluxes and of erosion flux parameters on a mud-sand bed where mud suspension can be limited by sand armoring.

## Recommendation

Our recommendations are set based on scientific and local knowledge and our project's findings. We come to a set of suitable choices for soft, hard and hybrid measures. The recommendations are site specific.

First of all, we realize that coastal protection in the face of structural erosion cannot rely only on creating bigger and stronger dikes; dikes can be built to withstand any undercutting by erosion and increased wave attack, but not against acceptable costs. Therefore the project aims at halting the erosion with measures that maintain a shallow foreshore and viable mangrove areas.

A potential sediment deficit from upstream Mekong River exists but is not clearly demonstrated here. Even if the deficit is real, it cannot be reduced within the project and should be considered as a boundary condition. The situation may be different for the Saigon Dong Nai system, which appears as a dominant supplier for the Go-Cong area. Vietnam authorities controlling operations on this river system should be alerted. If we consider river supply as a given condition, then any hard coastal protection structure will be unable to increase the amount of sediments transported alongshore. Nourishments may in part mitigate this imbalance.

On a local scale, coastal erosion and accretion depend on the balance between sediment deposition and erosive forces of waves and currents. Deposition directly depends on the nearshore sediment concentration, and on the conditions for fine sediments to settle. Erosion is a function of the local bed shear stresses and the degree of mud consolidation. It is useful to consider an upper limit of what to expect in terms of sedimentation rate. We estimate this upper limit of accretion in the LMDCZ in the order of 5-40 cm/yr (depending on SSC). Paradoxically, at some certain degree high wave conditions may be favorable for accretion when combined with tides and suitable protection, while they may at the same time lead to strong erosion in unprotected areas. Therefore, the design of coastal protection measures should aim at minimizing the destructive effects of the waves while allowing their accretive effects in combination with tides.

From Schüttrumpf (2017) we may summarize the design considerations as follows. Any coastal protection structure should ensure the following requirements:

- Be porous enough to ensure water exchange, sediment transfer and water quality
- Be as high as possible to reduce wave impacts
- Be able to withstand extreme wave heights
- Be able to trap sand, silt and clay.

Ideally, the solution should be a combination of structural and non-structural measures, e.g. offshore breakwaters with gaps in combination with nourishment and mangrove planting. Where erosion is severe and waves are high, such as in Go-Cong, damping waves should be a priority, whereas the opposite prevails in less energetic environment such as Phu-Tan. A wide



mangrove belt of more than 500 m is a necessary condition for its sustainability but not sufficient in case of high-energy conditions. In this sense, we could recommend hard measures in Go-Cong but soft measures in Phu-Tan, although our model results and the experience of breakwaters in U-Minh confirms that breakwaters would also work for Phu-Tan. In both cases, model experiments on sandbar protections give good results in terms of accretion and lack of scouring, but we have no result from existing experiments to backup these results. In the following, we propose design options, including the design of limited full-scale pilot experiments.

### Go-Cong

The proposed measures for Go-Cong are:

- **HARD MEASURES:** breakwater with I-shape or T-shape structure, 300m from shore, with crest elevation above the highest water level (2.2m). It should be composed of sections 600m wide with gaps of 70m,
- **SOFT MEASURES:**
  - Nourished sand bar, with shore-parallel structure 500m from shore, 70-m wide, and crest level at mean sea level.
  - Mangrove seeding and planting to reach a 500 m belt
  - Bamboo or melaleuca fences for mangrove erosion control
- **PILOT EXPERIMENT:** we suggest carrying out a pilot experiment with the two methods above, each covering a coast section of about 2 km.

Note: erosion seaward of the breakwater will likely continue as suggested by bathymetric evolution and probable river sediment deficit from the Saigon-Dong Nai river system. Accretion inside the breakwater may also be limited by river sediment flux deficit if no nourishment is proposed. As opposed to the West coast, no monitoring along the Go-Cong coast has been conducted following the implementation of geo-tubes and thus little information is available on existing experiments. Pilot experiments with monitoring should provide more insight on this matter.

### Phu-Tan

The proposed hard measures for Phu-Tan are:

- **HARD MEASURES:** porous or concrete pile breakwater with shore-parallel structures 300m from shore, and crest elevation above the highest water level. It can be composed of sections 600m wide with gaps of 70m.
- **SOFT MEASURES:** a combination of:
  - Nourished sand bar, with shore-parallel structure 500m from shore, 70-m wide, and crest level at mean sea level.
  - Mangrove seeding and planting to reach a 500 m belt
  - Bamboo or melaleuca fences for mangrove erosion control



Note: erosion seaward of the breakwater may be mild as suggested by bathymetric evolution and expected under relatively low-energy conditions (waves, tides) and sediment supply from around the peninsula. We may expect toe erosion for breakwaters on the other hand, while sandbars should adjust to wave forcing (according to flume experiment and models). Surrounding areas should not be dramatically altered as suggested by model results.

### ADVANTAGES/DISADVANTAGES

		Advantages	Disadvantages
<b>Phu-Tan</b>	<b>Breakwater</b>	Proved efficient (U-Minh)	No natural mangrove regeneration (U-Minh)
	<b>Sandbar</b>	Efficient in models Environment friendly	No hindsight (refer to Indonesian project)
	<b>Wood fences</b>	Proved efficient (Kien Giang) Adapted to low-energy conditions Environment friendly	Short lifespan
<b>Go-Cong</b>	<b>Breakwater</b>		No hindsight
	<b>Sandbar</b>	No scouring Nourishment	No hindsight May be less efficient inside structure

### COST ESTIMATION

Protection type	Cost (\$/m)	Lifespan	Damage
Breakwater	800	30-50 yr	Unknown
Sandbar	500	10 yr	15-20% /yr
Bamboo fences	50	2 yr	50% /yr

Existing breakwaters in Phu-Tan cost \$700-800/m. This is estimation as no local example is available. Note that for concrete breakwater on soft ground, foundation needs to be addressed (e.g., geotextile filter mat is needed in case of thick soft mud layer; for a thin layer, mud should be removed to expose the sand layer). The maintenance cost then needs to be assessed and will depend on breakwater type, logistical and environmental parameters (extreme wave energy). Existing hard structures are too recent for feedback on longevity, but concrete breakwaters have a usual life expectancy of 30-50 years (evidence of geo-tubes alterations in Go-Cong is to be considered). Damages and their cost are unknown so is dismantling cost.

The cost of initial implementation of breakwaters and sandbars is not expected to be largely different. At about \$4/m<sup>3</sup> of sandbar, the cost is estimated at \$500/m for a 70m wide bar but \$800/m for a 120m wide bar (180 m<sup>3</sup>/m). We estimated a lost rate of 15% (at Phu-Tan) and 20% (at Go-Cong), based on physical and numerical modeling. Impact on local geomorphology and ecology is unknown.

From existing experiments, the cost of **wood fences** is given at \$50/m, i.e., more than 10 times cheaper than the implementation of hard measures. However, wood fences need regular maintenance, as their life span is about 2 years and damages are about 50%/yr. Because they are set in accessible shallow water and material is low cost, wood fences remain cost-effective and environment friendly.

### Summary of recommended protections

	Options	Measures	Crest level (m)	Width (m)	Distance from shore (m)	Unit Length (m)	Gap between units (m)	Initial Cost (\$/m)	Damage (%/year)
<b>Phu-Tan</b>	1	Sandbars L=7km; V= 0.7 Mm <sup>3</sup>	0	70	500	1000	200	500	15
		T-fences (GIZ type)	Scale of fences are smaller than GIZ's					50	50
	2	Porous breakwaters	1.1	N/A	300	600	70	N/A	N/A
		T-fences (GIZ type)	Scale of fences are smaller than GIZ's					50	50
	3	Concrete pile breakwater porosity >=20%	1.1	N/A	300	600	70	N/A	N/A
		T fences (GIZ type)	Fence scale smaller than GIZ's					50	50
<b>Go-Cong</b>	1	Sandbars L=15.5km V= 2.56 Mm <sup>3</sup>	0	70	500	1000	200	800	20
		T fences (GIZ type)	Fence scale smaller than GIZ's					50	50
	2	Porous breakwaters	2.2	N/A	300	600	70	N/A	N/A
		T-fences (GIZ type)	Fence scale smaller than GIZ's					50	50

### Porous fences and mangrove restoration

Porous breakwaters were successfully implemented in U-minh with the observed deposition rate of about 40 cm/y. Similarly, bamboo/melaleuca fences, which are porous barriers, can increase accumulation as shown in recent studies (order of 15 cm/y in Kien Giang; Cuong et al. 2015). The calm conditions provided by these fences can promote flocculation, and also increase settling by scour lag (e.g., more deposition during flood than entrainment and export during ebb tides). Importantly, where implementing concrete breakwaters can be cumbersome and expensive, soft fences are set in shallow water and thus cost effective and relatively easy to implement and environment friendly.



Example of soft structures: mangroves planting protected by wood/bamboo fences in Ca Mau

Our investigation underlines the variable nature of shoreline changes, often advancing and retreating from year to year or on longer cycles. Soft measures can more easily be adapted to this variability. During an erosive phase, soft fences and mangroves can suffer damages and retreat but remain sources of damping, then be rebuilt and prepare a more favorable phase. Therefore, for cost effectiveness and consistency with intrinsic morphodynamics, soft measure is recommended as a complement to hard measures if erosion is dramatic.

In addition, our investigation on mangrove restoration shows that breakwaters at U-minh did not permit natural mangrove regeneration despite large sediment accumulation rates, while wood fences in Kien Giang proved effective. Our explanation is that concrete pile breakwaters were not porous enough to allow seedling transport to muddy shores while wood fences were more permeable. The addition of gaps in breakwater might remedy this problem to some extent. If not, seeding or planting is recommended immediately after accumulation. It is recommended to use root control bag raised seedlings for transplantation to ensure high survival rate and shorten maturation time. In doing so, exposition time is an important factor. Optimal conditions for seed trapping and colonization are around or below the max height water level (MHWL). Lessons learnt from French Guiana by our team members are that only few good temporal windows are present each year, depending on topography and tides.

Our study of existing mangrove species around the LMDCZ, successful restoration and environmental conditions (salinity, tides, soil chemistry, sediment type) led to the recommendation of mangrove species in study sites. In Go-Cong, we selected *Avicennia marina* as pioneer belt, with *Rhizophora apiculata* planted behind. In Phu-Tan, *Avicennia marina* was selected.

Site	Salinity	Tidal range	Altitude	Recommended Species
Go-Cong	15-26	3.5 m	-0.5 to +0.7 m	<b>Avicennia marina &amp; Rhizophora apiculata</b>
Phu-Tan	25-30	1.5 m	0.2 tot 1.5 m	<b>Avicennia marina</b>

### Note on capacity building

Besides the scientific objectives of the project, building capacity for continuation of the initiated studies and for conducting similar future projects is one of our targets. The knowledge and technology transfer to Vietnamese colleagues (particularly in field surveys, data analyses and physical/numerical modeling) have taken place through a very close collaboration over the entire duration of the project. This will have positive impacts beyond the project. The outcome of the video camera survey (WP3) was not as successful as initially expected due to contractual, logistic and technical difficulties, resulting in a short period for the data collected; however, the survey can be considered as a success for capacity building (in installing, operating, data collection/processing and image analysis), thus building a good starting base for long term monitoring. A major weakness for LMD studies is lack of consistent monitoring and this is particularly true for the coastal zone.

As for capacity building, the project also contributes to the scientific basis for Integrated Coastal Zone Management (ICZM). Important contributions are expected with respect to the methodologies in numerical studies (e.g. regional to local modeling, calibration and validation using in-situ measurements and remote sensing) and to the techniques for field surveys and data/image analysis. Another contribution is the actual results. These have generally contributed to generate substantially new knowledge on erosion mechanisms: the role of river flux, coastal redistribution, and mangrove squeeze, in comparison with expected relative sea level variations. Geographically, the respective coastal zone of influence of the Mekong and Saigon-Dong Nai river systems were demonstrated and quantified for the first time, with implications for erosion and coastal management. At local scales for accretion mechanisms, our results reveal the role of cross-shore transports in shallow mud coast environments, and the efficiency of combined waves, tides and winds when protection is given there. They contradict the use of classical littoral transport paradigm for understanding and devising protection measures in the LMDCZ and offer new ones.

### Further suggestions

The objectives of this project specifically aimed at dynamical coastal processes that have a direct impact on shoreline changes. The global impact of relative sea level variations was not considered apart from what is known from the literature. Relative sea level change processes, especially anthropogenic land subsidence, can affect the delta plain as well as the coastal zone and increase flood risk, especially if less sediment loads are deposited on the plain. Expanding coastal studies to including relative sea level changes may be considered as a logical continuation of this project. Other aspects that should be pursued further concern inter-annual to multi-decadal variability, including natural drivers from storms to El Nino/La Nina oscillations, and long-term evolution of the coastal zone. Simpler bulk models may be used for long-term assessment or/and use of morphological acceleration procedures in 2D or 3D models.

Continuing research projects will be required for a sustainable protection against coastal erosion and an ICZM (Integrative Coastal Zone Management) in the LMD. They should rely on:

1. Development of an integrated monitoring program: bathymetry/topography using different techniques to cover the entire subaerial/subaqueous coastal and estuary zones. This should also include river bed/bank erosion and subsequent river morphology changes, which together with information on land use and human interventions, will contribute to a better quantification of the drivers of sediment budget in the LMD coast. Including the monitoring of biotic components of the delta ecosystems may also be required for sustainable management of the LMDCZ.
2. Development of an integrated database: building an organized, accessible and continuously maintained LMDCZ database with quality control is of primary importance in order to make use of large amount of data generated in the numerous studies from different actors, national and international institutions.

## Summary reports of work packages



Chapter 1 Observing the evolution of shorelines, river fluxes and coastal waters (WP1 & WP3)

Part 1 Satellite sensing of shoreline changes (WP3)

Part 2 Mekong river sediment flux (WP3)

Part 3 Coastal video-camera monitoring (WP3)

Part 4 In-situ measurements (WP1)

Chapter 2 Regional sediment budget from 3D models (WP2)

Chapter 3 Local hydrodynamics and sediment dynamics (WP4- WP5)

Part 1 Local wave climate (WP4)

Part 2 Regional to local hydrodynamics (WP4)

Part 3 Local sediment dynamics (WP5)

Chapter 4 Protection measures from coastal erosion (WP6)

Communications

References

## Chapter 1

### Observing the evolution of shorelines, river fluxes and coastal waters (WP1 & WP3)

We start here with the satellite observation of shoreline changes (WP3), as it is the best way of introducing and objectifying our present knowledge of coastal erosion in the LMDCZ. Then we proceed to estimate the total Mekong river sediment discharge into coastal waters and, if possible, its trend over the last years and decades. Finally, we report on the project's coastal surveys.

## Part 1

### Remote sensing of shoreline changes

Anthony et al. (2015) presented a first synthetic analysis of erosion/accretion along the whole LMDCZ (over 600 km of coast). Graphs of shoreline (m/year) and coastal area (km<sup>2</sup>/year) change rates between 2003 and 2012 were analyzed from high-resolution SPOT 5 satellite images. Phan et al. (2017) reproduced this exercise recently for the period of 1973-2015 from Landsat images. In the same time, in the course of this project, SIWRR conducted its own investigation for the period 1990-2015, using a combination of Google Earth images, SPOT images and in-situ observations. The three studies show local differences but similar patterns of erosion/accretion at regional scale. These are the same patterns predicted by our regional model (see WP2). The good comparison between all these outcomes reveal a strong indication of a natural large-scale redistribution process in the LMDCZ. However, at local scales, in Go-Cong and U-Minh for example, discrepancies suggest other processes: deficit of river supply, coastal squeeze, and subsidence, etc.

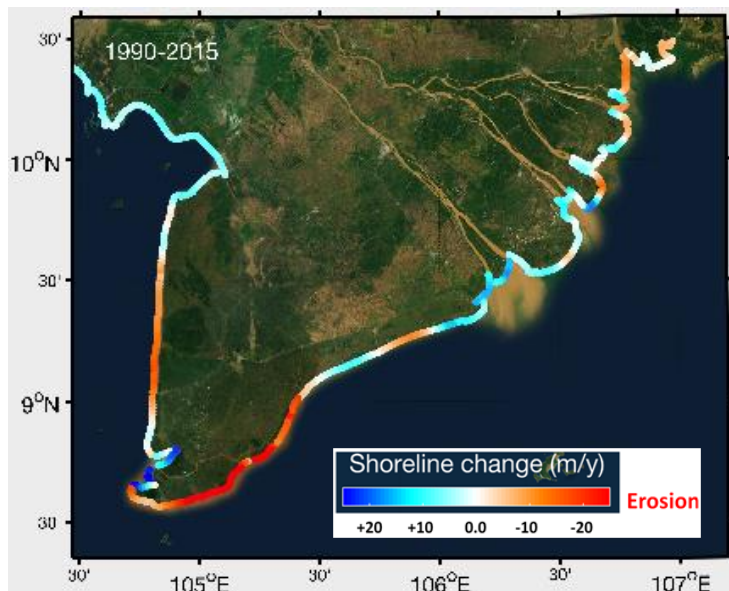


Figure 1: Map of shoreline change rates in m/y estimated from satellite images from 1990-2015. Red/blue colors are erosive/accretive shores. Local variations were filtered to improve readability and highlight subregional variations

Figure 1 shows shoreline change rates (erosion in red and accretion in blue) for the period 1990-2015. The first observation of this result is that the coastline is not in a state of general erosion as sometimes suggested by local knowledge. There is mean erosion over the whole coast of only 0.6m for a standard deviation of  $\pm 10$ m. The mean value is below uncertainty range of observations. As an illustration, Phan et al. (2017) found small accretion in average over the period 1973-2015. Therefore, the global rate of the system is uncertain. The evolution of this global rate is also fluctuating. Figure 2 shows the global rates of the system by periods of 5 years since 1990. Not only the global rates are low (less than 5m/y) but they are also fluctuating without any clear trend, although the last 10 years indicate erosion while the previous 16 years were accretive.

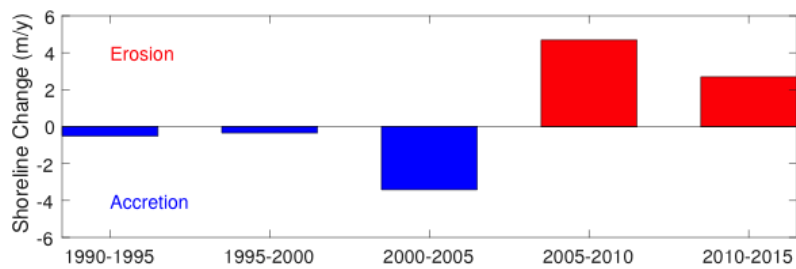


Figure 2: LMD CZ global rates of shoreline change (m/y) by periods of 5 years since 1990.

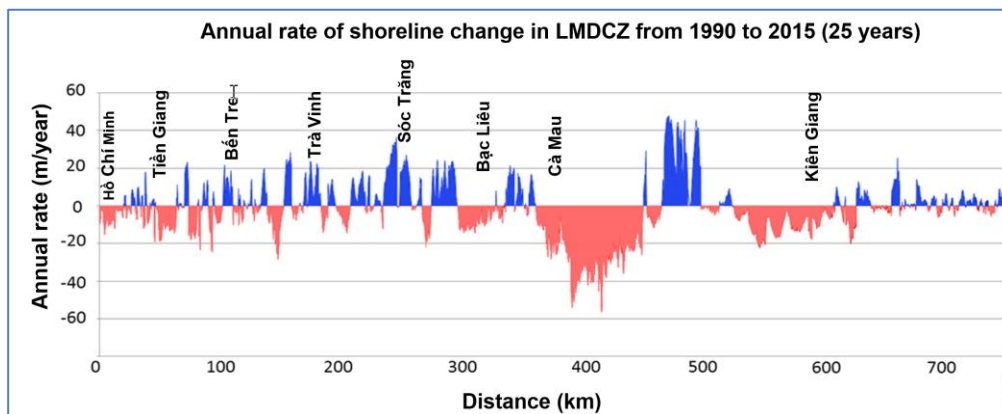


Figure 3: Average annual shoreline change rates (m/y) along the 700 km of LMD CZ from 1990 to 2015. It shows the main subregions of LMD CZ: estuary area, East coast and West coast.

More importantly maybe, there are large subregional variations in the LMD CZ system (*Figure 1* and *Figure 3*). These are morpho-dynamically consistent coastal areas:

- **Estuary area:** from Vung Tau to Soc Trang, with large local variations but mostly accreting. On the other hand, Go-Cong (Tien Giang) at the extremity of the estuary zone has experienced consistent erosion in the last decades, but Go-Cong is under the influence of the Saigon-Dong-Nai, not the Mekong River.
- **Eastern coast:** from Soc Trang to Ca Mau, presents the largest erosion
- **Western tip of peninsula:** presents the largest accretion
- **Western coast:** from Ca Mau to Kien Giang, with increasing erosion
- **Northwestern coast:** from Kien Giang north is mostly accreting although local erosion problems were experienced there.

The largest subregional erosion is on the southern shores of Ca Mau (30-50 m/yr), but the largest accretion zone is just downstream along the western peninsula's tip (30-80 m/yr). The regional area surrounding the peninsula's tip is therefore an important area of erosion and accretion that seems to be connected and interdependent. The estuary area is marked by large local variations (*Figure 3*).

Local spatial fluctuations in the estuary area are also associated with temporal fluctuations. *Figure 4* presents a map of a number of fluctuations (switching between erosion and accretion, or vice versa, from one period of time to another) during the five periods of 5-year interval between 1990-2015. Yellow areas are either constantly eroding or accreting during the 25-year period. We see that the estuary area is a subregion of largest local fluctuations, sometimes eroding, sometimes accreting but globally prone to accreting. The peninsula is more consistent.

The West coast and part of the East coast show fluctuations but there are large areas of consistent change rates around the peninsula's tip (with erosion on the East coast and accretion on the other side). The other consistent area of change rates is the Go-Cong coast. Comparison with our model results suggest that the peninsula has experienced strong natural redistribution, while Go-Cong has a deficit of sediment river supply from the Saigon-Dong Nai River.

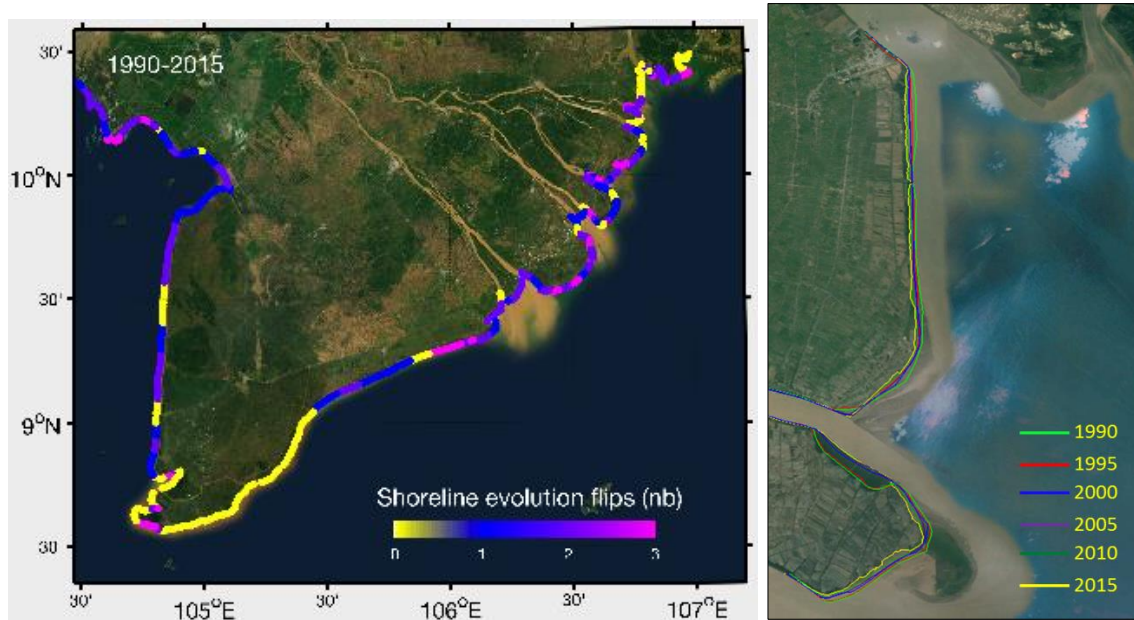


Figure 4: left: number of fluctuations of erosion/accretion (change of sign of change rates) during the five 5-year periods between 1990-2015. Right: shoreline evolution for Go-Cong where erosion has been consistent from decades, contrasting with the much more fluctuating estuary area.

## Part 2

### Mekong river sediment flux

Weathering and mechanical erosion, which constrain the transport of sediment and associated elements (e.g. trace elements, organic matter) from the continent to the ocean, are attributed to a combination of natural processes related to geomorphology, tectonic activity, and climate influences as well as land cover (e.g., Milliman and Mead, 1983). Additionally, human disturbance may affect erosion and sediment supply to estuaries, deltas or coastal zones. Therefore, in recent years, there has been increasing concern about the global river sediment balance, particularly with respect to its response to climate change and anthropogenic impacts (e.g., Syvitski et al., 2005). However, important uncertainties persist, mainly due to the non-stationary nature of sediment fluxes and the use of dated and/or questionable data (short-term sampling, inappropriate sampling frequency and/or data collected before dam/reservoir construction, deforestation or climate changes; see Walling, 2006).

The rivers draining the Himalaya Mountains into Southeast Asia are recognized as significantly contributing to suspending particulate matter (SPM) delivery to the global ocean (Milliman and Meade, 1983). In this key area, recent and rapid changes in population and economic growth have strongly affected the functioning of the river-systems leading to major human pressure on its sustainable development. Therefore, South-East Asian Rivers are good indicators of the strong influence of anthropogenic activities on suspended sediment transport. For example, in Taiwan, the fluvial sediment load in the Lanyang His River System has more than doubled during the last three decades due to road construction. In contrast, the sediment flux of Chinese rivers has declined with the construction of large reservoirs (Yellow, Changjiang, Yangtze rivers). However, available estimates of particle delivery to the oceans are often derived from “average” values (e.g. monthly values) and datasets of inadequately documented rivers. The general poor reliability is high variability of water and solid discharges, which would require continually updating fluvial data. Therefore, **predicting the change of sediment fluxes in Southeast Asia represents a major challenge for environmental sciences, especially considering the complexity and nonlinear interaction between natural and anthropogenic impacts.**

Originating from the Tibetan plateau, the Mekong River is the largest river basin in Southeast Asia, and is shared by six riparian countries: China, Myanmar, Laos, Thailand, Cambodia, and Vietnam (*Figure 5*). In recent years, the basin has faced rapid development related to water resources management, including various hydropower plans and large irrigation schemes (King et al., 2007). Reservoir operation and climate change are considered among the most influential drivers of future hydrological change in the Mekong, but other drivers are potentially as important, i.e., land cover change, new irrigation and water diversion schemes, and urbanization (Keskinen et al., 2010). The impact of reservoir operation on the Mekong basin was extensively studied<sup>4</sup>. Although reservoirs in the upper Mekong basin have trapped most of the sediment from the upper reaches, little information is available on the impact of dams on sediment load

<sup>4</sup> The Mekong River Commission (MRC), the Asian Development Bank (ADB), the United Nations Education Scientific and Cultural Organization (UNESCO), the National Natural Science Foundation of China (NNSFC), the World Wild Fund (WWF), the US National Science Foundation (NSF) and the Office of Naval Research (ONR).



in the lower Mekong basin (especially in the Mekong Delta) and on the sediment flux by the Mekong River to the sea. In addition, most analyses were based on “recycled” database and/or used inadequate sampling frequencies, including monthly to weekly sampling. The serious lack of long-term, accurate sediment data in the Mekong River critically undermines our knowledge of sediment flux into the estuary (e.g., Walling, 2008).

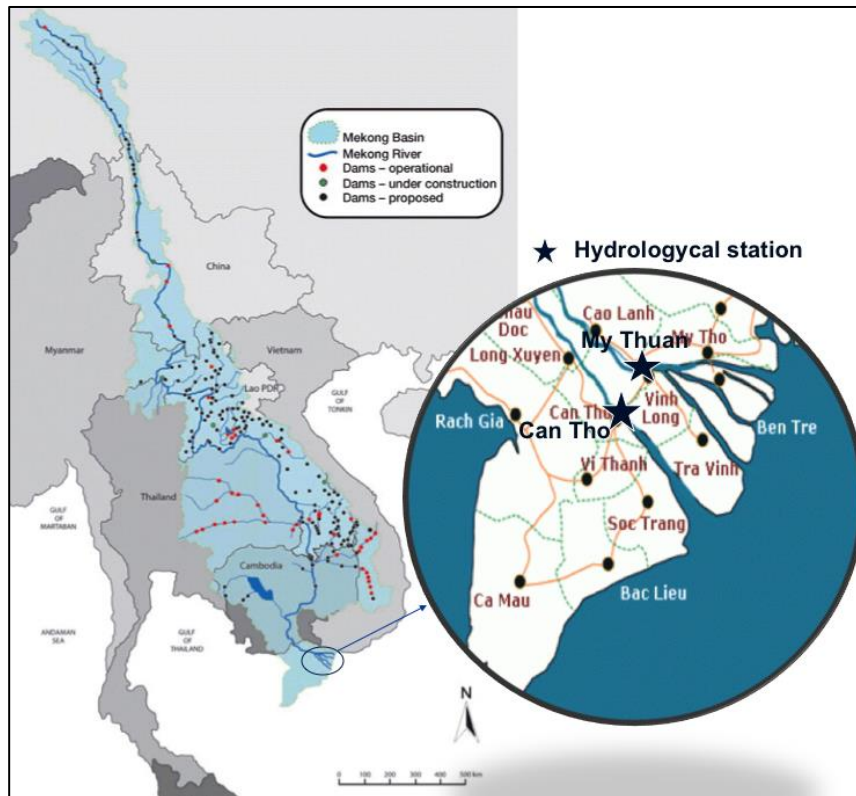


Figure 5: Hydrological network of the Mekong River Basin. Mekong River originates from the Tibetan plateau and flows through a narrow deep gorge. The Mekong River then flows through Myanmar, Lao PDR, Thailand, and Cambodia before it finally drains into the sea creating a large delta in Viet Nam covering a total drainage area of 795,000 km<sup>2</sup>. Hydropower represents a key activity in the Mekong River basin, particularly in China and Lao PDR. About 73 projects in the lower part are operating and 29 projects are under construction.

In the present project, we use an extensive dataset of hourly water discharges and twice-daily suspended sediment concentrations (SSC) collected between 2009 and 2016 at two strategic sites: Can Tho and My Thuan gauging stations<sup>5</sup>. My Thuan and Can Tho stations quantify the discharges of the two main distributaries of the Mekong River: Tien and Hau Rivers (Mekong and Bassac), after flowing through the Plain of Reeds and Long Xuyen Quadrant, including water distribution through main irrigation channels of these regions. These stations, located about 100km from the ocean, are also influenced by sea tides. Sediment concentrations were collected twice per day (during ebb tide and flood tide) according to the Vietnamese national standard. The water discharges were estimated from hourly measurements of river stage and a stage-discharge rating curve regularly checked and updated. The sediment flux was then estimated from water discharge and sediment concentrations. Note that before 2009, no regular

<sup>5</sup> The data was supplied by the Vietnam Institute of Meteorology, Hydrology and Environment (IMHEN).

accurate data on water discharge and sediment concentration was available on the lower Mekong River (including Thailand, Cambodia and Vietnam areas).

### Mean discharge of the lower Mekong River

Based on the high resolution database of water discharge and sediment concentrations from the 8-year monitoring period (2009-2016), the annual water discharge and sediment flux of the Mekong River at Can Tho and My Thuan stations were calculated and are presented in *Table 1* and *Figure 6*.

Year	CanTho station		MyThuan station	
	Annual Flux (Mt/yr)	Q annual (m <sup>3</sup> /s)	Annual Flux (Mt/yr)	Q annual (m <sup>3</sup> /s)
2009	37.4	6381	40.7	6948
2010	11.1	4929	14.7	5410
2011	32.2	7660	53.6	8572
2012	12.5	5774	17.3	6363
2013	15.0	6582	23.7	6888
2014	16.4	6482	22.7	6791
2015	8.4	4347	9.1	4737
2016	8.5	5151	13.6	5645
<b>Max</b>	37.4	7660	53.6	8572
<b>Min</b>	8.4	4347	9.1	4737
<b>Average</b>	17.7	5913	24.4	6419

Table 1: Annual water discharge and sediment flux at Can Tho and My Thuan stations during the 2009-2016 period

The results show high variability of annual sediment fluxes in the two distributaries. For Can Tho station, the annual sediment fluxes ranged from 8.4 (in 2015) to 37.4 Mt/yr (in 2009) around the average value of 17.7 Mt/yr. For My Thuan station, fluxes ranged from 9.1 (in 2015) to 53.6 Mt/yr (in 2011) around the average value of 24.4 Mt/yr. The annual water discharges and sediment fluxes at Can Tho and My Thuan show a similar temporal evolution (Figure 2).

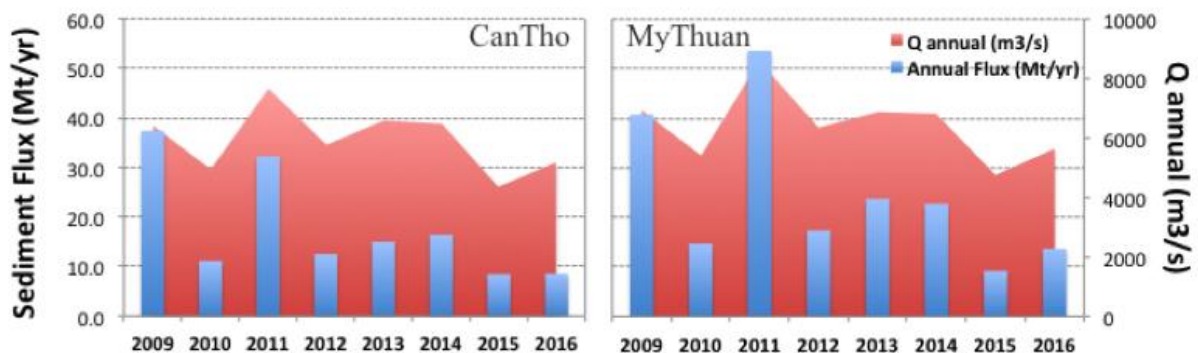


Figure 6: Evolution of annual water discharge (Q-m<sup>3</sup>/s) and sediment flux (Mt/yr) of the Mekong River at Can Tho and My Thuan stations from 2009 to 2016.

Considering that the sum of sediment fluxes at both Can Tho and My Thuan stations represents the sediment flux by the Mekong River to the lower delta, we observed that **the sediment flux transported by the Mekong River varied strongly between 18 and 86 Mt/yr with an average value of about 42 Mt/yr during the study period.** This value is similar to estimations at Chau Doc and Tan Chau stations (a bit further upstream) of about 45 Mt/yr by Nguyen et al. (2017; report in Vietnamese), based on daily measurement of water discharge and sediment concentrations during 2008-2016. The specific sediment yield of the whole Mekong River watershed was estimated for the same period at 53 t/km<sup>2</sup>/yr.

### The role of regional climate

Although eight years of observation cannot be considered a "long-term survey", the dataset covered various hydrological conditions. Using water discharges on the same locations for the period 2000-2008, combined with the data used in the present study (*Figure 7*), we show that maximum and minimum water discharges occurred in 2011 and 2015 (i.e., during our survey period). These extremes are clearly associated with historic **La Nina and El Nino events** in the region, which set conditions for extreme wet and dry seasons respectively (2015 saw one of the strongest El Nino event with severe dry conditions in Southeast Asia). Hydrological conditions are also strongly correlated with annual sediment fluxes. At both gauging stations, extreme annual sediment flux values (highest and lowest) were coincident with extremes of annual water discharge and mostly consistent with occurrences of ENSO phases. High correlations (> 0.8) for annual and even monthly averages confirmed **the dominant role of hydrological conditions on sediment input to the Mekong River.**

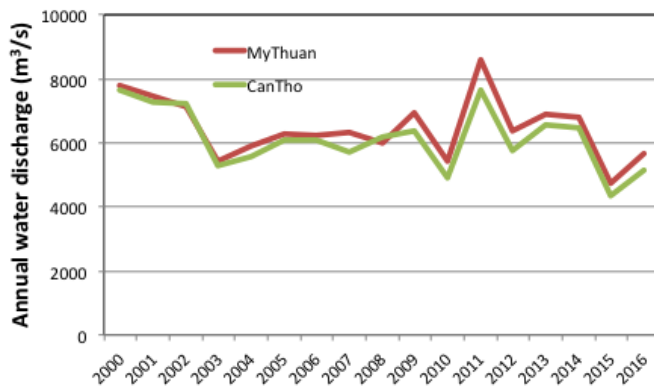


Figure 7: Variation of annual water discharge measured at Can Tho and My Thuan stations during 2000-2016. [2000-2008: data from Koehnken (2014) based on daily water discharge; 2009-2016: this study]

### The role of hydropower plants

During the study period (2009-2016), several big hydropower dams started operating in the upper Mekong river basin (e.g., the Xiaowan Dam in 2010, the Jinghong Dam in 2011 and the Nuozhadu Dam in 2015). However, contrarily to regional climate variability, no clear inflection was observed on our data in so-called double-mass plots, indicating no or weak direct impact of these new dams in the lower Mekong delta. A similar observation in dam impact was shown in other studies (e.g. Wang et al., 2011). For example, Wang et al. (2011) showed that sediment load at station Mukdahan in Laos did not decrease after the completion of the Manwan Reservoir in 1993, but instead increased by ~50%. **This increase of sediment concentration (also seen in other studies) can be explained by multiple causes: land-use changes and a**

**general intensification of human disturbance in the lower Mekong basin during the last 20 years; river bed-bank erosion due to imbalance between sediment transport and sediment trapped in the reservoir (the process termed “hungry waters” by Kondolf, 1997); and sand mining.** More generally, our combination of available published data for the pre-dam and post-dam period shows a complex spatial and temporal pattern. Nevertheless, **our estimation of sediment flux in the lower Mekong River is on the lower end of previous estimates (about 90-160 Mt/yr). Whether it is the expression of a real trend or a bias due to the low temporal resolution of historical studies, it is uncertain to say from the data alone.** In order to evaluate precisely the effect of sediment trapping in the new reservoirs, a long-term observation (> 10 years) is needed. The dataset started in 2009 in various locations is a step in that direction.

### Conclusion

Based on high temporal resolution (hourly/twice-daily frequency) of water discharge and suspended sediment concentration at Can Tho and My Thuan stations during 2009-2016, we observed that the annual Mekong sediment flux at these strategic sites strongly varied and was closely correlated with hydrological and regional climate conditions (specifically, ENSO). Considering that the total sediment flux of both stations represents the sediment input to the ocean by the Mekong River, we estimated this input to be ~42 Mt/yr. This value is much lower than that estimated during pre-dam periods (before 2003: 90-160 Mt/yr). However, the accuracy of previous studies is weakened by the scarcity and low frequency of data collected before 2009. In addition, we did not find any correlations with new dam construction in the 2009-2016 data (consistent with other recent studies). The sediment load in the lower Mekong basin may be already affected by trapping of sediment in upstream reservoirs but it may also be resilient (hungry waters) or affected by various other anthropogenic activities, such as sand exploitation, reforestation and soil-conservation. However, continuous, long-term, high-resolution monitoring must validate our assumptions and current results.



## Part 3

### Coastal video-camera monitoring

Installation of video cameras was a challenge. The first step was capacity building and training of a Vietnamese SIWRR team with no previous experience with video cameras and their image processing. For installation, the challenge was lack of coastal structure and logistic (power, internet, permit), as opposed to previous installations in Vietnam (e.g., Nha Trang and Hoi An). The solution was to use solar panels for energy and store data locally rather than sending images through Internet. This was conducted for Go-Cong, but not for Ca Mau, even less accessible. Analysis was performed based on a few months of collected data available now. Clearly, this part of the project is related to capacity building on one hand, and setting the bases of longer term monitoring on the other hand. Nevertheless, interesting results are already at hand.

### Implementation

Installation of 4 cameras on 2 sites at Go-Cong was undertaken during one-day field trip on May 30 2017 (*Figure 8*). Poles were implemented with solar panels and connection boxes fixed 3 meters from the ground. The calibration of the cameras consists of finding the optical distortion parameters inherent to all lenses. Those parameters, called intrinsic parameters, are unique for each camera and crucial for proper image rectification. Fortunately, these parameters are fixed and can be evaluated before installation (at SIWRR premises). The calibration step is absolutely necessary for this type of camera. The level of distortion can be appreciated by looking at the horizon line on original and corrected pictures.



Figure 8: Installation of video cameras at Go-Cong on two poles each hosting 2 cameras

Then, the rectification process or geolocalisation consist in mapping each pixel of the picture taken from a camera to a geographic position. For this we determined the extrinsic parameters of the camera, i.e., the camera position file (*Figure 9*).



Figure 9: Camera image calibration and rectification. Original (left) and corrected images (right): the horizon line forms a circle arc in the original image and a straight line on the corrected image. On the original image, all ground control points are shown with their respective projection in pixel space. A 3-axe reference frame is drawn on each point to check consistency of geographical reference system.

The next step of the setup consists in defining the zone of interest or the Region Of Interest (ROI). There are several reasons for defining a specific region. First, the rectification is only valid to a central part of the image (and resolution is coarsening far from the camera). Secondly, as much land as possible needs to be removed to optimize the detection of light structures on the sea. Finally, image processing requires large computing resources and computing time will also be shorter if we only treat a specific region of images.

In order to analyze coastline variations from the video system, we must first process secondary images. Four types of secondary images are produced. The first one is a 10-min average of all frames. This allows us to remove high frequency signals (wave propagation). Coastline and sandbar location (where waves are breaking) can be determined from these average pictures. In another type of image analysis, we extract a line of pixels in each frame and stack them together. This forms a picture, which is the size of pixel length in one direction, and of the number of frames in the other. When swell is dominant, the wave crest is easily detected from cross-shore stacks.

## Shoreline changes

Shoreline detection methods are usually based on image color properties. On sandy beach environment (where video cameras are traditionally used), shoreline detection rely on the color difference between sand (high value of red color) and sea (high value of blue or green). However, one should be noted that Go-Cong is a mixed sand-mud environment. In addition, the shore's upper limit is protected by concrete (grey) while the water is charged with small sediments, which gives a brown color. As classical methods would not fail in such condition, we implemented a new indicator based on light intensity and its gradient. That probably makes the first method adapted to delta systems. However, another limitation is that most of the detected shoreline here is along the concrete dike, while lines detected at low tides are of coarser resolution. Therefore, averaging over longer periods, i.e., monthly, would improve accuracy on the budget analysis of the intertidal zone. As the video system is now up and running, it will prove a useful monitoring tool and provide accurate shoreline changes.



Figure 10: Low tide in Go-Cong on June 6 (left) and September 1 (middle). Right: shorelines during June 1.

The results reported here are for the monitoring period from June 1 to September 3 2017 (summer monsoon), and only on one set of camera S1, as it has the longest dataset. Only parts of the video data were collected so there are gaps or missing data for some weeks. Overall, a total of 7 weeks of S1 video data was transferred. From the available recorded video, no swell was detected, as this summer monsoon season was of very calm conditions with no extreme weather in the Go-Cong area.

**No significant shoreline change was detected either from these images, which suggests that no significant accumulation of sediment occurred during summer 2017. The capacity of sediment supply by the Soai Rap River is questionable (Figure 9).**

### Wave period

During 2017 summer monsoon, no important swell was detected and characterization of wave dynamics from stack images is more limited in this case. Yet, wave period was evaluated and the daily average wave period was found in the 5-7 sec range over the 3-month monitoring period (Figure 11).

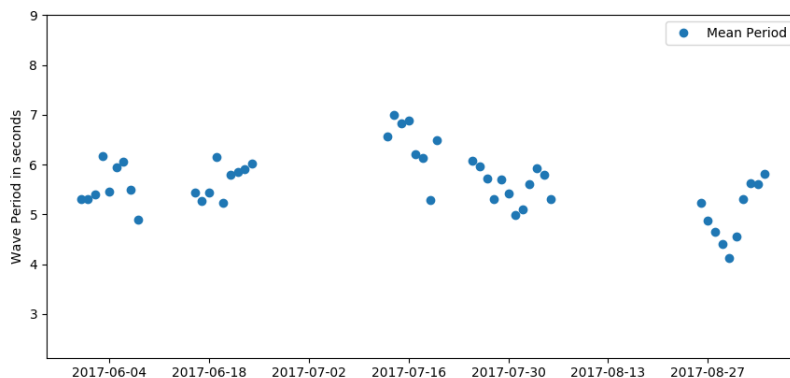


Figure 11: Daily mean wave period computed over the entire monitoring period.

### Wave height and bathymetry profile from swash detection

Swash is the layer of water that washes up on the beach after an incoming wave has broken. Swash is tightly coupled with the beach slope and wave height. On the same principles as for coastline detection, we can automatically detect the swash line out of a stack and obtain its varying position and length (distance from the position of bore collapse to the upper limit of



the shore face). By following the swash line during successive tides we can reconstruct a cross-shore profile of the intertidal zone (*Figure 12*).

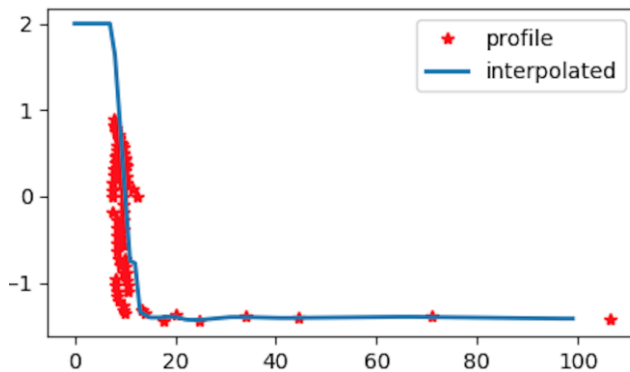


Figure 12: intertidal zone bathymetry profile estimated from swash line detection.

We also computed the swash length from standard deviation of swash line position. The result suffers from coarser resolution when the swash line is farthest from the camera (low tide). Yet, in association with beach slope and wave period, we can use it to inverse the Stockdon parametrization and estimate wave height over the monitoring period of summer monsoon (*Figure 13*). The result confirms small wave height (about 10 cm in average and 30 cm max over the whole period).

### Conclusions from video camera analysis

Not enough data were yet collected to provide a complete description of various expected parameters. In addition, the monitoring period over which this report is based is very low-energy and no change is observed in beach morphology. However, this is a powerful result on its own because accretion would be expected during the wet season if river supply were to be efficient. It underlines the poor supply capacity of the Soai Rap River (the Saigon-Dong Nai river system) at the present time and suggests indication as a probable reason for the observed severe erosion in the Go-Cong area.

As no incoming swell was detected, wave parameters such as wave height and celerity could not be assessed through classical methods, but new methods were devised to estimate the heights of small wind waves. In addition, the observation system is now set up and running in the Go-Cong area and will continue providing data throughout the winter monsoon season to capture seasonal variations of beach and wave parameters. We will be particularly interested in the erosion rate associated with high-energy waves from the northeast monsoon.

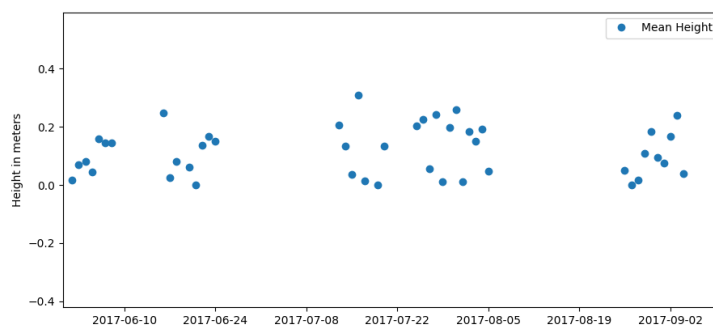


Figure 13: Wave height computed over the entire monitoring period from swash detection.

## Part 4

### In-situ measurements (WP1)

In-situ measurements were primarily conducted for validating and calibrating models and satellite imagery. These data were also compared with published data and the current knowledge gained from previous field observations. In particular, it helped us better assess the erosion effect in the subaqueous delta, which can be compared with the modeling of bed evolution and satellite observation of shoreline changes.

This summary is based on the two field surveys carried out in Oct 2016 and Feb-Mar 2017. The survey data included water level, vertical distribution of current velocity, wave parameters and suspended sediment concentration, collected at two mooring stations (fixed stations) located 12-14km offshore at Go-Cong and U Minh (see *Figure 14* for locations). These mooring stations provided time-series to capture a neap-spring tidal cycle of 15 days during each campaign. During the surveys, “instantaneous” wave and current parameters were measured for a period of 30 min at 183-186 marine sampling stations (Fig.1) using two cruising boats. Water samples of 5 relative depths over the water column and seabed sediment samples were collected at these locations for analysis of salinity, suspended sediment concentration, and grain-size distribution.

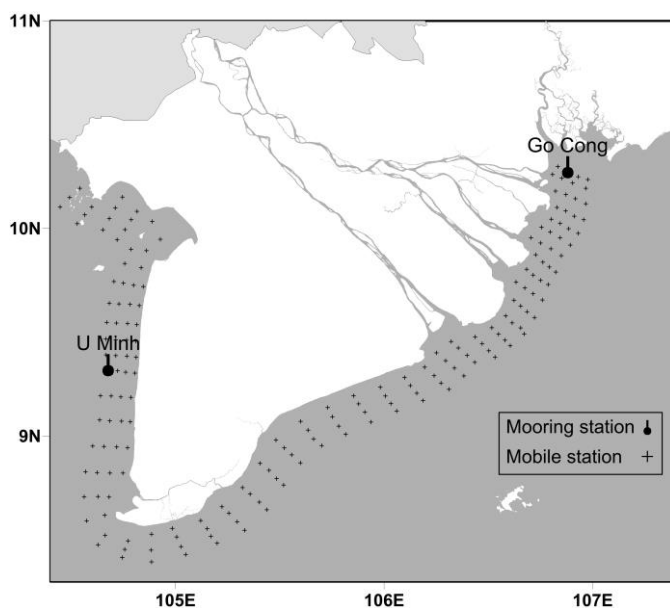


Figure 14: Map showing the locations of two mooring stations at Go-Cong and U Minh and 186 mobile stations along the east and the west seas.

### Hydrodynamics

Time series data of water level, current velocity and wave at the mooring stations at Go-Cong and U Minh are summarized in Tab. 1. Water level fluctuations at Go-Cong are typical mixed, mainly semi-diurnal tides with higher tidal ranges in Oct 2016 than in Feb-Mar 2017 (Tab. 1). Maximum tidal ranges were about 3.7 m in Oct and 2.8 m in Feb-Mar. Water level variations in Go-Cong show a change of tidal regime between the two surveys. In Oct 2016, the tide is mixed, mainly semi-diurnal while in Feb-Mar, the tide is mixed, mainly diurnal. At U-Minh, tidal ranges are generally less than 1 m. There is a not significant difference in tidal range

between the two periods. Maximum tidal ranges are about 0.8 m in Oct 2016 and 0.7 m in Feb-Mar 2017.

Current velocities at both stations Go-Cong and U Minh show that ebb currents are dominant, especially during the first field survey in Oct 2016 (Tab.1). At both stations, current velocities measured in Oct 2016 are higher than velocities observed in Feb-Mar 2017. At Go-Cong in Oct 2016, measured velocities are strong and peaks of ebb currents are usually about 1.5 times higher than those of flood currents. Depth averaged velocities show that maximum ebb and flood currents are about 1.7 m/s and 1 m/s, respectively. In Feb-Mar 2017, ebb current velocities are slightly higher than flood velocities. Maximum ebb and flood velocities during the 15-day period are about 0.8 m/s and 0.7 m/s. At U Minh, current velocities are generally less than 0.5 m/s and ebb currents are dominant, especially during SW monsoon. In Oct 2016, maximum ebb and flood velocities are about 0.6 m/s and 0.3 m/s. During Feb-Mar 2017, max ebb and flood currents are about 0.4 m/s and 0.3 m/s.

*Wave data measured in SW and NE monsoonal season are typical of wave regimes at Go-Cong and U Minh stations. During SW monsoon, the U Minh station was wavier than Go-Cong (*

*Table 2).* Although maximum significant wave heights at U Minh and Go-Cong are about 1.5 m and the 15-day mean significant wave heights (Hs) at U Minh and Go-Cong are about 0.9 m and 0.4 m. During NE monsoon, wave heights at Go-Cong are higher than those at U Minh. At Go-Cong, Hs and Hmax (maximum height in the wave spectrum) are respectively about 1.6 m and 2.3 m; at U Minh they are approximately 0.6 m and 1.0 m. On average, mean Hs values are about 0.8 m at Go-Cong and 0.3 m at U Minh.

Station	Survey period	Tidal range (m)			Depth-mean velocity (m/s)		Hs (m)		Hmax	
		Max	Min	Mean	Max ebb	Max flood	Max	Mean	Max	Mean
Go-Cong	16 Oct - 31 Oct 2016	3.69	1.89	2.58	1.68	1.01	1.5	0.4	2.0	0.6
Go-Cong	25 Feb - 12 Mar 2017	2.84	2.11	2.46	0.84	0.71	1.6	0.8	2.3	1.2
U Minh	17 Oct - 02 Nov 2016	0.83	0.42	0.61	0.64	0.3	1.6	0.9	2.4	1.3
U Minh	25 Feb - 12 Mar 2017	0.70	0.40	0.60	0.37	0.3	0.6	0.3	1.0	0.5

Table 2: Summary of tidal range, current velocity and wave height at the mooring stations Go-Cong and U Minh.

Along the Mekong Delta, short-term wave measurements during Oct 2016 show a prevailing SW direction causing the western side of the Mekong Delta is more directly affected by wave than the eastern side. Wave directions were almost perpendicular to the west coast; whereas in the east coast wave directions were more scattered (*Figure 15* left). Average and maximum significant wave heights were about 0.7 m and 1.2 m for the West Sea and 0.5 m and 1.4 m for the East Sea. Wave data measured in Feb-Mar 2017 indicate strong NE monsoon events with dominant E-NE wave directions in both East and West Seas (*Figure 15*, right). The strongest wave heights were observed at the beginning of the survey in the eastern side off Cua Dai and

Ham Luong river mouths with a maximum significant wave height of 3.2 m. Peaks of wave heights were usually higher than 1 m on both sides of the LMDCZ. On average, significant wave heights were about 0.8 m in the East Sea and 0.5 m in the West Sea. These observations were consistent with climatology (see WP4).

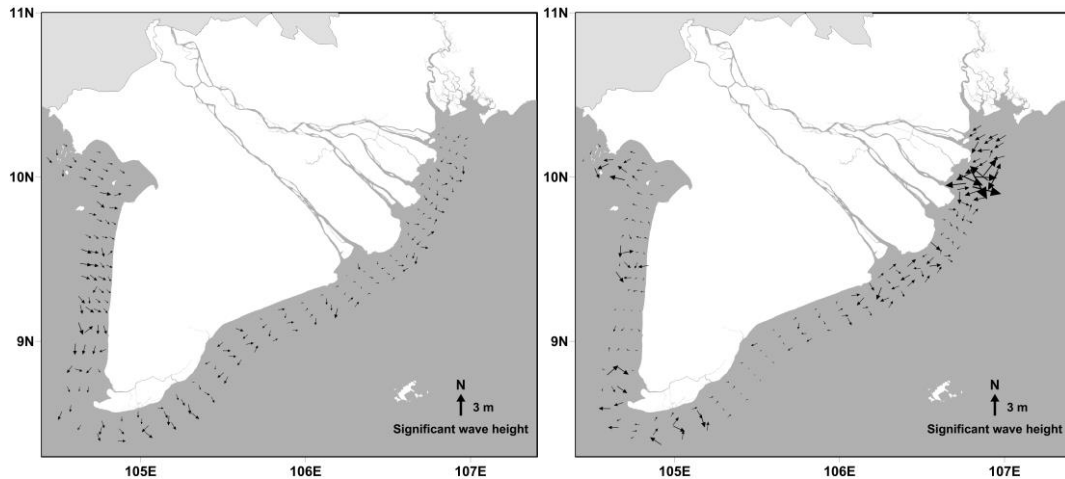


Figure 15: Vectors of significant wave height along the Mekong Delta coast during SW monsoon (left) and NE monsoon (right).

### Sediment grain size distribution

Sediment grain-size distribution along the Mekong Delta is shown in Figure 3. During the wet season (Oct 2016), the clinoform in the estuary zone, from Cua Tieu to Dinh An, was influenced by strong river runoff and fine sediment discharge. Silt was found near the river mouths and on the lower foreset of the estuary zone. Off Dinh An and Bassac river mouths, a range of mixed sediment from fine silt to very fine sand were found, with prevailing coarse silt sediment. Elsewhere in this area, sediments were composed of sand mixture ranging from very fine to medium sand, with fine sand being dominant (*Figure 16*, left). Along the East coast and West coast, south of the Bassac river mouth to Rach Gia, most seabed sediments had fine silt grain-size. There were small areas with fine sand near the cape of Ca Mau in front of Bo De mouth and near Ha Tien.

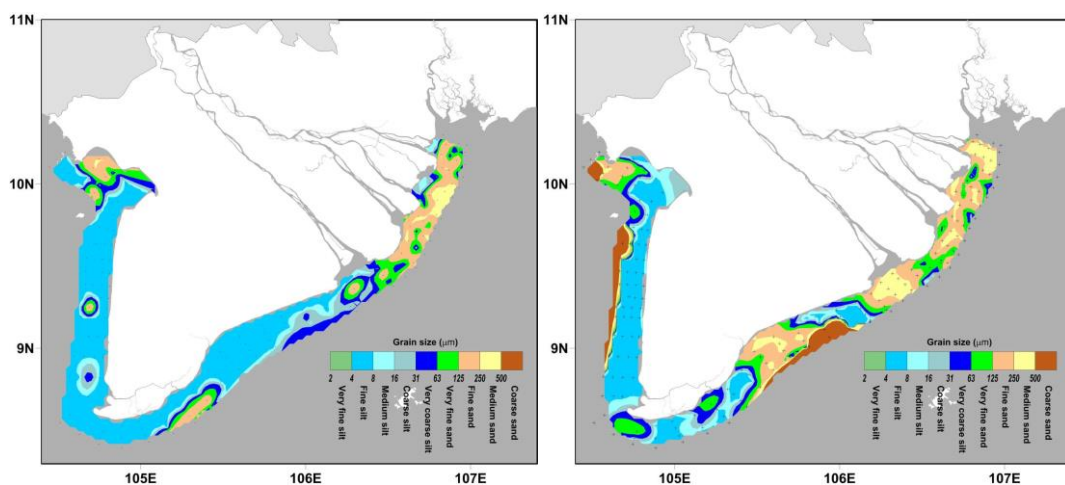


Figure 16: Grain size distributions of sea bed sediment along the Mekong Delta coast, which were collected during SW monsoon (left) and NE monsoon (right).

During the winter monsoon (dry season) in Feb-Mar 2017, the distribution of surface sediments along the LMDCZ changed significantly, especially along the Estuary zone and East coast (Figure 16 right). Along the estuary zone, the fine silt observed in front of the river mouths during the wet season was no longer found during the dry season. In the estuary zone also, coarser sand was observed with grain-size ranging from fine to medium. Along the East coast, a large part of fine-grained sediments (mainly fine silt) detected in the wet season were gone and replaced by coarser sediment. Two small patches of very fine sand were found in front of Bo De mouth and in the cape of Ca Mau. Along the West coast, fine silt remained in the dry season but coarse sand was found at some offshore locations. The origin of this sand patch is unclear but shell fragments in these samples may possibly have affected the grain-size analysis.

This picture of sediment grain-size distribution during winter monsoon shows (as expected) a large influence of waves and currents on sediment mobility along the LMDCZ. After strong NE monsoon events, fine-grained sediment were likely re-suspended and transported southward from the estuary zone along the Ca Mau peninsula. Coarser sediments may also have moved from the estuary zone. The large sand patch located near Bac Lieu is sometimes (in other surveys) found further downstream along southern Ca Mau, which the zone of strongest erosion (see Chapter 1). This suggests transitory movements of mud and sand during intra-seasonal as well as seasonal periods.

### Bathymetry Survey

A bathymetry survey was conducted in the study sites of Go-Cong and Phu-Tan district areas. Bathymetry was measured across the subaqueous delta, from the prodelta to the nearshore region, but was limited to a maximum depth of 2 m; shallower waters were not accessible by boat (Figure 17 and Figure 18). Bathymetry profiles were compared with previous bathymetry surveys by MONRE (over a decade ago), which gave us a measure of erosion, as seen on the subaqueous delta rather than the shoreline (two strongly connected regions; Eidam et al., 2017). It confirms that large erosion observed in Go-Cong actually extends far offshore over the whole mudflat (with a concave shape). On the other hand, Phu-Tan does not show any sign of erosion in the subaqueous delta at least up to 2 m depth, anywhere along the district. If there is local erosion there, then it is a shallow process, not necessarily related to large-scale alongshore transport (see WP2).

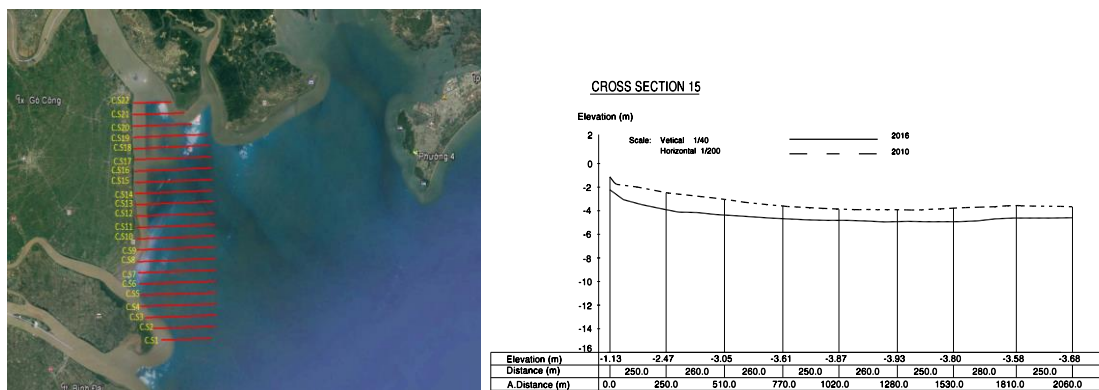


Figure 17: Bathymetry measurements along the Go-Cong coast in Oct 2016. Left: survey transects; right: transect 15 compared with a previous survey in 2010. Note the strong erosion of the whole cliniform, representing many Mtons of sediment loss.

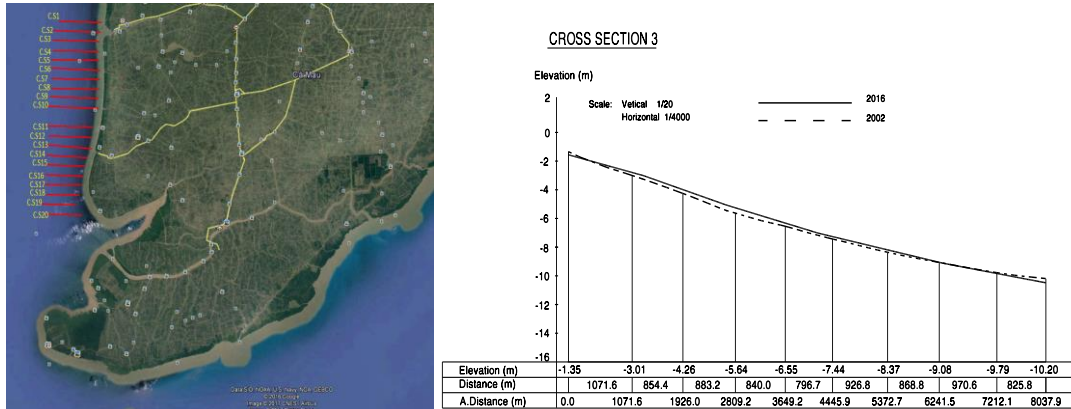


Figure 18: Bathymetry measurements along the Phu-Tan coast in Oct 2016. Left: survey transects; right: transect 3 compared with a previous survey in 2002 (14 years before). Note that no signs of erosion are visible here contrarily to Go-Cong.

## Conclusions

The survey data were used for the calibration of the regional and local high-resolution models. It provided valuable insight on evolution of forcing (particularly wave forcing) near the coast. It also helped settling the issue of contrasting values of sediment concentrations (SSC) measured in the LMDCZ. It confirmed the adequacy of our new satellite product, while revealing the evolution of SSC when approaching very shallow nearshore waters (very few data was previously available due to the difficulty of approaching these shallow depth by boat or land). For the regional models, satellite imaging specifically processed for this project, and validated by our measurements, were used in priority because it provided statistical reliability and synopticity (coherent spatial patterns, see WP2).



## Chapter 2

### Regional sediment budget from 3D models (WP2)

This WP presents an innovative approach based on three-dimensional coupled hydro-morphodynamical modeling. The delta is considered as a system including the coastal ocean with its complex hydrodynamics driven by winds, waves, tides and salinity fronts. The response of the coastal system is assessed in terms of sedimentary balance. One essential goal is to distinguish the part of morphodynamic evolution that is intrinsic to the system (natural redistribution process) from other processes attributable to human activity: river supply deficit, mangrove belt reduction, coastal squeeze, and subsidence. Another important aspect of the problem is to identify oceanic regions involved in sediment erosion (nearshore zone, mudbank, continental shelf; see *Figure 19*).

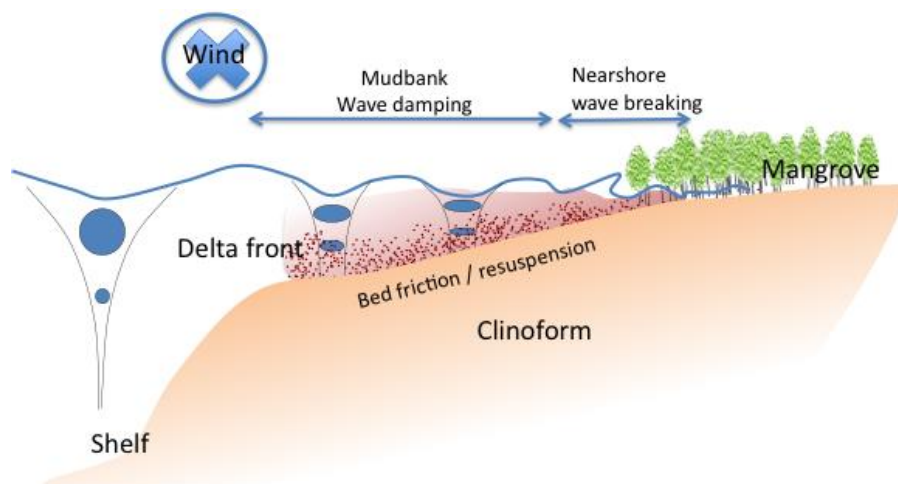


Figure 19: Schematic view of coastal regions and main driving forces in the LMDCZ

A particular aspect of delta dynamics and particularly the Mekong delta is the feature of a shallow cliniform of about 10 km that has a profound impact on wave damping and friction-related erosion (*Figure 19*). On sandy environments or maybe other delta systems with deeper coastal zones, surfzone erosion due to wave breaking is the dominant process. But here it is different, as will be shown, which justifies the use of regional models solving coastal dynamics up to the prodelta and continental shelf area, as opposed to focusing only on the surfzone with nearshore models. The robustness of the results relies on calibration and validation from in-situ data, laboratory experiments and satellite sensing.

### Models

The objective of the regional study was to build robust and reliable hydrodynamic numerical models of the LMDCZ, including tides and wave forcing and the 3D stratified ocean circulation with eddies produced from instabilities of the main currents. In the project, we use a multi-model approach akin to an ensemble approach in order to lower the error bar of any individual model alone. Our model of

choice is CROCO (Coastal and Regional Ocean Community model), a French code built upon the well-known Regional Oceanic Modeling System (ROMS; Shchepetkin and McWilliams, 2005; Blaas et al, 2007 for sediment modeling). We compare it to DELFT3D, which has been already applied to the LMDCZ with success (this study; see also Vinh et al., 2016). The tidal solutions are validated against coastal satellite altimetry data, salinity (

Figure 20) against in-situ data collected during the project, and sediment concentrations mostly against estimations from ocean color satellite images and in-situ data (sediment characteristics are given by laboratory studies).

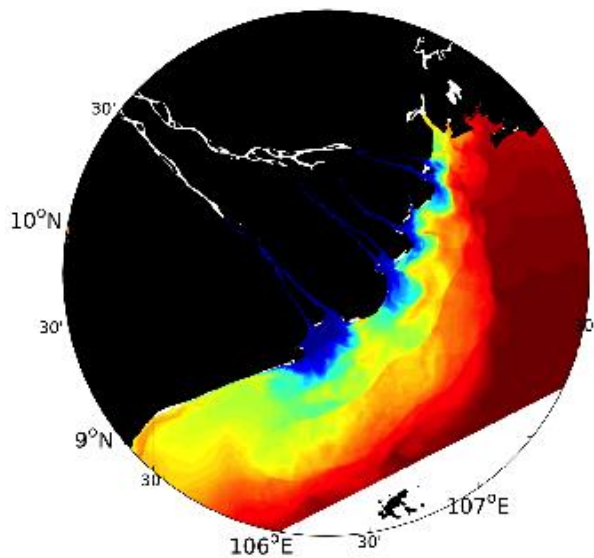


Figure 20: Snapshot of surface model salinity in October 2014 showing the fresh water plume in the coastal zone of Mekong river runoff. The good effective resolution of our models can simulate much of the turbulent behavior of the plume.

### Satellite data comparison

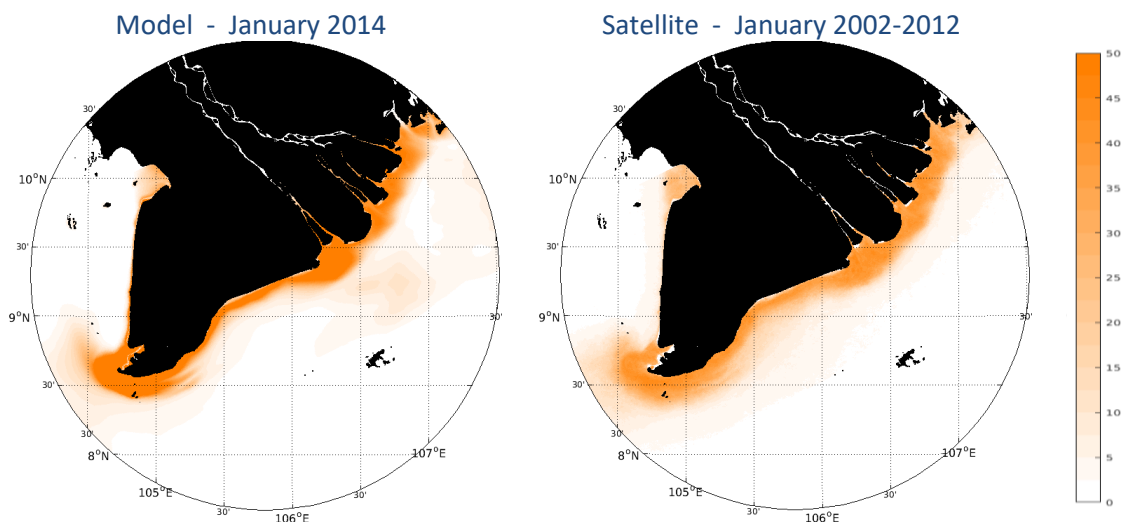


Figure 21: Comparison of monthly mean surface sediment concentration (mg/l) between model and satellite analysis from MERIS 2002-2012. The satellite product actually presents a 10-year monthly climatology of surface particulate matter (assumed close to SSC), while the model shows the monthly means for 2014.

Due to high variability of physical and biogeochemical processes in the coastal ocean, traditional approaches based on oceanographic ship surveys and in situ time series, although essential, are time-consuming, expensive and maybe more importantly here of limited use for synoptic patterns. Remote sensing on the other hand is a powerful mean of capturing synoptic or climatological patterns, which is essential to calibrate and validate regional patterns in models. In situ data, such as those gathered in the frame of this project, remain obviously necessary to validate the satellite products and models. From a specific study of this project, monthly means of suspended particulate matter concentration (SPM) were produced using the best available satellite products and specifically designed new algorithms for data inversion.

### Sediment properties: lab study

Suspended and deposited sediment were collected during the two coastal surveys of the project (SIWRR), another field survey onboard IRD ALIS vessel (June 2014, VITEL campaign) spanning from the Bassac estuary to the adjacent coastal zone, and from additional surveys conducted in the Bassac estuary by SIWRR (2016). Some of the samples were analyzed at the CARE laboratory (HCMUT), where flocculation properties and settling velocities were estimated (published in Gratiot et al., 2017). This study was important for model calibration, suggesting that a relatively simple sediment model with two important size classes (floculi and fine sand) can be used. For these classes, we neglect flocculation processes and consider this model a pseudo-cohesive one, due to the implicit assumption of flocculation in the choice of settling velocities. Using these analyses, the match between model and satellite climatologies is very good in comparison with that previously shown in the literature (*Figure 21*).

### Sediment transports and budget

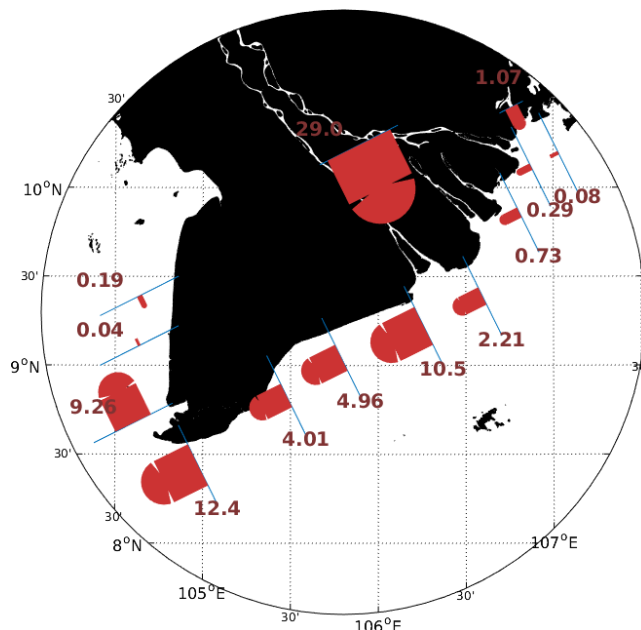


Figure 22: Annual (2014) alongshore fluxes of mud sediment (Mton/y) across various coastal sections (blue lines).

We used a regional setup for a full 3D model of the LMDCZ. The sediment model parameters (classes, sizes, settling velocities, critical bed shear stress and erosion rates) were calibrated using in-situ samples, laboratory analysis, and the best satellite climatology specifically generated for the LMDCZ. The model solutions show that, schematically, river sediments are

supplied in summer to the estuary area and transported in winter to the Ca Mau peninsula (Figure 22). The coastal circulation is driven by essentially by winds, and to a lesser extent by tides and river buoyant plumes. However, sediment transport is done through a repetitive cycle of re-suspension and deposition, so that sediment concentration measured along the coast is essentially a result of re-suspension due to wave-induced bed shear stress over shallow areas (clinoform). Yet, alongshore transports set the patterns of erosion and deposition by concentrating or dispersing the re-suspended sediments.

## Erosion patterns

In agreement with satellite observation of shoreline evolution (Chap. 1), we find that the Mekong deltaic coast is locally non-equilibrated. In other words, it experiences large redistribution of sediments by hydrodynamical processes, and its morphology is in constant evolution with both erosion and accretion zones. In the model, we integrate the net erosion flux (erosion minus deposition) over the whole mudbank area up to the delta slope. This is only a proxy of shoreline evolution but it provides the best comparison with observations (Figure 23 and Figure 24).

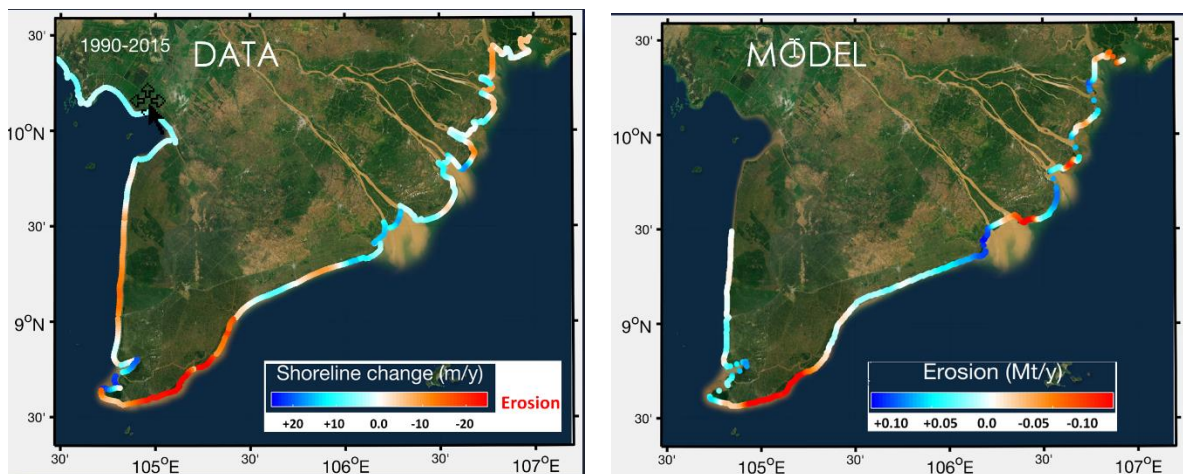


Figure 23: Comparison of 1990-2015 observed shoreline change rates (m/y) and modeled net coastal erosion in 2014 (Mton/y) along the whole Mekong delta coastline. In both cases, similar tendencies are present in four main zones: West coast (Ca Mau to Kien Giang), Ca Mau Head, East coast (Ca Mau to So Trang) and Estuarine zone (Soc Trang to Vung Tau).

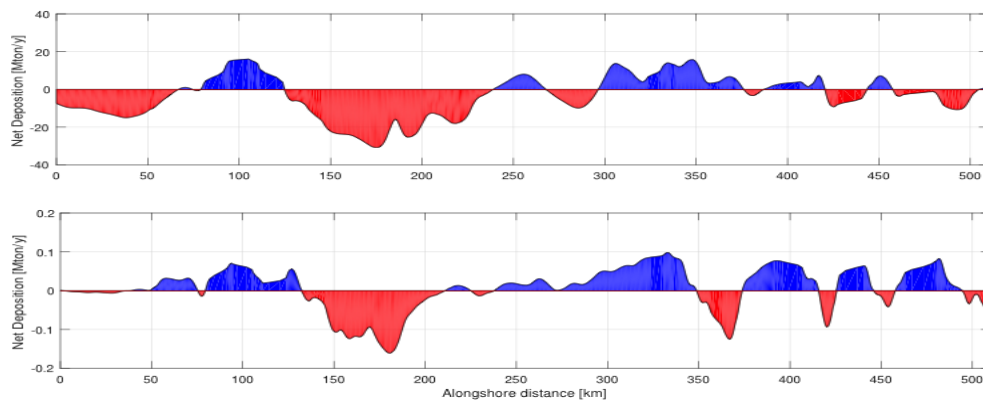


Figure 24: same as Figure 3 but presented on one-dimensional plots. The main sub-regions are well represented in the model (local variations respond to local processes not represented in a regional

model). Top: the observed shoreline change rates (Mton/yr) 1990-2015; bottom: the modeled net deposition in 2014

This result implies that shoreline change is actually an integrated result of net erosion over the whole shallow subaqueous delta of about 10 km wide, not just the surfzone or intertidal zone. There are obviously cross-shore exchange processes at fine scales that are not well represented in our regional model.

The LMDCZ is thus divided in the model as in observations into 4 subregions of distinct morphodynamics:

- The estuary zone, from Vung Tau to Soc Trang, is mostly in accretion
- The East coast, from Soc Trang to Ca Mau is mostly in strong natural erosion
- The Western peninsula's tip is in strong accretion as it receives the eroded sediments from the East coast in its southern area
- The West coast from Phu-Tan (Ca Mau) to Kien Giang shows signs of erosion (Tran Van Thoi, U-Minh) but of moderate intensity

## River supply

The fact is that Go-Cong, in the estuarine region, has experienced strong erosion in the past decades suggests a deficit of sediment intake. The most obvious candidate is a large reduction of the Saigon - Dong Nai river supply due to upstream damming and other anthropic activities. This is supported by a sensitivity test of the model. In this experiment, we lower the upstream river sediment concentration by 75 % (in both Bassac and Mekong branches and in the Saigon-Dong Nai river system).

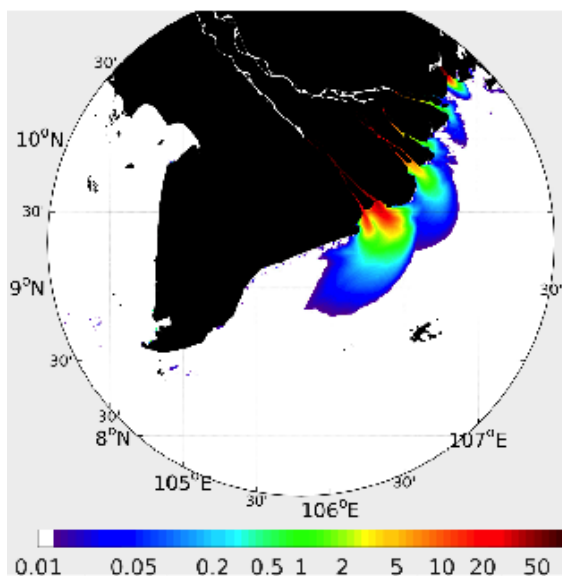


Figure 25: Sensitivity of coastal surface sediment concentration to river supply. The difference of SSC in mg/l is between two simulations with upstream river SSC fixed at 200 mg/l and 50 mg/l. The color scale is logarithmic and blue colors represent very small concentrations.



Figure 25 shows SSC difference between the two simulations after a month of simulation. It turns out that only the estuarine zones are significantly affected by the change in concentration, but the signal of change is much lower as it gets to the mouth area (only 20% of the source signal) and it propagates very little to the other coastal areas (to the south). It means that almost all sediments are deposited near the river mouth and only slowly travels southward. The process explaining the compensation of reduced river supply is called “hungry waters”, i.e., the river compensating for the reduced sediment load by eroding bottom sediments that have accumulated for years (Kondolf, 1997).

Go-Cong shores being so close to the dams and reservoirs of the Saigon Dong-Nai rivers are more vulnerable to damming than the Mekong estuaries because the nearest dams are much farther upstream. On the other hand, reduction in river supply is not likely to affect downstream Ca Mau peninsula at the same timescale. Therefore, increased erosion in the East and West coast must be explained for now by other mechanisms: weakening of mangrove belt protection, subsidence (estimated at 3cm/year), coastal squeeze, and may be others.

## On nearshore dynamics

So far, our results were based on the idea that in a deltaic, mud-dominated environment like the LMDCZ, with very shallow (often less than 5m) mudbanks (or of mixed-sediment) protecting the shoreline, erosion is not confined to the nearshore zone. With this assumption, a regional model with sufficient resolution of the mudbanks (about 10km wide across-shore) can provide a relevant solution. The main processes at work is then a combination of sediment deposition from the rivers in summer, re-suspension by waves (with tidal modulation) in winter and subsequent transport to the south of the suspended sediment, mostly by wind-driven currents. The good “prediction” of erosion rates by the regional model tends to validate our initial assumption.

However, some studies on LMDCZ erosion (e.g., GIZ study of Soc Trang erosion, 2011) have made different assumptions. Assuming that the shoreline behaves as sand-dominated beach, one can apply a one-line model, which is a simple model of shoreline response to a wave-driven longshore sediment transport in the surf zone (<1 km wide). In this case, the transport processes involved over the remaining section of the mudbank are neglected. We checked this assumption with a one-line model and compared the results with observations, as done previously with the regional model. With the one-line model we could not predict the observed regional patterns of net erosion and only the estuary area shows significant erosion/accretion due to “favorable” orientation of the coastline to wave direction in some places.

The results of the one-line model can be added to that of the regional model to improve model prediction, at least in the estuaries. But, more importantly, it is not a good predictor of regional processes. Erosion in the LMDCZ results from processes affecting the whole shallow subaqueous delta. A problem in using one-line models for the Mekong delta is that all wave dissipation is assumed to occur during breaking in the nearshore zone. However, the very shallow (<5m) and wide muddy area (order of 10km), extending from the coast to the delta front, has large bottom orbital velocities, that can affect the sediment bed all the way. This is what explains the far extension of delta front in winter, well spotted from aeroplanes and satellites. In addition to shallow water argument, muddy seafloors, which are combinations of elastic, plastic, viscous, and porous media, can cause higher dissipation of ocean surface-gravity waves than sandy seafloors (e.g., Elgar and Raubenheimer, 2008). Therefore, wave dissipation



along the LMDCZ is not confined to the surfzone, nor is sediment transport and erosion. Eventually, there are cross-shore processes that exchange sediments across the coastal mudbank, whether associated with tidal or residual wave effects. These cross-shore transport processes are not well understood and modeled because they are weaker than alongshore transports and hard to reveal, but our results suggest that they have an important role in shoreline evolution.

## Chapter 3

### Local hydrodynamics and sediment dynamics (WP4-WP5)

A study of regional and local wave climate was conducted using the TOMAWAC wave model (Benoit et al, 1996). Because waves are the main forcing of sediment re-suspension, a proper assessment is needed, which was used as a general reference to all modeling activity, even though each modeling group used their own wave models as part of coupled systems. It confirms the difference of wave action in the East and West coasts and the dissipation role of mudflats, which need to be well represented in models to avoid overestimating wave energy in the coastal area.

For downscaling information from regional to local scales, two state-of-the-art numerical models were used (TELEMAC-2D, MIKE21). After the setup of forcing conditions, calibration and validation with data, these models were used to simulate and analyze hydrodynamics, followed by a morphodynamical study (WP5) addressing local sediment budget analysis: transport and erosion. The following chapter on protection measures will then present this work.

## Part 1

### Local wave climate

The main objectives were:

1. Build a regional wave model of the East and West Sea using a spectral wave model.
2. Calibrate the numerical model using recent field measurements collected over the area of interest.
3. Validate the model against another series of field measurement.
4. Implement local model grids for the coastal areas of Go-Cong and Phu-Tan.
5. Determine the wave climate for a 8-year period.
6. Analyze wave characteristics relevant to the planning of coastal protections.

### Regional approach

Two specific grids were developed for the coastal areas of Go-Cong and Phu-Tan. The computed domain for Go-Cong covers the whole East sea as shown in *Figure 26*, while the computed domain for U-Minh is smaller. This is because Phu-Tan located in the West Sea is not affected by the northeast winter monsoon conditions. Grid resolution ranges from 500 m nearshore to 40 km offshore (25 km in the West sea grid). Wave boundary conditions were provided by the East sea regional model (for the West sea grid). Wind fields over an 8-year period (2009-2016) were collected from the US NOAA archive on a global 30 arc-second resolution grid (1km) and interpolated at the nodes of the regional grids.

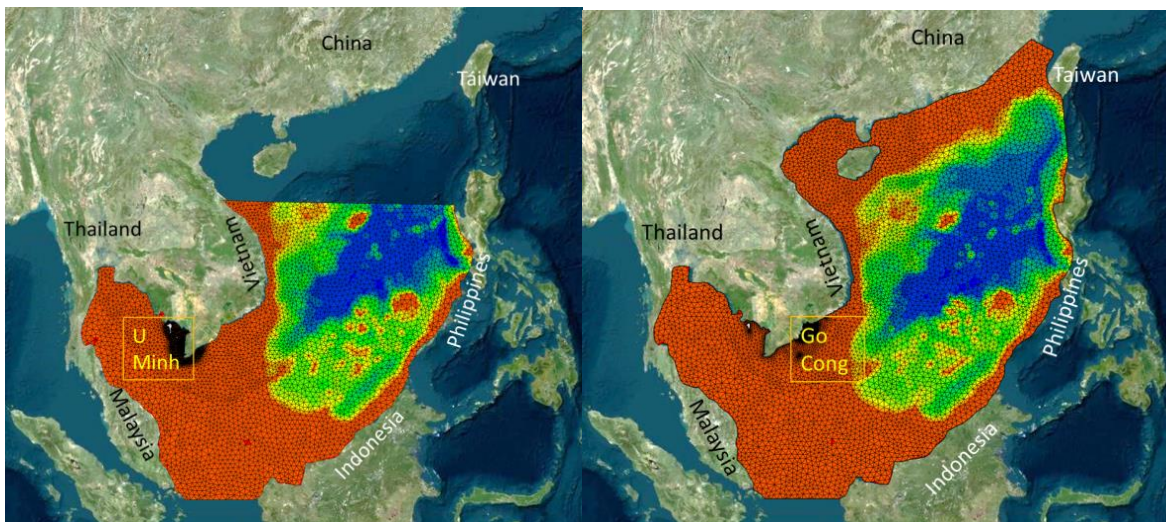


Figure 26: Computational domain for Go-Cong and Phu-Tan (West Ca Mau) coastal areas

The model calibration was carried with the observed wave data over a period of 16 days during two in-situ survey campaigns in the course of LMDCZ project (16-31 Oct 2016 and February-March 2017) at two locations in Go-Cong and Phu-Tan. Comparisons of measured and simulated time-series of significant wave height are given in *Figure 27* (Go-Cong). The comparisons between observed and computed wave heights show good agreement at the two

locations (see also Table 3), confirming the applicability of the wave model at a local scale. Local grids developed for the computation of local hydro-morphodynamics show further improvement owing to their higher resolution (Figure 28), although these grids are too expensive to run for a wave climate study (they are used for hydro-morphodynamics in WP5-WP6).

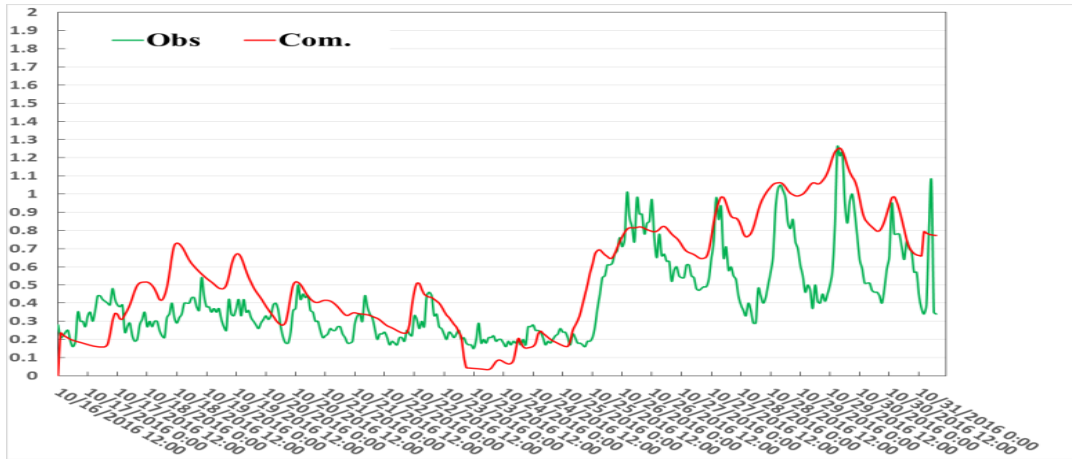


Figure 27: Comparison between computed and observed significant wave height  $H_s$  (m) off Go-Cong from 16/10/2016 to 31/10/2016

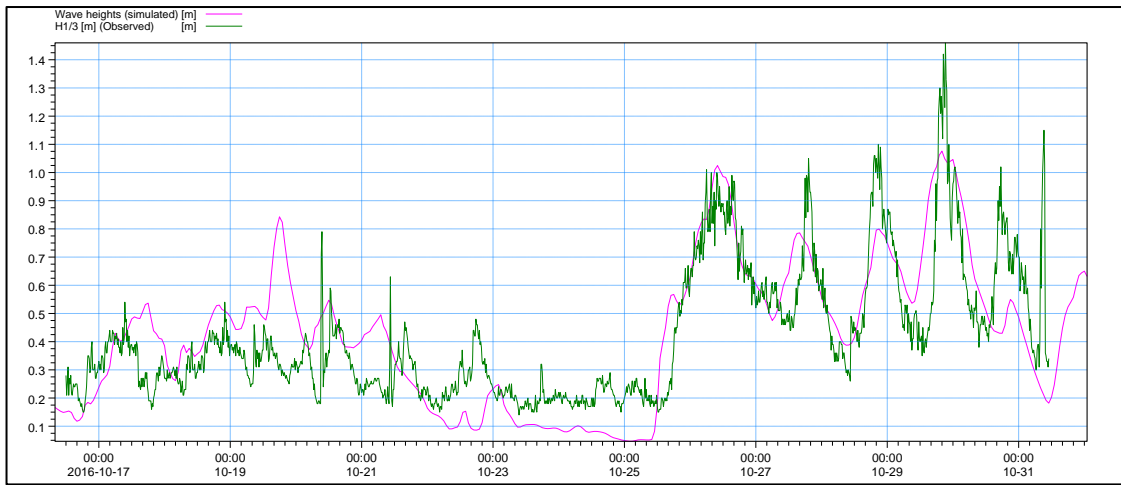


Figure 28: Same as Figure 27 but using local model grids used for hydro-morphodynamics (WP5-WP6). High resolution allows improvements in the wave simulation.

Point	Error Index			
	Mean error (ME)	Root mean square error (RMSE)	Standard deviation of error (SD)	Scatter index (SI)
Go-Cong	0.055	0.235	0.228	0.558
Phu-Tan	0.055	0.236	0.229	0.270

Table 3: Error index between computed and measured significant wave height at the two locations considered for calibration from 16/10/2016 to 31/10/2016.

The regional wave model was then applied to simulate wave conditions during a period of 8 full years, from 2009 to 2016. The model results include time series of significant wave height, mean wave direction and wave period. From these time series a number of statistical analyses were performed to characterize the wave climate at the two sites of interest, including histograms of wave height, wave period and wave direction, as well as wave roses. The spectrum and seasonal variability of wave height and direction are analyzed by plotting wave roses at a number of points (3 in each local model). Here is just a summary of results.

### Go-Cong wave climate

Three points in Go-Cong zone (GC5, GC6, GC7) about 1.5km offshore were considered for detailed statistical analyses (*Figure 29*). The wave roses indicate that there are two distinctive seasons for waves. From October to March, under the effect strong northeast monsoon winds, the dominant wave direction is in the E and ESE angular sector. From April to September, the waves are affected by southwest summer monsoon winds and the dominant wave direction is SSE. The wave directions are almost perpendicular to the shoreline during winter monsoon and almost parallel to the shoreline during summer. Due to strong wind events, wave heights in winter monsoon are also much higher than in the summer.

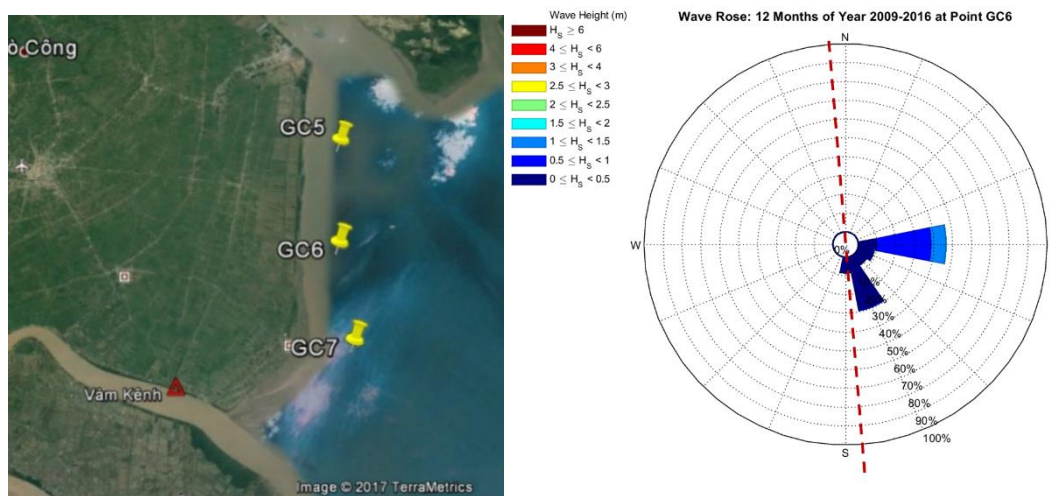


Figure 29: Right: locations of the 3 points considered for statistical analyses in the Go-Cong coastal zone. Left: an example of wave rose at point GC6 in Go-Cong area based on the 8-year simulation.

Histograms for the Go-Cong coastal zone are provided here as examples for the significant wave height (*Figure 30*), mean direction and wave period. A summary of results of the statistical analysis is given in *Table 4*.

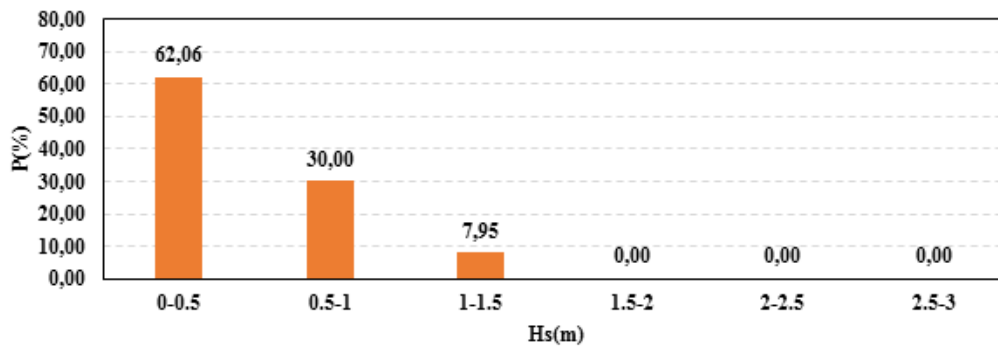


Figure 30: Histogram of significant wave height at point GC6 in Go-Cong coastal zone.

Significant wave height	< 0.5m	P = 62.1%
	0.5m – 1m	P = 30.0%
	1m – 1.5m	P = 8.0%
Wave direction	E	P = 46.5%
	ESE	P = 9.4%
	SES	P = 25.4%
	S	P = 13.2%
Wave period	2s – 6s	

Table 4: Wave statistical analysis in Go-Cong coastal zone (point GC6)

Based on our statistical analysis, the wave characteristics in the Go-Cong area presents the following features:

- The wave direction has a two-regime seasonal pattern: summer monsoon conditions from April to September and winter monsoon conditions from October to March.
- During winter monsoon, the dominant wave direction is E and ESE, while in summer the dominant wave direction is SES and S. Results on wave direction during the two seasons show that the occurrence of East direction is dominant at about 47%, and there is 25% and 13% occurrence for SES and S directions respectively. The other wave directions have an occurrence probability lower than 10%.
- The wave heights during two seasons are quite different. High wave conditions occur more frequently during winter monsoon than in the summer season. The probability of wave height less than 0.5m is dominant with more than 60%, and it is about 30% for wave heights in the range of 0.5m-1m. Sea-states with over 1 meter-height have a probability of less than 10%.

### Phu-Tan wave climate

Three points in West Ca Mau (UM5, UM6, UM7) about 2 km offshore were considered for detailed statistical analyses (*Figure 31*).



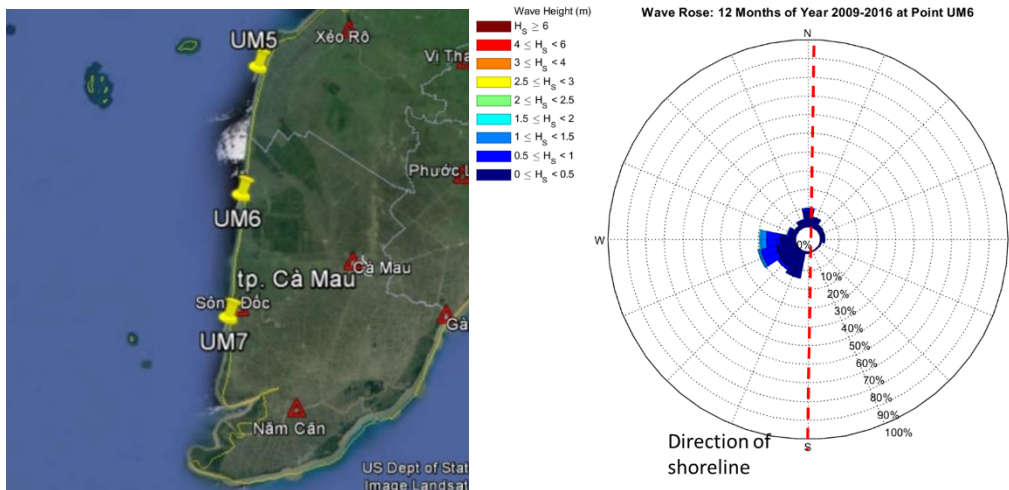


Figure 31: Locations of the 3 points considered for statistical analyses in the West Camau coastal zone. An example of wave rose at point UM6 in the U Minh area based on the 8-year simulations. UM7 is more representative of Phu-Tan, but the results are similar between UM6 and UM7)

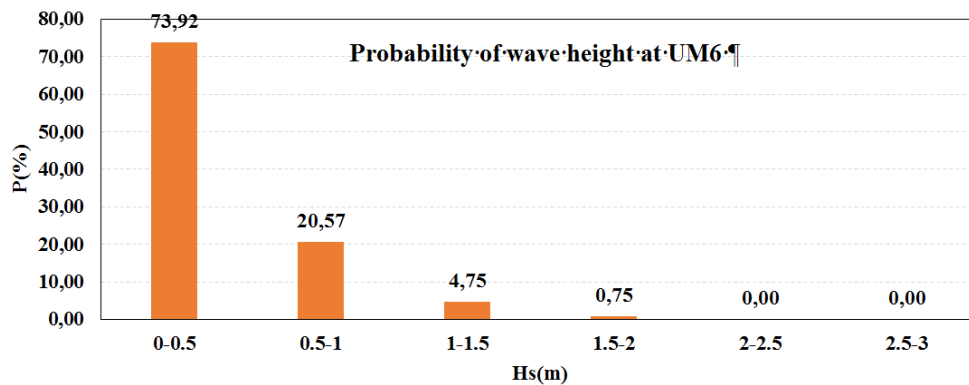


Figure 32: Histogram of significant wave height at point UM6 off West Ca Mau.

The wave roses indicate a more complicated picture in this area compared to Go-Cong. The dominant wave direction during the winter monsoon is in E, NE, and ENE depending on the location of the considered points. In summer, from April to September, the waves are affected by the southwest summer monsoon winds and the dominant wave direction is from W to WSW. The wave roses also show that the wave directions are perpendicular to the shoreline during the summer season and almost parallel to the shoreline during winter (opposite to the Go-Cong area). The wave height in summer is also higher than in winter. This is related to the effective fetch for the generation of waves, which is clearly shorter for southwest winds in the West Sea. Examples of histograms at UM6 are provided here (Figure 32). A summary of results of statistical analysis is given in Table 5.

Significant height	wave	< 0.5m	P = 73.92%
		0.5m – 1m	P = 28.08%
		1m – 1.5m	P = 4.78%
		1.5 m – 2 m	P = 0.73%
Wave direction		NE-ENE-E	P = 25.79%
		W-WSW-SW-SWS	P = 54.48%
Wave period		2s-4s	P = 80.50%

Table 5: Wave statistical analysis in U Minh coastal zone (point UM5)

Based on this statistical analysis, wave characteristics in the West Ca Mau coastal area present the following features:

- The wave direction has two distinctive seasonal regimes: summer conditions from April to September and winter conditions from October to March.
- In winter, the dominant wave direction varies between E, NE and ENE while in summer season the dominant wave direction is from W to SSW. Results on wave direction during the two seasons show that the occurrence of directions from W to SWS is dominant with about 55 % while the occurrence of directions E, NE and ENE is about 26 %. The other wave directions have an occurrence probability lower than 5%.
- The wave heights are quite different between the two seasons. High wave conditions occur more frequently in summer. The probability of wave height less than 0.5 m is largely dominant with about 74 %, and it is about 28 % for wave heights in the range 0.5 - 1m. Sea-states with over 1 m height have a probability of 5 %.
- The dominant wave period lies in the range 2s – 4s, with an occurrence probability of 80%.

## Part 2

### Regional to local hydrodynamics

The main objectives and steps of this WP4 task were:

1. Building a hierarchy of coupled wave-current regional to local configurations, as a necessary step for testing protection measures.
2. Calibrating/validating the models using the project's field survey and other available published or unpublished data.
3. Checking the flow regimes for consistency with the 3D study of WP2.

#### Setup

Regional models were setup in WP4 essentially to force the local models that are presented in the following section (WP5). TELEMAC and MIKE models were used, solving the nonlinear shallow-water equations on unstructured grids with finite element method. Here, we present some of TELEMAC results (MIKE's results are generally consistent). The circulation model is coupled with the same wave model (TOMAWAC) used previously for studying regional and local wave climate. The regional computational grid resolution is from 10 km offshore to 200 m in the coastal zone and estuaries, where SIWRR high-resolution bathymetry data was used. The offshore open boundary conditions include astronomical tides extracted from the global database. Upstream water discharges are taken from monitoring data at 2 gauge stations in Can-Tho and My-Thuan (*Figure 33*; see also WP3). Surface wind forcing is extracted from the NOAA archive.

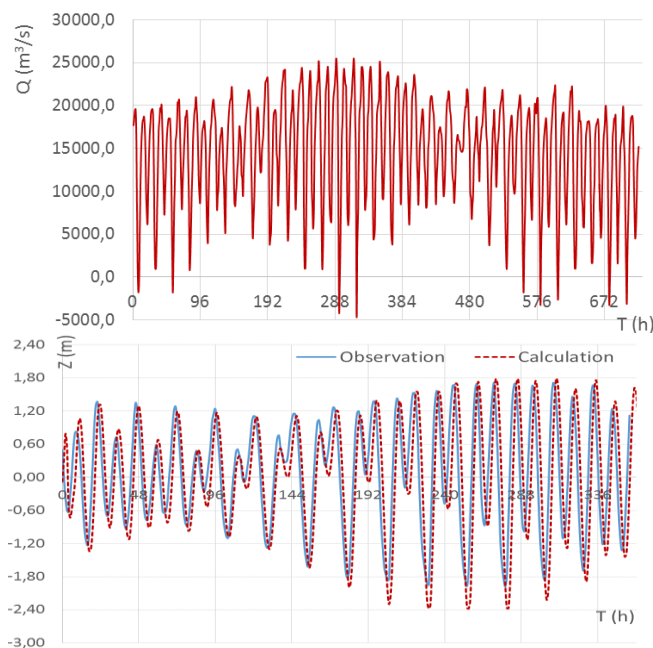


Figure 33: Top: River discharge time series during August 2014 at My-Thuan; bottom: Comparison of sea level from model and from in situ monitoring from 01/08/2014 to 15/08/2014 at a coastal position in the East Sea.

The simulations were made for two typical seasons in the year, one for the northeast winter monsoon (January and February) and one for the southwest summer monsoon (August and September). The 3D model investigation showed that these typical months are representative of seasonal cycle and annual mean results are qualitatively very similar to averages made of these typical months (true also for the sediment budget). This justifies choosing shorter simulations of typical months, and saving computer power for increasing model horizontal resolution. At the start of the project, the forcing and calibration data were not yet available and simulations were made for the year 2014. A first step of calibration was done with 2014 data (e.g., *Figure 33*). Then, validation was done for the survey periods of Oct 2016 and Feb-Mar 2017.

Results from the calibration/validation step (complete series of tables and figures are available in WP4 reports) show that model tidal wave components, in particular K1, O1 and M2, are in overall good agreement with the monitoring data. The comparisons of water level at Ong-Doc station in the West Sea are less accurate than those of the East coast. This is quite usual and likely due to the complex geography of the sea and interaction of overlapping zones of small amplitude diurnal tides (West Sea) and high-amplitude semi-diurnal tides (East Sea). Uncertainties are enhanced by inaccuracies in bathymetry and bottom roughness. In any case, the results of the flow model can be used with confidence to obtain tidal induced currents over the local study sites.

**This 2D model setup is similar to that of the 3D regional model of WP2, but simpler and cheaper to run, as there is no vertical dimension and associated salinity-driven dynamics, and we focus on typical months of the seasonal cycle.**

### Coastal circulation

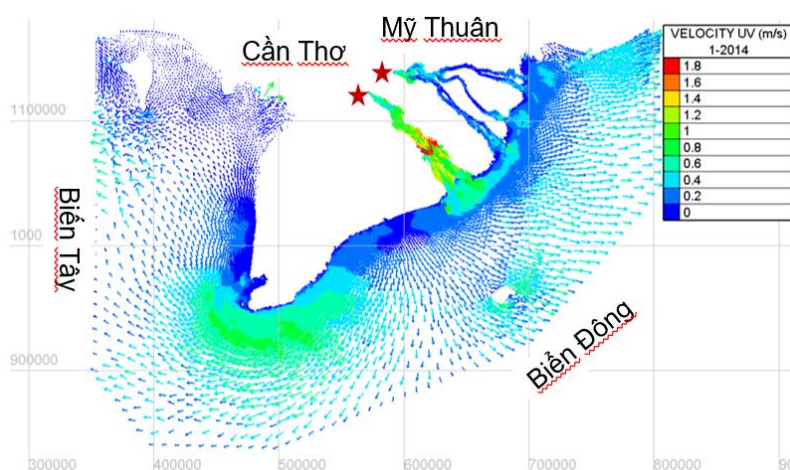


Figure 34: Instantaneous velocity field at 6 a.m. on Sep 9 2014.

As for the 3D model, tides and winds produce a very variable velocity field instantaneous values much larger than the residual (*Figure 34*), which explains that the residual transport of tracers (suspended sediments) can be different from the transport by the mean flow, which is dominantly parallel to the shore. In particular, onshore sediment flux can be significant despite weak residual cross-shore velocities. Similarly, waves and instantaneous currents, not mean currents, drive sediment re-suspension. Strongest velocities are in rivers, estuaries and around the Ca Mau cape. The residual flow is generally along the coast, from the northeast to the

southwest and into the West Sea. The average velocity in January can reach 0.25 m/s in the Ca Mau cape. This is an important factor in assessing pathways from the estuary zone to the rest of the LMDCZ.

One drawback of using a 2D model is that river plume dynamics cannot be solved, as they are associated with salinity fronts, actively sustaining geostrophic currents (see WP2). However, our 3D study shows that the dominant forcing of sediment transport is wind (first) and tides. Plume circulation is not insignificant but for the study areas of Go-Cong and Phu-Tan, they are not essential.

### Wave modeling

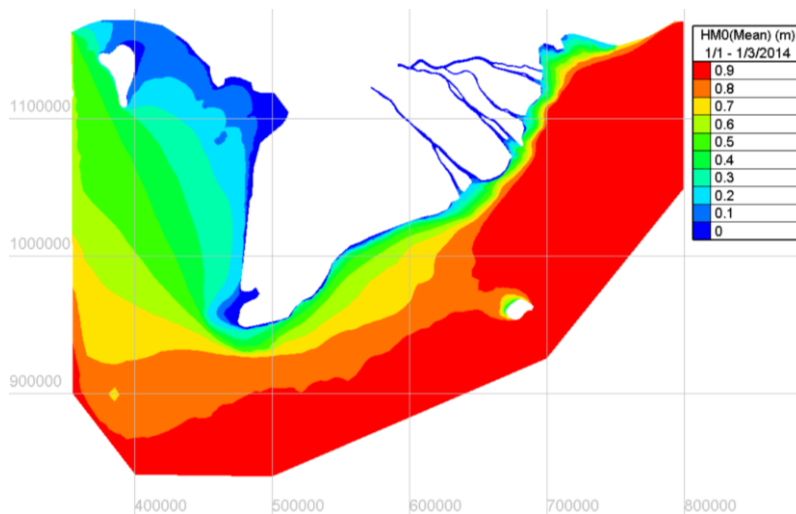


Figure 35: Mean wave height  $H_s$  for winter monsoon (January/February 2014)

The analysis of average wave height  $H_s$  in January and August are generally very consistent with the wave climate results presented in the previous section. In the East Sea, waves are much larger in winter than summer, while it is the opposite in the West Sea. Figure 35 emphasizes the large dissipation of offshore waves as they interact with the shallow subaqueous delta. There is at least a 50% decrease over the coastal platform, which has implications for sediment re-suspension, as already mentioned before. Models not resolving this dissipation mechanism would over-estimate bed-shear stress and erosion. Also, due to refraction, coastal waves tend to have smaller angles with the coastline, with implication for surfzone currents (see WP2).

These hydro-dynamical fields were next interpolated onto local model grids so that the sediment budget simulated at these scales is relevant to our study of protection measures. This is presented in the following section.

## Part 3

### Local sediment dynamics (WP5)

Local models using the coupled TELEMAC and MIKE modeling system (circulation-waves-sediments) were implemented for the Go-Cong and Phu-Tan districts. The grids have variable mesh size with refinement of a few meters in the coastal zone. The regional models of WP4 were used to force the local models at the offshore boundaries. The models are calibrated and validated using in-situ and satellite observations for waves, currents, and sediment concentrations. It confirms the findings from the 3D regional model (WP2) showing a pathway from the East coast to the West coast around the peninsula head and sediment transported to Phu-Tan along this pathway. In general, Phu-Tan has less erosion than Go-Cong due to weaker wave and tidal forcing and the presence of a pathway around the peninsula's tip that can carry sediments from the East Sea to the West Sea.

#### Phu-Tan model

Both MIKE and TELEMAC were applied to the west coast of the LMDCZ (*Figure 36*) in the West sea from Bay Hap to Ong Doc River, i.e. the southern portion of the West coast. The results of these models were consistent in many aspects. The main difference is quantitative and appears on the amount of sediment accumulation behind protection structures (see Chap. 4; WP6). The average offshore extension of the grid is about 40 km and it is about 120 km alongshore. The offshore open boundaries are imposed from the tidal database (see previous section), and the river discharges are given from gauges (small flow of about 10 m<sup>3</sup>/s).

In TELEMAC, the sediment is considered as non-cohesive (or pseudo-cohesive) with four representative sizes, the main size class being that of flocculi (20 microns), with small settling velocity (see WP2). A pseudo-cohesive approach is justified by the dominance of flocculi as long as bed stratigraphy is not of major importance. The pseudo-cohesive approach has the advantage of fewer control parameters for calibration. Fine flocculation processes in very shallow water, particularly calm water inside structures (breakwaters, mangroves) is not simulated but the cohesive model of MIKE provided a more reliable approach in this case.

Two periods are considered, Jan-Feb (the winter NE monsoon) and Aug-Sep (the summer SW monsoon) of year 2014. The survey period (2 weeks in Oct 2016 and Feb-Mar 2017) was also simulated for validation purposes. Comparison with observed sediment concentration was used for calibration, e.g., satellite observations provided specifically for this study (*Figure 36*) and in-situ observations collected during the surveys.



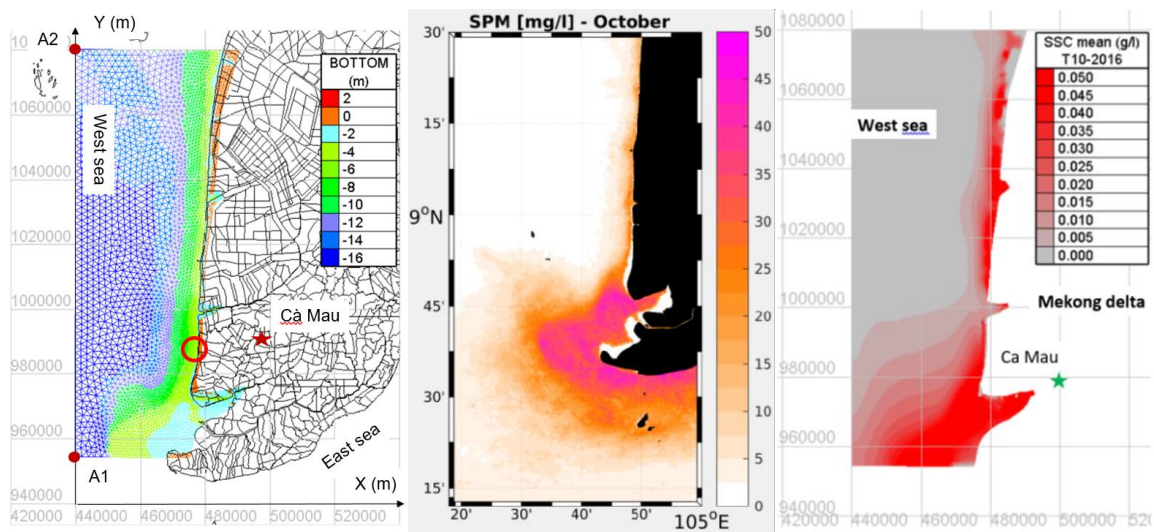


Figure 36: Local grid of the Phu-Tan area and averaged sediment value in October from satellite observations (climatology) and present modeling (2016).

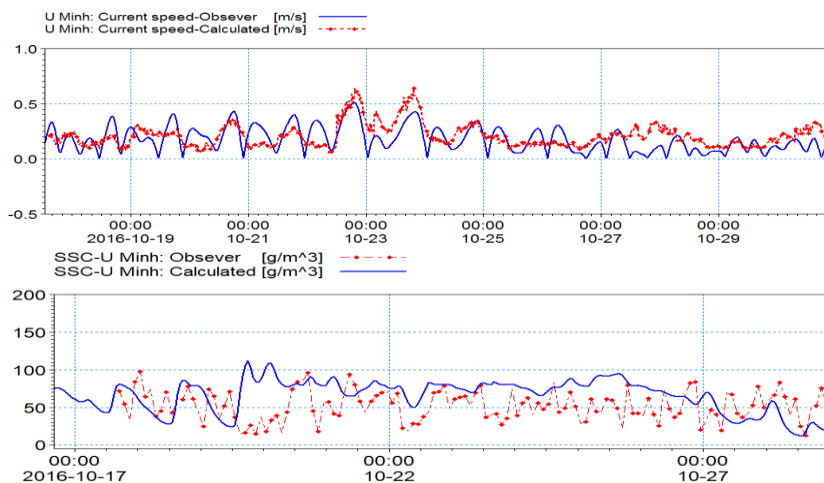
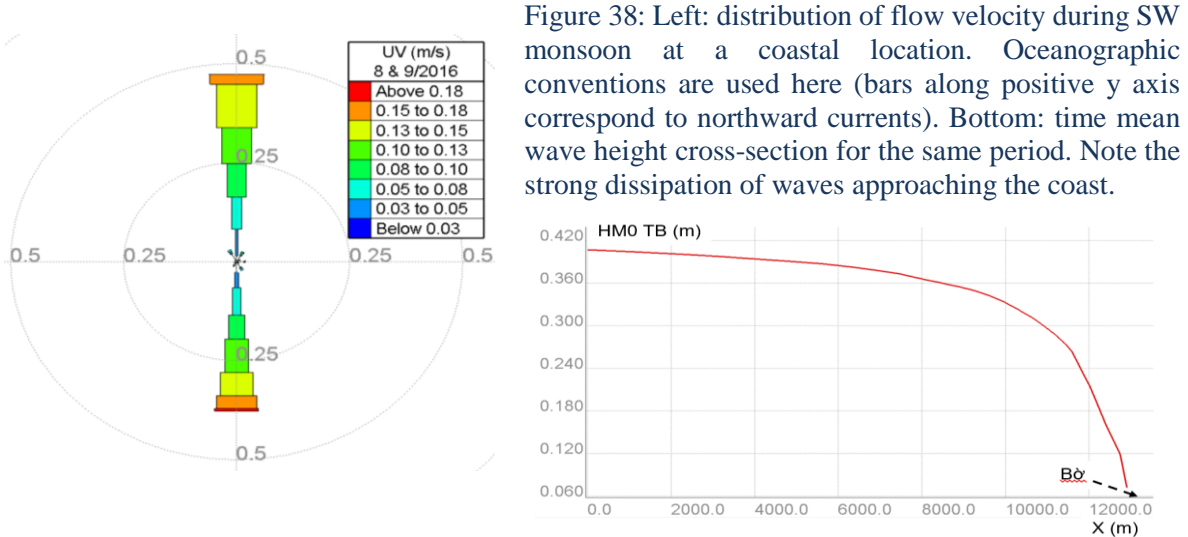


Figure 37: Comparison of SSC at west coast In-situ stations during the SW monsoon (Oct 2016)

The local simulation tends to confirm a connection between the East and West seas. It also shows a dominant northward flow from Ca Mau cape. The largest currents are during summer monsoon as expected from the wind field. In summer, alongshore flow is dominant (Figure 38), although some cross-shore transports are present. The flow has two main directions: northward and southward along the west coast, and a maximum speed of ~20 cm/s. The mean flow is essentially to the north, but closer to shore, a thin southward flow is simulated that can carry sediments, and higher cross-shore velocities are also noted in these very shallow waters.

The average wave intensity tends to increase northward along the coast. There is strong dissipation of waves approaching the coast (Figure 38), due to shallow waters and mild slopes. Wave intensity drops rapidly within 1000 m from the shore. Within 500 m, the wave height is less than 0.3 m before breaking over a relatively large surf zone. Near the Ca Mau cape, the mean wave height falls faster than further north because the bathymetry is shallower due to large volumes of mud that has accumulated there. The average wave angle shows a nearly normal direction to the coast due to refraction, which means that only weak longshore drift is

generated. As suggested in WP2, longshore drift in this area as in most areas of the Ca Mau peninsula is probably not a major driver of sediment transport, owing to strong wave dissipation over the shallow subaqueous delta.



Coastal waves greatly affect the concentration of suspended sediment. This result is consistent with patterns observed from satellite imagery and is explained by the strong interaction of the sea bed with wave orbital velocities, creating wave dissipation on one hand and sediment re-suspension on the other. As a result, wave breaking has a relatively minor role here and more generally in the LMDCZ (as opposed to steep sandy beach environments), apart from some areas in the Estuary zone. Erosion is thus spread over a wide coastal area and not only the surf zone.

Phu-Tan Area	South	Center	North	Whole area
In (1000 m <sup>3</sup> )	44.7	49.7	49.4	
Out (1000 m <sup>3</sup> )	54.4	68.2	35.1	
Balance (1000 m <sup>3</sup> )	-9.7	-18.5	14.3	-13.9

Table 6: Sediment budget analysis for the Phu-Tan area, combining winter and summer monsoons. The budget is split between 3 areas: South, Center and North.

Table 6 shows the budget analysis of the Phu-Tan area, split into South, Center and North (the southern area being the most affected by fluxes from the Ca Mau cape). The sediment flux tends to increase northward, creating divergence in the south and center of Phu-Tan district. Therefore, if sediments are carried from around the Ca Mau peninsula, currents can redistribute the load irregularly along the coast. Specifically, over the combined winter and summer months (assuming that they are representative of the whole year), the southern areas appear to erode more than the northern area of Phu-Tan, which seems accretive, according to the model.

This result is not inconsistent with satellite observations for recent years (Figure 39), which shows similar weak erosion/accretion patterns. However, the numbers are small and very fluctuating from a decade to another in observations (U-minh erosion is more steady). The small magnitude of erosion/deposition in this area means that interannual forcing variability or changes in the mangrove belt can easily modify the patterns. Actually, these volumes of accumulation presented here amount to less than 1 cm/yr. Deposition can probably be

augmented in very shallow water if protection is given (see WP6). As will be seen, the maximum accumulation that can be expected from tidal onshore flow in these waters is 10 cm/yr or more if protection is given.

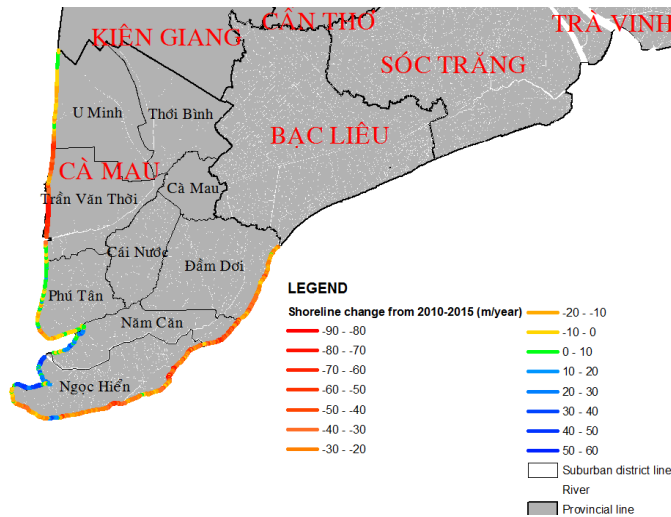


Figure 39: Satellite observation of shoreline changes for the Ca Mau Province from 2010 to 2015 (results from the present study).

## Go-Cong models

TELEMAC and MIKE were both applied at the scale of the Go-Cong coastal zone (*Figure 40*). MIKE is our model of reference and we present here a summary of its results. TELEMAC results applied the Go-Cong area allowed us checking the consistency of our modeling approach. MIKE setup is based on MIKE21 coupled wave-current-sediment dynamics. River forcing is the same as for the other models, and offshore conditions are provided by MIKE regional model. Upstream river conditions are given from field data and from a one-dimensional MIKE11 hydro-morphodynamic model simulation. Offshore open boundary conditions are from the regional model (WP4). Here, the sediment is considered as cohesive and three layers represent the bed (Teisson et al., 1993). Simulations are provided on two periods: January and September 2014.

As opposed to Phu-Tan area, the dynamics of Go-Cong are strongly influenced by Soai Rap River (the Saigon-Dong Nai river system) and Cua Tieu River (Mekong). Therefore, the flow direction is mainly north and northwest at rising tide and south and southeast at falling tides. In this area, currents are stronger during the Southwest summer monsoon than the Northeast winter monsoon. However, it is the opposite for wave energy and therefore for sediment erosion. There is erosion along Go-Cong during the winter monsoon and accretion during summer monsoon (*Figure 41* and *Table 7*).

As said before, the role of Soai Rap River and to a lesser extent the Cua Tieu River are particularly important, naturally leading to a direct accumulation of sediments along Go-Cong. We conducted a test of river supply reduction to quantify this effect. With 75% sediment reduction of upstream river discharges, the model predicts a large reduction of deposition in the coastal area (*Table 2*). This is true for the nearshore area as well as the whole mudbank area (offshore). There is more than 50% reduction of coastal sediment. Some of the 75% river deficit is compensated by an increase of erosion in the river downstream of the source. This is

consistent with the process of “hungry waters” allowing some compensation of river discharge reduction (Kondolf, 1997). Nevertheless, if supply reduction is affected so close to the coastal zone, as is the case with the Saigon-Dong Nai system, “hungry waters” have no time to cover the whole deficit.

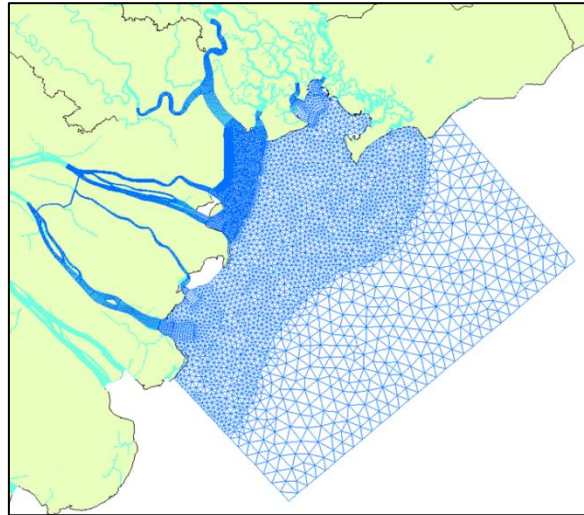


Figure 40: Mesh used for the Mike model around Go-Cong.

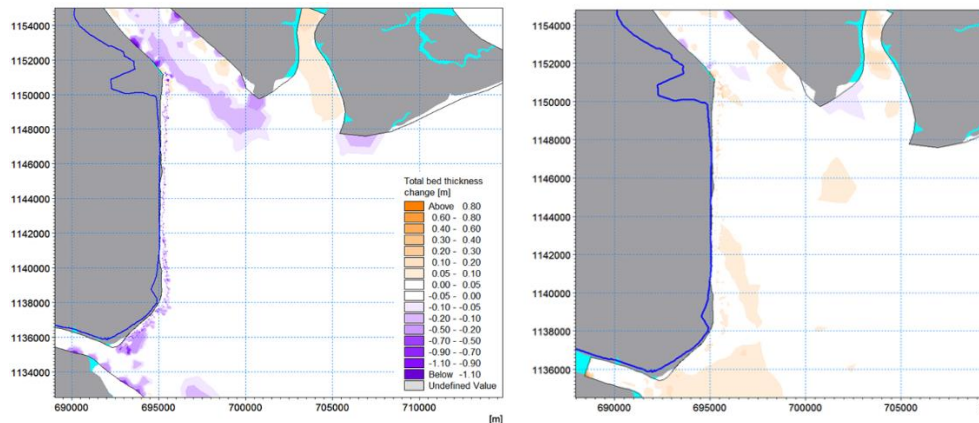


Figure 41: Distribution of erosion and accretion after one month: Northeast monsoon (left), Southwest monsoon (right).

Period	Offshore region (10 <sup>6</sup> m <sup>3</sup> )		Nearshore region (10 <sup>6</sup> m <sup>3</sup> )	
	Accretion Volume	Erosion Volume	Accretion Volume	Erosion Volume
January 2014	11.1	-17.6	<b>0.4</b>	<b>-1.1</b>
75% less river sediment supply	8.0	-17.8	<b>0.3</b>	<b>-1.1</b>
September 2014	34.4	-11.8	<b>0.8</b>	<b>-0.2</b>
75% less river sediment supply	15.1	-12.5	<b>0.3</b>	<b>-0.2</b>

Table 7: Total accretion and erosion in study area after one month

## Conclusions

Local sediment transport behavior seems well simulated by the two-dimensional models (hydrodynamics, waves, sediment transport). Consistency was found with satellite observation and in-situ surveys. During the wet summer season, high sediment concentrations are found in the direct flume of rivers, whereas the turbid plume is stretched eastward with a low level of suspended matter along the West coast during the northeast winter monsoon. During this period, sediments move from East to West around the peninsula head and could be a contribution to the general deposition balance of the Phu-Tan coast. All simulations show that waves play an important role in coastal erosion. Those results are in agreement with the 3D numerical simulations with non-cohesive sediment in WP2 and with the mechanism described by Hein et al. (2013).

Local sediment transport and morphological simulations were undertaken on the West coast (Phu-Tan area). The general behavior agrees with observations. It leads to erosion during summer and accretion during winter. Erosion does not seem correlated with wave direction, but rather seems driven by wave energy (re-suspension) and coastal wind direction driving suspended sediment transport. Different models were used but they give overall consistent behavior. During the project a set of sediment transport and morphological modeling was established. Applying non-cohesive sediment modeling was a difficult task but it provided interesting results.

One particularly interesting result for Go-Cong, confirming the result of the 3D regional model is the important role of the Saigon-Dong Nai River. A 75% reduction of river supply upstream is translated into more than 50% reduction of accretion in the coastal area of Go-Cong.



## Chapter 4

### Protection measures from coastal erosion (WP6)

#### Design philosophy

First of all, we realize that coastal protection in the face of structural erosion cannot rely only on creating bigger and stronger dikes; dikes can be built to withstand any undercutting by erosion and increased wave attack, but not against acceptable costs. Therefore the project aims, where practically feasible, at halting the erosion with measures that maintain a shallow foreshore and viable mangrove areas.

A potential sediment deficit from upstream Mekong River exists which cannot be reduced within the project and which should be considered as a boundary condition. The situation may be different for the Saigon-Dong Nai system as operations on this river system are under control from Vietnam authorities (as opposed to the Mekong River). If we consider river supply as a given condition, then any hard coastal protection structure will be unable to increase the amount of sediments transported alongshore. Nourishments may in part mitigate this imbalance.

On a local scale, the erosion and accretion of the coast depends on the balance between the sediment deposition and the erosive forces of waves and currents. Deposition depends directly on the nearshore sediment concentration, and on the conditions for fine sediments to settle. Erosion is a function of the local bed shear stresses and the degree of mud consolidation. It is useful to consider an upper limit of what to expect in terms of sedimentation rate. For cases where a sheltered region is created, i.e., a mangrove area, an area sheltered by T-groins or other longshore dams, the tide is mainly responsible for exchanging the sediment. The total inflow in one tidal cycle equals the tidal volume times the nearshore concentration; the outflow depends on the efficiency in capturing the sediment. If we assume complete effectiveness as an upper limit the sedimentation rate per year is then:

$$\text{MaxSed (m/y)} = \frac{\text{Tidal Range (m)} \cdot \text{SSC (kg/m}^3\text{)} \cdot 700 \text{ tides/y}}{\text{bed density (kg/m}^3\text{)}}$$

With average tidal range in the order of 1.5-2.0m an average nearshore concentration of 100 mg/l then leads to an upper limit of accretion in the order of 10 cm/yr (depending on SSC). Given that the efficiency of capturing is never perfect we should not expect large expansion of mangroves in such areas, but at best a halting of erosion. From satellite, in-situ observations and models we see a large range in nearshore concentrations between 50 and 3000 mg/l with the higher concentrations often linked to stronger wave action and low tide phase (mean tidal values range from 50 to 500 mg/l). Paradoxically, at some certain degree higher wave conditions may be favorable for accretion when combined with tides, while they may at the



same time lead to strong erosion. Therefore, the design of coastal protection measures should aim at minimizing the destructive effects of the waves while allowing their accretive effects (in combination with tides).

From Schüttrumpf (2017) we may summarize the design considerations as follows. Any coastal protection structure should ensure the following requirements:

- Be porous enough to ensure water exchange, sediment transfer and water quality
- Be as high as possible to reduce wave impacts
- Be able to withstand extreme wave heights
- Be able to trap sand, silt and clay. Especially trapping of silt and clay is a crucial task and not easy to ensure under turbulent hydraulic conditions

Ideally, the measure should be a combination of structural and non-structural measures, e.g. offshore breakwaters or T-groynes in combination with nourishment and mangrove planting. In the following, we will summarize the lessons learned from field studies. We will then discuss the results of physical model tests to assess the impacts of coastal structures and sand bars; these are needed for instance to design the crest height of the structures. We then report the main findings from the modeling studies, where both the existing situation and various design options have been simulated, and end with proposing design options, including the design of limited full-scale pilot experiments.

## Field studies



Figure 42: Example of existing concrete pile breakwaters in Ca Mau (July 2017).

In the course of this project, we conducted a series of field trips to the study sites to evaluate the effect of existing protection structures. This survey was very valuable to our understanding of these effects and for guiding our final recommendations.

## Erosion in U-Minh area: effects of existing pile breakwaters

Our survey (*Figure 42*) confirms that erosion stopped at U-Minh, although the mangrove line is constant; there is no evidence of mangrove expansion but planting. The sediment deposited

inside the breakwaters must have come in by tidal exchange, as the water level inside the breakwater closely follows the level outside. This suggests that as long as the breakwaters are porous enough to allow the tide in, there can be a sufficient exchange of sediment.

### Erosion in Go-Cong area and geotube effect

Based on bathymetric survey differences, there is huge erosion ( $>20 \text{ Mm}^3$ ) in the first 2 km from the shoreline over 6 years. The differences need to be verified for biases between the two periods of measurements. However, the comparison in the West coast of Ca Mau does not show such a large difference, which means that there is consistency between satellite analysis of shoreline changes and bathymetric surveys.

The geotubes have been implemented in Go-Cong. However, there is very little evidence of small accretion; no effect of vegetation growth; there are still large waves accessing the shore. Unfortunately, no collecting data system was setup for the site to monitor effects of these pilot geotubes.

### Satellite analysis of shoreline changes

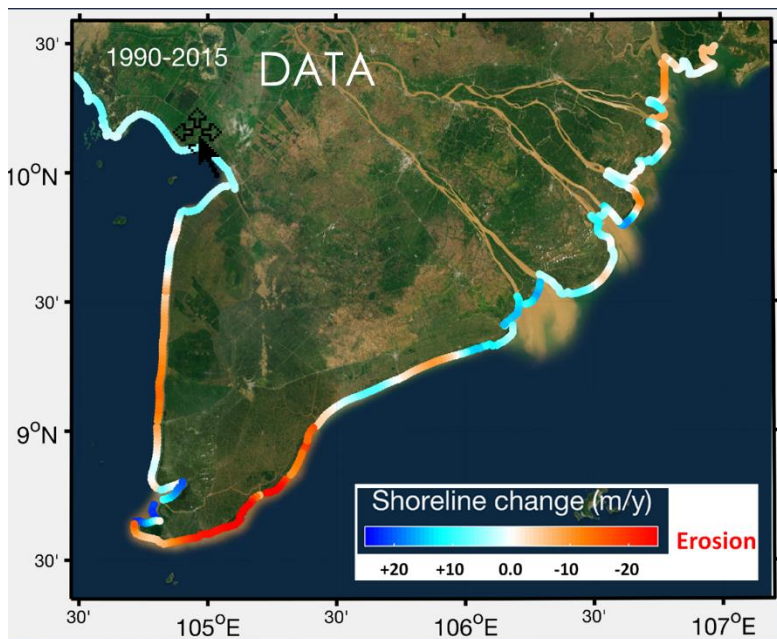


Figure 43 : Shoreline changes (m/yr) averaged over 1990-2015 from our satellite observation study (WP3).

**Go-Cong:** Shoreline analysis (Figure 43; WP3) shows consistent erosion in Go-Cong from 1990 to 2015. This is unique within the Estuary zone. Our understanding is that Go-Cong shores may be under direct influence from the Saigon-Dong Nai river system, rather than the Mekong River.

**Phu-Tan:** Phu-Tan is a very different subregion, showing interannual variability between mild erosion and mild accretion as opposed to U-Minh, which has showed consistent erosion in recent years. Consistently, our bathymetric survey compared with a survey performed about 15 years before shows little evolution. If there is local erosion, then it may be due to local causes or interannual climate variability.

## Mangrove width and sustainability

We revisited the results of Phan et al. (2015) (see report on Mangrove Erosion and *Figure 44*). They estimated that a critical mangrove width is needed in many cases around the LMDCZ to sustain the coastal mangrove belt. Using satellite data, we recomputed the relation between mangrove width and erosion/accretion; but the response is more varied in our results and probably need to be separated into more coherent subregions. A clear relationship between mangrove width and erosion/accretion was only found locally for a small part of the coast. The southern east coast has suffered massive erosion in spite of having mangrove fringes sometimes, at several kilometers wide. On the west coast, where there is little evidence of large-scale erosion of the seabed, mangrove erosion is possibly the result of coastal squeeze, mainly because of aquaculture activity.

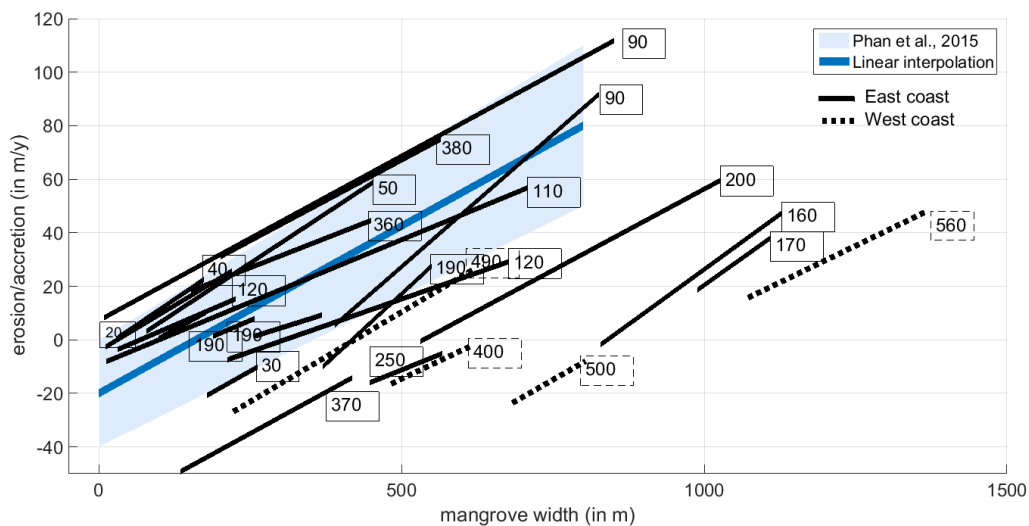


Figure 44: Synthesis of areas presenting a significant correlation between mangrove width and erosion/accretion

More specifically:

- The Estuary coast (0 to 280km) shows alternate signs of erosion and accretion even at small scales (sectors of 10km in length). This indicates that the coast is highly dynamics and resilient. Sediment supply from the river mouths is redistributed by ocean dynamics, with some adjustment and feedbacks of mangrove vegetation. Only 11% percent (32 km over 280 km) of the shoreline shows a direct linear relationship between mangrove width and the rate of erosion/accretion. For the remaining 89% of shoreline, the hypothesis of Phan et al. (2015) is not valid and the dynamic equilibrium is not dominated by mangrove resiliency, but by another driving factor: ocean forcings and/or human pressure and/or a variation of the fluvial sediment supply.
- The East coast (281-379 km) is dominated by large-scale erosion (97%), even if this coast has the largest mangrove belt, up to 2000m. Results of numerical simulations (WP2) shows that the dominating factor is a large scale (hundreds of km) readjustment of the geomorphological forms under the ocean forcing. In this sector, the interplay of waves, tides, and winds do not supply enough sediment along shore. The natural development of mudflats is limited and the mud bed remains too low to offer optimal

conditions for mangrove growth. While severe erosion in this regional unit results from natural geomorphic readjustment, we should bear in mind that mangroves, even under erosion, contribute actively to shore defense. In other words, the erosion rate would be larger without mangrove fringe.

- Go-Cong suffered chronic erosion during the last 20 years (not any phase of accretion, the dynamic equilibrium is disrupted). The mangrove is very scarce and the sand mud mixture is not necessarily the best environment for mangrove restoration. In the light of geomorphic and modeling results, we may assume that erosion is predominantly due to a reduction of sediment fluxes from the Saigon-Dong Nai system. Sediment supply being a key factor, measures of mangrove restoration would probably be improved by associated sand and mud nourishments.
- The West coast suffers mangrove squeeze in which aquaculture activity might be a significant driver. While the coast has been eroding in recent years without strong geomorphological adjustments (the coast remains linear); we may assume that mangrove squeeze enhance erosion. From the literature, we identify two possible factors: mangrove is not large enough to ensure wave dissipation, turbulence decrease and flocculation; the presence of aquaculture farms and/or dykes limits the tidal prism with negative effects on sediment trapping (Winterwerp et al., 2013).

The conclusion from these studies is that a minimum width of 500 m is required for a healthy mangrove belt, but not sufficient to prevent erosion (necessary but not sufficient condition). In addition, protection structures can prevent mangrove seeds from flowing through and thus prevent restoration. Soft fences are more permeable than concrete piles but planting may be required for mangrove restoration even for efficient sedimentation. Exposition time above the sea surface is also a critical factor, i.e., there is a critical height for mangrove seeds to anchor and colonize, which is related to temporal windows permitted by tides. Studies of the LMDCZ on this matter should benefit from experience acquired in other tropical regions (e.g., French Guiana).

## Laboratory Studies

Two methods to reduce wave energy were investigated in the laboratory: a new type of porous breakwaters and wide, shallow sand banks. Details can be found in the report on physical models (WP6).

### Porous breakwaters

The conclusions of flume experiments for the selected porous breakwater is that it may work as a means to reduce **wave transmission**, but it must be much higher than the still water level: for a zero relative freeboard  $R_C/H_{m0}$ <sup>6</sup> (crest level at water level), transmission is more than 50%

<sup>6</sup>  $R_C$  is the free board height, i.e., the difference in height between the top of the structure and mean sea level.  $H_{m0}$  is a measure of significant wave height (assumed here equal to  $H_S$ ).

(Figure 46). In practice this means that the crest level should be well above mean high water (MHW). Also, we note serious reflection, which can produce some amount of scouring on the seaward side of the breakwater.

Preliminary tests with kaolinite sediment showed that sediment is clearly transported through the breakwater, even without any tidal flow. With tidal flow cycles, we expect an easy exchange of sediment through the structure.

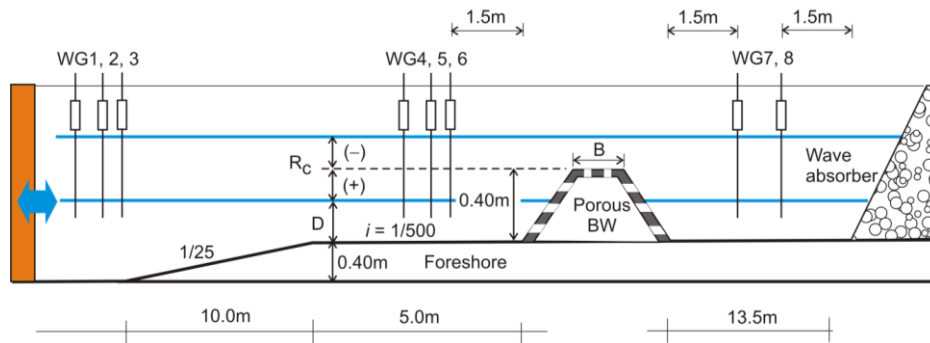


Figure 45: Flume configuration for porous concrete breakwater

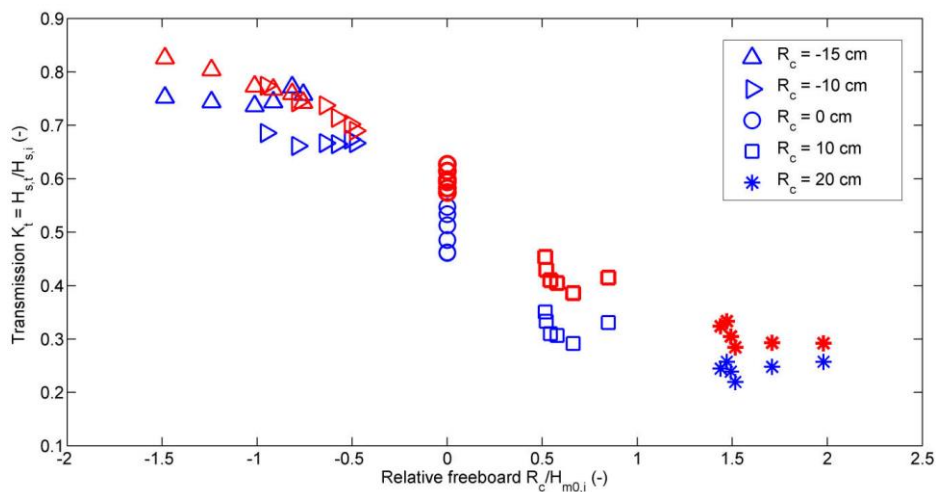


Figure 46: Transmission coefficient as a function of relative freeboard, for porous breakwaters

### Nourished sand bars

For the sand banks investigated, there is a significant reduction of the wave spectrum due to a wide sand bar (100-140 m). Here a negative freeboard (crest level under water level)  $R_c/H_{m0}$  of -0.5 reduces the wave heights to about 30%.

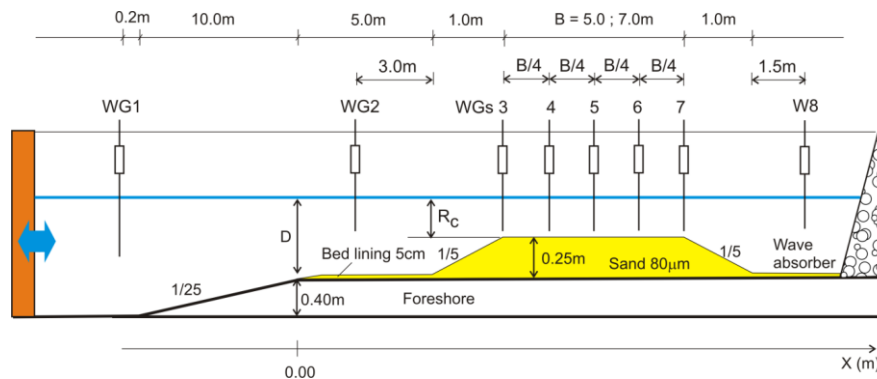


Figure 47 : Flume configuration for sand bar test

Deformation of the bar can be significant but positive damping effect remains over most tested wave conditions. Overall, the test of nourished sand bars appears positive, but the crest level should be about 0.5 m above mean sea level (MSL) to ensure significant wave damping under most circumstances.

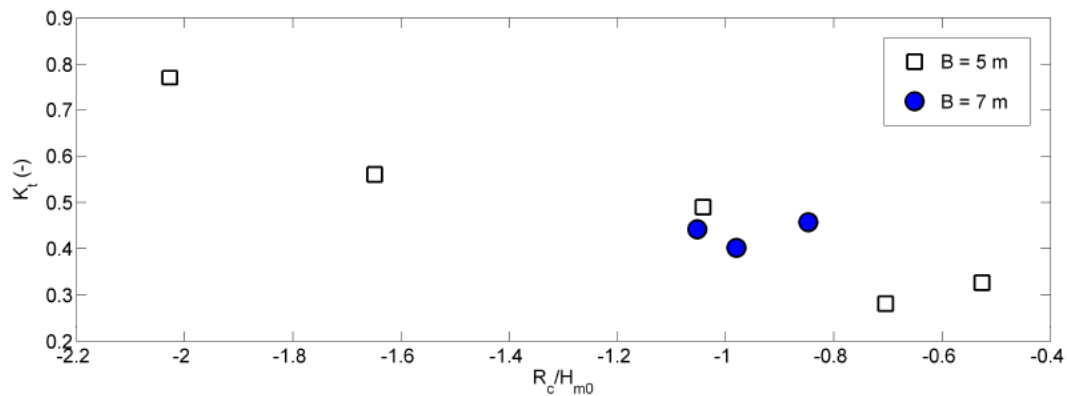


Figure 48 Transmission coefficient as function of relative freeboard, for wide sand banks

## Numerical modeling

### Regional modeling

Figure 24 shows the modeled-data comparison of main sub-regions of erosion/accretion (WP2) versus satellite survey. Note that local variations respond to local processes not represented in a regional model.

As seen before (WP2), regional models can provide (by comparison with data) valuable information for WP6. It shows the strong capacity of LMDCZ in redistributing sediments along shore at regional scales. It also shows that the whole shallow subaqueous delta should be considered for understanding erosion, not only the shoreline. Using sensitivity testing of river supply, the models also helped us reveal how Go-Cong appears as a consistently erosive subregion within a generally accretive region (estuary zone). The model results are sensitive to



river supply variations from the Sai Gon-Dong Nai river system (as opposed to other local areas of the estuary region influenced by the Mekong River). Phu-Tan is essentially a region of alternate mild accretive or erosion, receiving sediments from the East Coast of Ca Mau (naturally erosive). Local erosion there may thus have local causes or be subject to interannual climate variability.

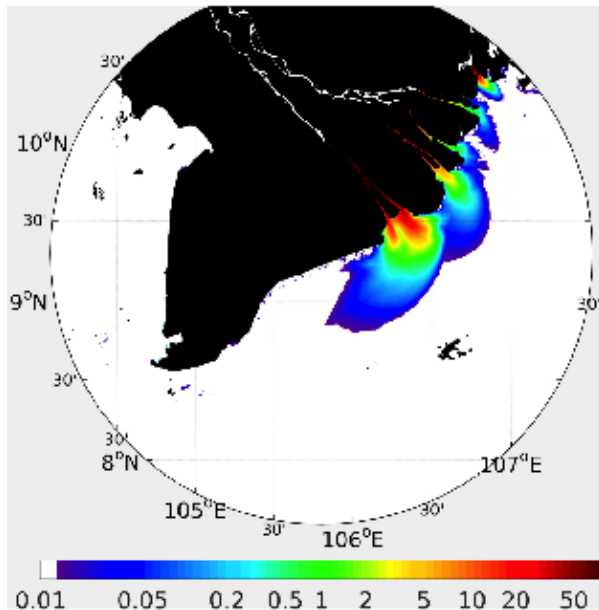


Figure 49: Sensitivity of coastal surface sediment concentration to river supply (WP2). The difference of SSC in mg/l is the response of a 75% reduction in river supply. There is exponential signal reduction away from the estuaries. It implies that river sediment deficit should first be seen in estuaries. It is the case for Go-Cong, which appears under direct influence from the Saigon-Dong Nai system, not the Mekong.

### Local modeling: Phu-Tan

Both MIKE and TELEMAC were applied to the west coast of the LMDCZ. The results of these models were consistent in many aspects. The main difference is quantitative and appears on the amount of sediment accumulation behind protection structures. The use of a cohesive sediment model in MIKE leads to larger sedimentation in calm waters. Generally, MIKE predicted higher SSC, which is favorable to accretion behind protections. These results were closer to observations of existing protections at U-Minh. Nevertheless, TELEMAC showed similar tendencies and sensitivities. We used the tests that it provided to complement our interpretation of results.

Local model testing is undertaken over representative months of high and low energy (Aug-Sep and Jan-Feb). According to the regional model, combined budgets from these months are qualitatively similar to yearly budgets. Confirming the result of the regional model, we show that, contrarily to sandy environments with steep beach profiles or more usual subaqueous delta profiles (deeper profiles; see Eidam et al., 2017), the effect of waves here is not confined to the surf zone, but extend further onto the shallow mud seafloors where bed shear stress is dominated by wave orbital velocities to a depth of about 10m.

Below is a summary of model test results in terms of mean bed thickness evolution for a combination of summer and winter months (Jan/Sep 2014), with comments that follow:

Phu-Tan simulations	Baseline	Breakwater	Sandbar
Jan/Sep 2014 Sedimentation (cm) in 2-km nearshore area	-1.8	-1.1	0.1
<b>Jan/Sep 2014 Sedimentation (cm) in area inside structure</b>	<b>-0.8</b>	<b>8.0</b>	<b>9.0</b>
Comments		Scouring Wind contribution to trapping	Sandbar deformation Wind contribution to trapping

**MODELED BREAKWATER:** The modeled breakwater is a shore-parallel structure 300m from shore, with gaps of 70 m, and has a crest elevation above the highest water level. Our results show that it can efficiently remove inshore wave energy. Because erosion results from wave-enhanced bed friction, the breakwater efficiently controls it. **The sediment budget changes from weak bed erosion to strong accumulation of tens of cm/y. This result tends to confirm the result of our survey on existing breakwater structures in U-Minh.** At U-Minh, erosion stopped and sediments accumulated inside the breakwater. Interestingly, accretion is much stronger during the SW summer monsoon because SSC is higher due to stronger waves outside of the protected zone, so that a larger sediment load can be brought inside and deposited. Without protection, the same waves would lead to offshore export of mud and erosion. Therefore, some amount of wave energy can be beneficial to accretion, provided that the nearshore area is protected. To confirm this, a model test with double wave height leads to 50% increase of sediment deposition inside the protected area.

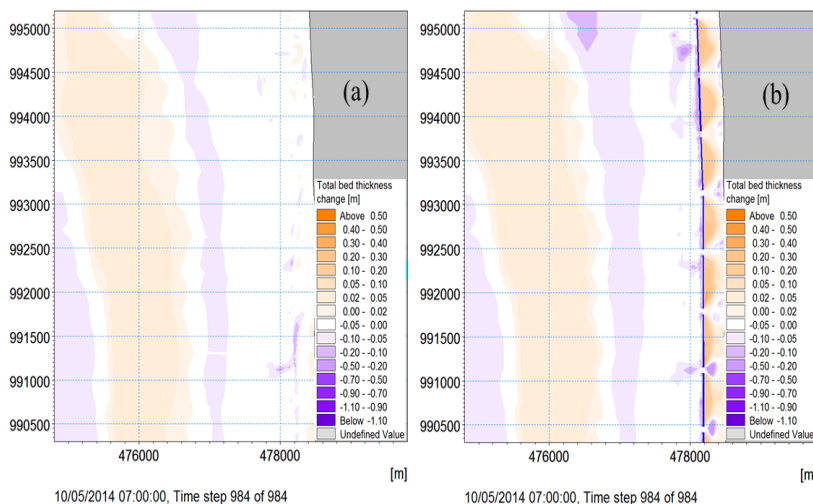


Figure 50: Monthly erosion and accretion off Phu-Tan district in Sep 2014 (SW monsoon). Left: without protection, erosion is apparent nearshore (on the right of the panel; Right: with breakwaters, strong accretion occurs, with scouring within gaps and at the offshore side of structures.

If tides are the main mechanism for onshore sediment transport, and we assume complete effectiveness of trapping processes, an upper limit for sedimentation rate can be estimated, depending on SSC. For SSC above 300 mg/l as measured during our nearshore surveys, accumulation of 30 cm/y, as observed in U-Minh and elsewhere (see our report on mangrove restoration; and Cuong et al., 2017) are possible. The present model helped us define the necessary conditions for such effective trapping to occur. We see here that not only waves must be efficiently damped but also tides must be allowed to carry sediments inside structures.

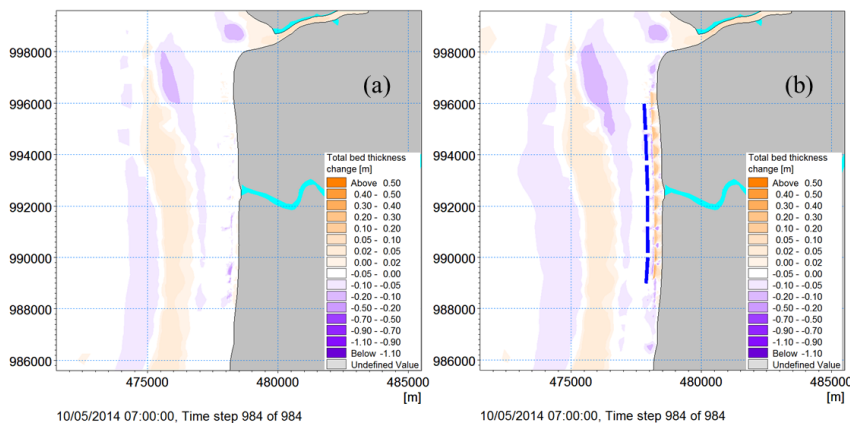


Figure 51: Same as previous figure but with sandbar for protection instead of concrete breakwaters. Accretion is also strong with sandbars, although a bit less than with breakwaters (20% less). However, scouring is absent here.

**NOURISHED SAND BAR:** We also tested the effect of a nourished sand bar. The modeled nourished sand bar is a shore-parallel structure ~500m from shore, 70 or 120 m wide, with gaps of 200m and height at mean sea level. The damping of waves by the bar was also an efficient process, provided that the bar width is in the order of a wavelength. Sandbars are a bit less efficient for wave blocking than a shore-parallel breakwater and has lower peak accretion inside the structure, but it has the **advantage of avoiding scouring at the breakwater foot and within the gaps, which leads to better overall trapping, and been environment friendly.** Finally, the addition of simulated mangrove effect on wave and flow dissipation showed to be a good complement to nourished sand bar as it carries wave damping further inshore and allows a more positive nearshore sediment budget in the model. As this is a preliminary experiment, the results remain qualitative.

### Local modeling: Go-Cong

Local modeling of the Go-Cong area (using MIKE as first choice) is also done over two representative months of high and low energy (Jan and Sep). It shows a clear impact of the T-groyne schemes on the flow velocities and a significant reduction of the wave heights. It also shows that the schemes are capable of enhancing sedimentation and reducing erosion in both monsoons. However, sand bank testing was not successful as no significant effect was seen on sedimentation and erosion rates. We believe that simulated sand banks were too low (MSL - 2m) and narrow for this area, defined by large waves and deeper bathymetry than in Phu-Tan.

**MODELED BREAKWATER:** The modeled breakwater is a T-groyne structure 300m from shore, and has a crest elevation above the highest water level (2.2m). It is composed of sections 600m wide with gaps of 30-50-70m (three scenarios). The model testing of protection measures shows that the breakwater has the capacity of allowing some inshore accretion, reversing the erosive tendency of the simulation without protection measures. Gaps between shore-parallel breakwaters were tested as well. It appears that the gap needs to be optimized to get the most effective accretion inside the structure and to reduce wave effect.. Therefore, damping waves appears as a priority for Go-Cong. It will not prevent erosion occurring further offshore, which eventually will affect the nearshore region and wall structures. Without raising again the sediment supply from the Saigon-Dong Nai river system, avoiding this problem will be difficult.

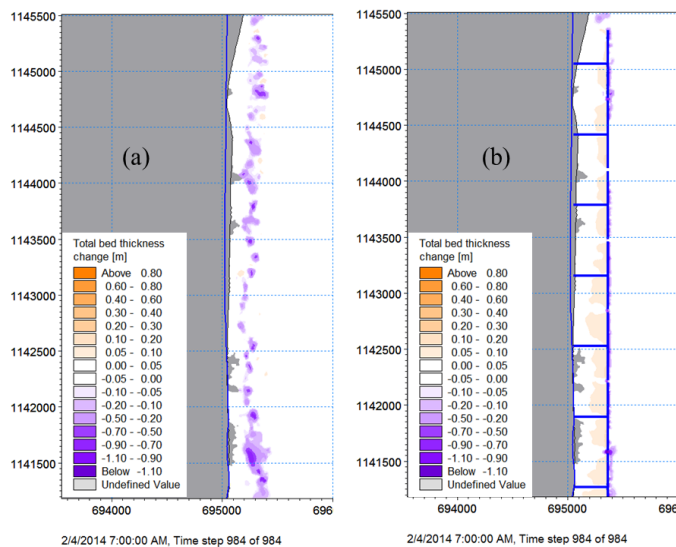


Figure 502: Distribution of erosion and accretion after one month of Northeast monsoon. Left: model erosion without protection measures; Right: model accretion with T-groyne structures (30m gap).

**NOURISHED SAND BAR:** We also tested the effect of a nourished sand bar. The modeled nourished sandbar is a shore-parallel structure 500m from shore, 50 or 70 m wide, with gaps of 200 m and crest level at mean sea level (deeper crest level proved inefficient in this high-energy environment). The model was first tested for sandbar integrity under high-energy NE monsoon waves. The results confirmed that of the physical model in producing only mild morphological changes on the outer slope of the bar. The damping of waves by the bar was less efficient than with breakwaters. Even though accretion inside the protection structure is lower, scouring is much reduced for sandbars compared with breakwaters. **The overall accretion with sandbars (over a section of 2km from shore) is higher by 30%.** Interestingly, during the low-energy season (SW monsoon), sandbars are more effective for accretion inside the protection structure, which adds to the overall efficiency. Finally, sandbar nourishment can also be useful as sediment storage in this sediment starved area. However, how helpful this might be for mangrove rehabilitation is an open question.

**SEDIMENT SUPPLY:** A test of sediment supply from the Saigon-Dong Nai river system was also performed. When sediment input is reduced by **75%** (100 km upstream), the net erosion increases along the coast of Go-Cong.

There is a **60%** deficit of sediment deposition in the coastal area (mostly in the wet season). The rest is deposited offshore or compensated by river erosion (“hungry water” process that limits the effective reduction of supply for downstream areas). Because in the reference simulation, erosion is almost balanced by accretion<sup>7</sup>, the deficit of accretion in the river supply experiment results in a large increase of net erosion over the combined two months of simulation (Jan and Sep): **0.67 Mm<sup>3</sup> erosion instead of 0.08 Mm<sup>3</sup>** (an order of magnitude). This result confirms previous suggestions from the regional model, indicating that erosion in Go-Cong is highly sensitive to the river sediment supply by the Saigon-Dong Nai river system. This is also confirmed by SIWRR surveys in recent years showing only thin layers of mud

<sup>7</sup> The Soai Rap River sediment flux is probably excessive in the reference simulation. The exact numbers are uncertain but recent studies of the Saigon Dong Nai river indicate low values associated with low SSC (J. Nemery, personal communication). This would need to be settled.

deposition during the low-energy season (summer), contrasting with thicker layers deposited further south in the mouths of Mekong branches (albeit with interannual variability).

Note that using breakwaters, river sediment deficit cannot be fully balanced by reduction of erosion and only half of net erosion is mitigated. This underline the fact that a full recovery of sediment in such a sediment starved area will require either local nourishment or modification of dam operations upstream on the Saigon and Dong Nai rivers.

Below is a summary of model test results in terms of mean bed thickness evolution for various scenarios and combination of summer and winter months (Jan/Sep 2014).

<b>Go-Cong simulations</b>	Baseline	Baseline -75% supply	Breakwater	Breakwater -75% supply	Sandbar	Sandbar -75% supply
Jan/Sep 2014 Sedimentation in 2-km coastal area (cm)	0.4	-1.2	0.8	-0.6	1.1	-0.3
<b>Jan/Sep 2014 Sedimentation inside structure (cm)</b>	<b>-2.8</b>	<b>-3.6</b>	<b>4.0</b>	<b>3.7</b>	<b>2.7</b>	<b>1.6</b>
Comments			Scouring	Scouring	No scouring Small bar deformation	No scouring Small bar deformation

Table 8: Sedimentation (mean bed thickness evolution in cm) over Jan and Sep 2014 in Go-Cong coastal area



## Recommendations

### Morphological model validation

- As for all other sensitivities and configurations, especially the test of reduced sediment input from the rivers, it is ever more important to assess the actual situation in order to explain the existing erosion at Go-Cong.

### Sand banks

- For the sandbars to work convincingly in Go-Cong the relative freeboard  $R_C/H_{m0}$  needs to be closer to -0.5; this means that we probably have to aim for a crest level of mean sea level + 0.0 m;
- The wider the better for long-term effect. From the physical and numerical model tests, a width of 70m seems appropriate.
- The amount of sand needed depends on the depth, but will be in the order of 170 m<sup>3</sup>/m in the Go-Cong area; if applied over the whole length it will be around 2.5 Mm<sup>3</sup>.
- This would at least in part restore the sediment budget in the nearshore area. For Phu-Tan, the volumes needed are probably less as the foreshore is much shallower.

### T-groyne schemes

- The simulations for the Go-Cong area showed a positive effect, in the sense of a reduction of erosion and an increase in sedimentation. However, mitigation appears to be hampered by river sediment supply deficit.

### Porous breakwaters

- At Phu-Tan, the breakwater is I-shape of porous type (see physical model test report) and location is 300 m offshore; Unit length is 600 m and gap between two units is 70 m; Crest elevation: +1.10 m;
- At Go-Cong, the breakwater is T-shape of porous type (see physical model test report) and location is 300 m offshore; Unit length is 600 m and gap between two units is 70 m; Crest elevation: +2.20 m (deeper topography);

### Pilot experiment

- We strongly recommend to carry out a limited but full-scale pilot experiment, testing both a section with breakwaters and one with a sandbar.
- The length of each at Go-Cong could be approx. 2 km long.
- In this case, it will be necessary to test these pilot configurations with numerical models for possible negative side effects.
- Both pilot sites should be placed some distance apart in the simulations so we can see the imprint of each of them;
- Based on these results, we could propose with more certainty a layout that provides maximum protection for the most critical sections.

## Communication

### Project Workshop

The LMDCZ project has organized 3 workshops as listed below:

- 1- Kick-off workshop on 12-13/11/2016 in Ho Chi Minh City
- 2- Technical workshop on 12-14/4/2017 in Ho Chi Minh City
- 3- Midterm workshop on 24-26/5/2017 in Hoi An
- 4- Final workshop on 26/1/2018 in Ho Chi Minh City.

The workshops attracted many international and national experts who eagerly contributed to the study, the decision makers at the central, provincial and local levels, various organizations and media. During the kick-off meeting, field trips were organized for many of the team experts. The technical workshop assembled most of the experts to share findings and experiences in an informal way. This was helpful for strengthening the group's cohesion and the direction of our work, just a month before presenting our preliminary results to the mid-term workshop in Hoi-An. During that workshop, very interesting exchanges occurred between scientist and decision makers, which helped us ascertaining our strengths and weaknesses.

### Project Website:

A website was implemented for the LMDCZ project (<http://lmdcz.siwrr.org.vn/?lang=e>), linked to SIWRR's website. All data collected during the project can be found on this website with more general information.

### Field trips and documentaries

We organized many field trips to study sites during the project. Some of them were for stakeholders to assess erosion problems with scientific experts. During one trip, a photo documentary was produced by one of our team experts on erosion sites and other Mekong delta areas. Towards the end of the project, a multimedia director from IRD filmed the study sites and interviewed the project's team to produce a film documentary, including many aerial shots from drones, that can be used for communication purposes.

## References

- Albers T et al. , 2013: Shoreline Management Guidelines: Coastal Protection in the Lower Mekong Delta.
- Anthony, E. J. et al. 2015: Linking rapid erosion of the Mekong River delta to human activities. *Sci. Rep.* 5, 14745.
- Benoit M., Marcos F., Becq F., 1996: Development of a third generation shallow-water wave model with unstructured spatial meshing. In: Edge, Billy L. (Ed.). *Proceedings of the 25th International Conference on Coastal Engineering, 1996*, vol. 1. American Society of Engineers Publications, 465–478.
- Blaas, M., C. Dong, P. Marchesiello, J.C. McWilliams, K.D. Stolzenbach, 2007: Sediment-transport modeling on Southern Californian shelves: A ROMS case study. *Continental Shelf Research*, 27, 832-853.
- Cuong, C.V., Brown, S., To, H.H., and M. Hockings, 2015: Using Melaleuca fences as soft coastal engineering for mangrove restoration in Kien Giang, Vietnam. *Ecological Engineering* 81, 256–265.
- Eidam, E.F., Nittrouer, C.A., Ogston, A.S., DeMaster, D.J., Liu, J.P. Nguyen, T.T., Nguyen, T.N., 2017. Dynamical controls on shallow clinoform geometry: Mekong Delta, Vietnam. *Cont. Shelf Res.* 147, 165–181.
- DeMaster, D.J., Liu, J.P., Eidam, E.F., Nittrouer, C.A., Nguyen, T.T., 2017: Determining rates of sediment accumulation on the Mekong Shelf: Timescales, steady-state assumptions, and radiochemical tracers. *Cont. Shelf Res.* 147, 82–196.
- GIZ, 2016 : Integrated coastal protection and mangrove belt rehabilitation in the Mekong Delta - Pre-feasibility study for investments in coastal protection along 480 km in the Mekong Delta.
- Gratiot N., A. Bildstein, Tran Tuan Anh, H. Thoss, H. Denis, H. Michallet, H. Appel, 2017: Sediment flocculation in the Mekong River estuary, Vietnam, an important driver of geomorphological changes. *Comptes Rendus Geoscience*, 349. 260–268.
- Guillou S., Thiébot J., Chauchat J., Verjus R., Besq A., Nguyen D.H. and Pouv K.S., *The Filling Dynamics of an Estuary: from the Process to the Modelling*, « Sediment Transport in Aquatic Environments», Ed. A. Manning, INTECH, Chap. 6, p. 125-146 (2011).
- Hervouet J.-M., 2007: *Hydrodynamics of free-surface flows: modelling with the finite element technique*. Wiley & Sons Ed., 360 pages.
- Hein H., Hein B., Pohlmann T., 2013. Recent sediment dynamics in the region of Mekong water influence. *Global and Planetary Change* 110 (2013), 183–194.
- Keskinen, M., Kummu, M., Kakönen, M., and Varis, O., 2012: Mekong at the Crossroads: Next Steps for Impact Assessment of Large Dams, *Ambio*, 41, 319–324.

King, P., Bird, J., and Haas, L., 2007: The Current Status of Environmental Criteria for Hydropower Development in the Mekong Region: A Literature Compilation, Consultants Report to ADB (Asian Development Bank), MRCS (Mekong River Commission Secretariat) and WWF (World Wide Fund for Nature), Vientiane, Lao PDR, 155 pp.

Kondolf, G.M., 1997: Hungry waters: effects of dam and gravel mining on river channels. *Environmental Management* 21(4): 533-551.

Le Hir P., W. Roberts, O. Cazaillef, M. Christie, P. Bassoullet, C. Bacher, 2000: Characterization of intertidal flat hydrodynamics. *Continental Shelf Research*, 20, 1433-1459.

Loisel H., A. Mangin, V. Vantrepotte, D. Dessailly, Dat Ngoc Dinh, P. Garnesson, S. Ouillon, J-P. Lefebvre, X. Mériaux, Thu Minh Phan, 2014: Variability of suspended particulate matter concentration in coastal waters under the Mekong's influence from ocean color (MERIS) remote sensing over the last decade, *Remote Sensing of Environment*, 150, 218-230.

Loisel H., 2013. GLobCoast : Remote sensing of Coastal water biogeochemical characteristics. International innovation, Research Media Ltd Ed., UK, August 2013, 38-41.

Lu, X.X. and R.Y. Siew, 2006 : Water discharge and sediment flux changes over the past decades in the Lower Mekong River: possible impact of the Chinese dams. *Hydrol. & Earth System Sciences* 10, 181–195.

Milliman JD and Meade RH., 1983: World-wide delivery of river sediment to the oceans. *J Geol.*, 91,1-21.

Minderhoud P.S.J., G. Erkens, V.H. Pham, V.T. Bui, L. Erban, H. Kooi and E. Stouthamer, 2017: Impacts of 25 years of groundwater extraction on subsidence in the Mekong delta, Vietnam. *Environ. Res. Lett.* 12.

Phan, H. M., Reniers, A., Ye, Q., Stive, M., 2017. Response in the mekong deltaic coast to its changing sediment sources and sinks. *Coastal Dynamics* (225), 311–322.

Phan, L.K., van Thiel de Vries, J.S.M., and Stive, M.J.F., 2015: Coastal mangrove squeeze in the Mekong Delta. *Journal of Coastal Research*, 31(2), 233–243.

Roberts W., P. Le Hir, R.J.S Whitehouse, 2000: Investigation using simple mathematical models of the effect of tidal currents and waves on the profile shape of intertidal mudflats, *Continental Shelf Research*, 20, 1079-1097.

Shchepetkin, A. F. and J. C. McWilliams, 2005: The regional oceanic modeling system (ROMS): A split-explicit, free-surface, topography-following-coordinate oceanic model. *Ocean Modeling*, 9/4, 347-404.

Schmitt, R. J. P.; Rubin, Z.; Kondolf, G. M., 2017 : Losing ground - scenarios of land loss as consequence of shifting sediment budgets in the Mekong Delta.

van Straaten, L. M. J. U. & Kuenen, P. H., 1958 : Tidal action as a cause of clay accumulation. *J. Sed. Petrol.*, 28, 406–413.

Syvitski J.P.M., Vörösmarty C.J., Kettner A.J., Green P., 2005: Impact of humans on the flux of terrestrial sediment to the global coastal ocean. *Science*, 308, 376-380.

Teisson, C., Ockenden, M. C., Le Hir, P., Kranenburg, C. & Hamm, L., 1993 : Cohesive sediment transport processes. *Coastal Engineering*, Vol. 21, pp. 129-162.

Walling DE., 2006: Human impact on land-ocean sediment transfer by the world's rivers. *Geomorphology*. 79, 192–216.

Walling, D.E., 2008. The changing sediment load of the Mekong. *Ambio* 37, 150–157.

Wang H., Saito Y., Zhang Y., Bi N., Sun X. and Yang Z., 2011: Recent changes of sediment flux to the western Pacific Ocean from major rivers in East and Southeast Asia. *Earth-science reviews*. 108, 80-100.

Winterwerp J.C., P.L.A. Erfemeijer, N. Suryadiputra, P. van Eijk and Liquan Zhang, 2013: Defining Eco-Morphodynamic Requirements for Rehabilitating Eroding Mangrove-Mud Coasts. *Wetlands*, 33, 515–526.

Winterwerp, J.C., W.G. Borst, and M.B. De Vries, 2005: Pilot study on the erosion and rehabilitation of a mangrove mud coast. *Journal of Coastal Research*, 21(2), 223–230.